Modeling Analysis of Rear Airbag Mounted Vehicle for the Enhancement of Crash Worthiness

Submitted by

Natif Keno Duguma

A Thesis Submitted to the Department of Mechanical Engineering

School of Mechanical, Chemical and Materials Engineering

Presented in Partial Fulfillment of the Requirement for the Award of the Degree of Master of Science in Automotive Engineering

Office of Graduate Studies

Adama Science and Technology University

June, 2023

Adama, Ethiopia

Modeling Analysis of Rear Air Bag Mounted Vehicle for the Enhancement of Crash Worthiness

Submitted by

Natif Keno Duguma

Advisor: Siraj Kedir Busse (Ph.D.)

A Thesis Submitted to the Department of Mechanical Engineering

School of Mechanical, Chemical and Materials Engineering

Presented in Partial Fulfillment of the Requirement for the Award of the Degree of Master of Science in Automotive Engineering

Office of Graduate Studies

Adama Science and Technology University

June, 2023

Adama, Ethiopia

ACKNOWLEDGMENT

I would like to acknowledge and give my warmest thanks to my advisor Dr. Siraj Kedir who made this work possible. His guidance and advice carried me through all the stages of writing my thesis. I would also like to thank my friends and family who have supported me and provided me with great insight into my research.

Also the author would like to thank Adama Science and Technology University for providing facilities and opportunities for this thesis.

Finally, I would like to thank the fact that this graduation thesis would not have been possible without the support of the software. Thanks to my friend Garbe Chukulu Jarso (Ph.D Candidate) for providing an excellent guide to the ANSYS Ls Dyna software.

DECLARATION

I hereby declare that this Master Thesis entitled **"Modeling and Dynamic Analysis of Rear Air Bag Mounted Vehicle for the Enhancement of Crash Worthiness"** is my original work. That is, it has not been submitted for the award of any academic degree, diploma, or certificate in any other university. All sources of materials that are used for this thesis have been duly acknowledged through citation.

________________	________________	________________
Name of student	Signature	Date

RECOMMENDATION

I, the advisors of this thesis, hereby certify that we have read the revised version of the thesis entitled **“Modeling and Dynamic Analysis of Rear Air Bag Mounted Vehicle for the Enhancement of Crash Worthiness**” prepared under guidance by Natif Keno Duguma submitted in partial fulfillment of the requirements for Master of Science in automotive engineering. Therefore, we recommend the submission of revised version of the thesis to the department following the applicable procedures.

Dr. Siraj Kedir

Advisor	Signature	Date

APPROVAL PAGE

We, the advisors of the thesis entitled "**Modeling and Dynamic Analysis of Rear Air Bag Mounted Vehicle for the Enhancement of Crash Worthiness**" developed by Natif Keno Duguma; hereby certify that the recommendation and suggestions made by the board of examiners are appropriately incorporated into the final version of the thesis.

______________________________	______________________	____________________
Major Advisor	Signature	Date

We, the undersigned, members of the Board of Examiners of the thesis by Natif Keno Duguma have read and evaluated the thesis entitled "Modeling and Dynamic Analysis of Rear Air Bag Mounted Vehicle for the Enhancement of Crash Worthiness" examined the candidate during the open defense. This is, therefore, to certify that the thesis is accepted for partial fulfillment of the requirement of a Master of Science in Automotive Engineering.

______________________________	______________________	____________________
Chairperson	Signature	Date
______________________________	______________________	____________________
Internal Examiner	Signature	Date
______________________________	______________________	____________________
External Examiner	Signature	Date

Finally, approval and acceptance of the thesis is contingent upon submission of its final copy to the Office of Postgraduate Studies (OPGS) through the Department Graduate Council (DGC) and School Graduate Committee (SGC).

______________________________	______________________	____________________
Department Head	Signature	Date
______________________________	______________________	____________________
School Dean	Signature	Date
______________________________	______________________	____________________
Office of Postgraduate Studies, Dean	Signature	Date

TABLE OF CONTENTS

Contents	Page
ACKNOWLEDGMENT	iii
ACRONYMY AND ABBREVIATION	iv
LIST OF TABLES	v
LIST OF FIGURES	vi
ABSTRACT	viii
CHAPTER ONE	**1**
INTRODUCTION	**1**
1.1 Background	1
1.2 Statement of the problem	3
1.3 Objective of the thesis	5
1.3.1 General objective	5
1.3.2 Specific Objectives	5
1.4 Scope of the thesis work	5
1.5 Limitation of the Study	6
1.6 Significance of this thesis work	6
1.7 Organization of the thesis	6
CHAPTER TWO	**7**
LITERATURE REVIEW	**7**
2.1 Introduction	7
2.2 Review of Related Literature	7
2.3 Review on Modeling Rear Impact and protective device	8
2.4 Detail Review of Airbag Materials	15
2.4.1 Necessary components for installation	17
2.4.2 Mounting Air Bag with Volkswagen Vehicle	17
2.5 Numerical Simulation Using Ansys LS DYNA	18
2.6 Summary of review	19
2.7 Research gap	19
CHAPTER THREE	**20**
MATERIAL AND METHOD	**20**
3.1 Introduction	20
3.2 Materials used	20

3.3 Methodology 20
3.3.1 Data Collection (Primary) 22
3.3.2 Material properties of the body of vehicles 23
3.3.3 3D model pick-up of front bumper beam 24
3.3.4 Data Collection (Secondary Data) 25
Theory of Airbag 25
Air bag Inflation time 30
3.3.5 Sizing and Selection of Air Bag filling Valve 31
3.3.6 Sensor Selection for Air Bag inflation 32
3.3.7 Installation position adjusted for sensor 34
3.3.8 Programming the Arduino ultrasonic sensor to measure distance 35
3.4 Concept on Rear air bag system 35
Air bag for Rear bumper portion system 36
3.5 Conceptual Design of Air bag shape with 3D Model 36
3.5.1 Parametric of air bag Design 37
3.5.2 3D Modeling 38
3.5.3 Ansys LS Dyna Boundary/Initial Condition’s 38
3.5.4 Assumption 39
3.5.5 Ansys LS Dyna Meshing 40
3.5.6 Grid independent Test based on grid convergence index (GCI) 40
3.5.7 The selected models mesh Generated 41
CHAPTER FOUR 43
RESULT AND DISCUSSION 43
4.1 Numerical Result of Airbag Design 43
4.2 Vehicle crash analysis 44
4.2.1 Car without Air Bag Tested Result 45
4.2.2 With Air Bag mounted at the rear end 49
CHAPTER FIVE 55
SUMMARY AND CONCLUSION 55
5.1 Summary 55
5.2 Conclusion 55
5.3 Recommendation 56
5.4 Future scope 56

REFERENCES 57
APPENDIX I 61
VEHICLE BODY MATERIAL TICKNESS 61
APPENDIX II 62
APPENDIX III 63
RESULT SUMMARY OF CRASH ANALYSIS 63
APPENDIX IV 65
RESULT UNDER MORE SEVERE DAMAGE CONDITION 65
APPENDIX V 67
FRONT CAR WITH AIR BAG 67
APPENDIX VI 74
CAR SPECIFICATION 74
APPENDIX VII 75
AIR BAG ARDINO BASED SENSOR CODE 75

ACRONYMY AND ABBREVIATION

FEA	Finite element analysis
ANSYS	Analysis Systems
CATIA	Computer Aided Three-Dimensional interactive application
LS-DYNA ANSYS	Livermore dynamic explicitly analysis software
GCI	Grid convergence index
SAE	Society of Automotive engineering

LIST OF TABLES

Table 2.1.Mechanical properties of the airbag (D. Bend jab Allah et al., 2019) 16
Table 2.2. Physical and mechanical properties of the airbag D. Bend jab Allah et al. (2019) 16
Table 3.1. Materials used 20
Table 3.2. Pick-up Car Specifications.. 22
Table 3.3. Volkswagen Specifications.. 22
Table 3.4. Properties of Steel 1006 23
Table 3.5. Mechanical Properties of Conventional Steel.. 24
Table 3.6. Properties of Nitrogen gas. 27
Table 3.7. HC-SR04 Ultrasonic Sensor 34
Table 3.8. HC-SR04 Ultrasonic Sensor Size 34
Table 3.9. Properties of Nylon 66 and Polyester. 36
Table 3.10 Air bag Shape Size based on rear crash zone of car 37
Table 3.11. Air bag Shape based on fixing location 37
Table 3.12. Output Parameters for all shapes 37
Table 3.13. Boundary/Initial Condition's 39
Table 3.14. Parametric Value for Air Bag Inflation mass flow 39
Table 3.15. Grid Refinement ratio of different Model... 41
Table 3.16. Grid Refined Stress value of different Model.. 41
Table 3.17 GCI of different Model 41
Table 4.1 Summary of Crash analysis without air bag 48
Table 4.2 Summary of Crash analysis with air bag 52

LIST OF FIGURES

Figure 2.1. Truck Rear Impact Energy -Absorbing Device (Li, 2018).. 8

Figure 3.1. Methodology of the Research.. 21

Figure 3.2. Bull bar Bumper 25

Figure 3.3. Sensor and airbag operating systems in the car.. 25

Figure 3.4. Detail of the air-bag inflation device.. 26

Figure 3.5 Conservation of mass in diverging tube 31

Figure 3.6. Fast Air bag filling Valve.. 32

Figure 3.7. Ultrasonic beams 33

Figure 3.8 Sensor Installation position 34

Figure 3.9 working of ultrasonic sensor on vehicle.. 35

Figure 3.10.3d model of bumper and Concept of airbag Shape 36

Figure 3.11 Free crash lengths for the rear impact 18

Figure 3.12 Vehicle with designed air bag mounted at rear 37

Figure 3.13. Vehicle without air bag mounted at rear 38

Figure 3.14 plot of Air Bag Inflation mass flow Rate 40

Figure 3.15 (a) Airbag- Mesh and (b) Two Cars, Mesh Generated............................... 42

Figure 4.1. a & b, Stress distribution and total deformation of air bag at maximum speed of rear vehicle 50m/s 43

Figure 4.2. c & d, Stress distribution and total deformation of air bag at maximum speed of rear vehicle 50m/s 44

Figure 4.3 a & b, Stress distribution and total deformation of Frontal car at rear car speed of.... 45

Figure 4.4 Average Dynamic stress on front vehicle during 25m/s & 50m/s speed of rear car... 46

Figure 4.5 Average dynamic deformation on front vehicle during 25m/s & 50m/s speed of rear car.. 46

Figure 4.6 Average dynamic internal energy absorbed on front vehicle during 25m/s & 50m/s speed of rear car.. 46

Figure 4.7 a & b, Stress distribution and total deformation of Frontal car at rear car speed of (6.25m/s & 12.5m/s) 47

Figure 4.8 Average dynamic stress on front vehicle during 6.25m/s & 12.5m/s speed of rear car 47

Figure 4.9 Average dynamic deformation on front vehicle during 6.25m/s & 12.5m/s speed of rear car 48

Figure 4.10 dynamic internal Energy absorbed during 6.25m/s & 12.5m/s speed....................... 48

Figure 4. 11 a & b, Stress distribution and total deformation of Frontal car at rear car speed of (25m/s & 50m/s) 49
Figure 4.12 Average dynamic stress on conventional automobile body during 25m/s & 50m/s speed of rear car 50
Figure 4.13 Average deformation of conventional automobile body during 25m/s & 50m/s speed of rear car 50
Figure 4.14 Average dynamic internal Energy absorbed of conventional automobile body during 25m/s & 50m/s speed of rear car 50
Figure 4. 15 a & b, Stress distribution and total deformation of Frontal car at rear car speed of (6.25m/s & 12.5m/s) 51
Figure 4.16 Average dynamic stress on airbag based automobile during 6.25m/s & 12.5m/s speed of rear car 52
Figure 4.17 Average dynamic deformation on airbag based automobile during 6.25m/s & 12.5m/s speed of rear car 52
Figure 4.18 Average dynamic internal Energy absorbed of airbag based automobile during 6.25m/s & 12.5m/s speed of rear car 52
Figure 4. 19 a, b, c & d, both rear car speed and Frontal car respectively during collision 54
Figure 0.2 a & b, Stress distribution and total deformation of both cars and Frontal car respectively at rear car speed of (12.5m/s) 69

ABSTRACT

Automobile manufacturers have a challenging task since car accidents scare survivors and complicate their socioeconomic circumstances. The energy absorption capacity of the restraint system is directly correlated with the severity of collisions. The rear car bumper is the most prevalent of the restraint system's components. But bumper is designed to reduce physical damage to the vehicle's structure by crushing or collapsing to absorb low energy collision energy. The objective of this research is to concentrate on the modeling and numerical analysis of popular light-duty vehicles' rear-ends systems with airbag mounting in place of bumper. The methodology used in this research included the creation of a 3D model using Ansys Space Claim and numerical analysis using Ansys LS Dyna. It also included the size determination of the rear air bag system based on the impactor vehicle's frontal end height and bumper width paralleled with the impacted car's rear end. A failure theory, such as bursting and internal energy, is used to calculate the thickness and size of the air bag in the early stages of the research. An air bag made of nylon 66 is applied to the rear impactor while a car is driving at its top speed, moderate and minimum. The research focuses on the analysis of impact strength, deformation, absorption of energy, and dynamic conditions. The investigation of an automobile with and without an airbag yielded the following results: the weighted averages of deformation, stress, and internal energy are 72.5mm and 34.59 mm, 555.24 MPa and 443.08 MPa, and 0.835 MJ and 2.458 MJ, respectively. Finally, this shows that a car with airbags reduces deformation by 52%, reduces stress by 20%, and absorbs energy 194% better than a normal system. Here, the airbag-based rear beam lessens stress and deformation, which is subject to the greatest strain at greater speeds as well as increases the quality of energy absorption on the front car. The air bag-based rear automotive system therefore improves crashworthiness by reducing deformation, stress, and raising internal energy with speed. Therefore as a result of minimizing deformation, stress and boosting internal energy with speed, the air bag-based rear automobile system enhances the crash worthiness. There for it is recommended to use air bag as crash safety protection device in place of conventional bumper.

Keywords: *Bumper, air bag, impact analysis, LS Dyna*

CHAPTER ONE

INTRODUCTION

1.1 Background

Automobile accidents endanger human lives and are a socioeconomic problem. Vehicle protection systems have to be given more thought as a result, and they are currently a popular area for study and development (Supriya et al., 2017). A motorized vehicle that offers frontal or rear al collision protection for the occupants or vehicle crashworthiness. It is accepted that rear collisions are one of the most frequent types of deadly auto accidents. The bumper systems also safeguard other safety-related equipment as well as the fuel, exhaust, cooling, and cooling systems. One of the car shields is the bumper, which is made of steel, aluminum, rubber, or plastic and attached to the front and rear of a passenger car. When a low speed contact occurs, the bumper system absorbs the shock, minimizing or avoiding damage to the car. The bumper, which can be found either in the back or front of an automobile, protects the passenger compartment in crashes. The bumper's primary function in a low speed collision inside a car is to cushion the impact and protect the occupants (Sudin et al., 2018).

In the early 1900s, the motor vehicle bumper was initially developed to shield the front and rear of the car from low-speed collisions. Bumpers were typically just plain beams that were held up by spring-like springs (Sudin et al., 2018). These bumper designs could not absorb energy since they did not store energy to be released in a rebound motion when contacted (unless sections were permanently bent or cracked under crash pressures) (Raj Kumar et al., 2019). According to the first bumper standard issued under the 1966 Act, FMVSS 215 external protection, commencing with the model year 1973, passenger cars had to be able to withstand frontal crashes at 5 mph and rear impacts at 2 1/2 mph against a barrier without any specific safety-related components being damaged (Report, 1981; Sonawane & Shelar, 2018) .

The researcher’s done the mechanical and deformation energy absorber, and the bumper reinforcement make up the rear bumper system. When a car is struck, airbags, a sort of automotive safety feature, deploy, creating a cushion of air that prevents someone from hitting their face on the dashboard or steering wheel. The front seats are often equipped with airbags. John Hetrick, an industrial engineer, was granted one of the key rights for automobile airbags on August 18, 1953(Kleisner & Zemčík, 2009). Following a collision in 1952, Hetrick designed an airbag that includes an air tank under the hood, expandable bags on the steering wheel, in the center of the dashboard, and in the glove compartment to protect people in the front seats, and an airbag on the back of the front chair to protect people in the back seats (Kleisner & Zemčík, 2009). The utility and consistency of airbag-equipped automobiles have been demonstrated later in the 1960s in detailed tests and regular use. The research, which was founded on data from 1985 to 1991, found that airbag-equipped automobiles had a 32% lower driver loss of life in frontal accidents(Kleisner & Zemčík, 2009).

It is constructed from an air pad, a flexible bag of textile fibers. Airbags inflate milliseconds after a collision is detected, protecting the body from the stiff inside of a car as it slows down. Airbags are meant to protect humans in frontal crashes.

Because the fundamental cohering behind an automobile body element in an advanced automotive safety control system is whether the mechanical component can absorb impact energy that may cause injuries to accident victims and if the interior of the vehicle body can resist a collision (Kurebwa & Mushiri, 2019). When a low-speed collision occurs between a vehicle and another car, the rear bumper scheme's primary function is to protect the tire, rear suspension system, and lamps. However, when a moderate-speed or high-speed collision occurs, the impact energy is transferred to further car parts. About 30% of collisions are rear-end crashes of all auto accidents, according to the National Highway Traffic Safety Administration (NHTSA) (Kahane J, 2013). These incidents are frequently the result of the other driver speeding, driving while distracted, driving while fatigued, failing to provide adequate space between vehicles, and driving aggressively. And also air bag system proposed in the previous work shows that as it is vehicle safety restraint system. It is an occupant restraint device that uses a cushion or flexible fabric envelope that may quickly inflate in the event of an auto accident. Its function is to cushion passengers during collisions and protect their bodies when they collide with interior objects like the steering wheel or a window. By lessening the force applied to any place on the body, including the steering wheel and dashboard, it reduces the number of injuries. There are two ways to do this: either by extending the time between applications of force, by distributing the force over more of the body. Most of the researchers were only focused on testing and effective implementation of the existing air bag system which is used in the interior, front and side of the vehicle.

Figure 2. 1 Side safety airbag system (Arun Kumar & Madhu, 2015)

As studied by (Yurchenko et al., 2021), Airbags and seat belts are essential safety features in cars to prevent car occupants from jumping out or hitting the interior structure during collisions. However, the high temperature and internal pressure of these gases can negatively impact the environment and cabin, especially in serious collisions and driverless vehicles. To increase the safety of vehicle occupants who are placed in arbitrary locations, advanced engineering solutions are needed. Employing a supersonic pulse ejector to entangle ambient air for aspirated inflator operation

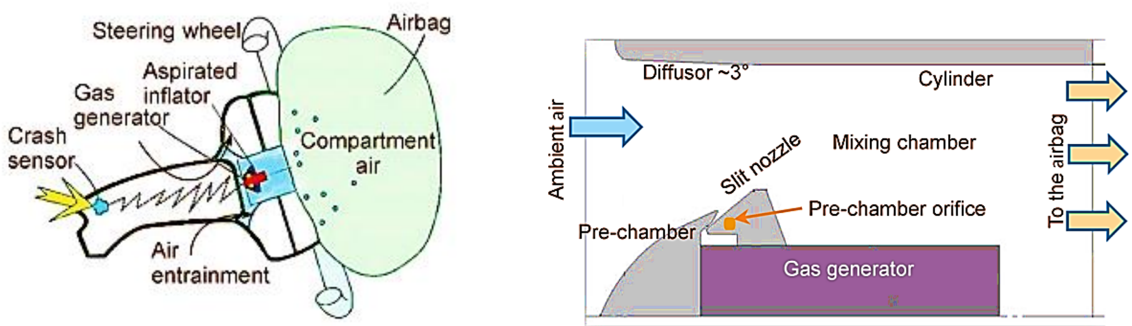

Figure 2. 2 Employing a supersonic pulse ejector to entangle ambient air for aspirated inflator operation

Therefore the goal of this research is to ascertain an air bag-equipped automobile rear bumper's capacity to absorb energy when impacted at a minimum, moderate speed and maximum. Crash analysis and design work are included in this research. After analyzing energy absorption, the novel airbag function is installed on the back bumper to use the appropriate airbag material to maximize energy absorption.

1.2 Statement of the problem

When the leading vehicle is stopped or driving extremely slowly, rear-end crashes are more common in metropolitan areas (Ma et al., 2022; Mohamed et al., 2017). 81% of rear-end collisions happen while the leading car is entirely stopped(Lee et al., 2007). Most crashes occur when the motorist follows the automobile in front of them too closely. According to the traffic flow observation, sedans and hatchbacks were more likely to be involved in rear-end collisions than other types of cars (Luo et al., 2020). Vehicles using the high-speed lane regularly drove next to one another, which raised the risk of rear-end collisions (Wang et al., 2019; Xi et al., 2019). According to the observation of driving behaviors, younger and higher-earning drivers are more likely to drive with fewer gaps, which raises the risk of a rear crash(Das et al., 2019). Shorter headway lengths and a higher risk of rear-end collisions are characteristics of drivers who frequently experience stress, fury, or hostility while operating a vehicle(Zhang et al., 2022).

Vehicle rear-end crash victims often suffer from whiplash and other neck injuries, closed head injuries, internal bleeding, internal organ damage, knee and shoulder injuries, as well as back and spinal cord injuries. Automobile deaths are a serious issue, especially lately (Kahane J, 2013). Due to insufficient energy absorption, the structural integrity of the rear end is damaged in an impact crash, killing any passengers. The airbag system suggested in the previous research shows that the majority of researchers were mainly focused on testing and effective implementation of the current airbag system, which is only used on the inside, front, and sides of vehicles. However, the original concept behind this research was to incorporate the idea of an airbag system into the vehicle's back compartment as a crash protection measure. Because rear-end collisions are frequent in urban locations, especially with traffic bottlenecks. According to this thesis, the concept of an airbag system incorporated at the rear bumper portion will increase energy absorption capacity, decrease vehicle body deformation during a collision, and lower the concentration of vehicle body stress during a high-speed impact. Customers are to blame for production failure, and material optimization and design modification are study gaps in vehicle crash analysis, and the research on moderate and high-speed impact analysis is lacking.

The air bag system suggested in the previous research shows that the majority of researchers were mainly focused on testing and effective implementation of the current air-bag system, which is only used in the inside, front, and sides of vehicles. However, the original concept behind this research was to incorporate the idea of an airbag system into the vehicle's back compartment as a crash protection measure. Because rear collisions are frequent in urban locations, especially with traffic bottlenecks. According to this thesis, the concept of an airbag system incorporated at the rear bumper portion will increase energy absorption capacity, decrease vehicle body deformation during a collision, and lower the concentration of vehicle body stress during a high-speed impact. Customers are to blame for production failure, and material optimization and design modification are study gaps in vehicle crash analysis and the research on moderate and high-speed impact analysis lacking.

The innovative concept in this research is the incorporation of an air bag system into the vehicle's back end. In this thesis, the idea of an airbag system integrated into the rear section is expected to boost energy absorption capacity while reducing deformation and stress concentration on the vehicle body during minimal, moderate, and high-speed impacts. With a fast filling valve method that fills the air bag in less than a millisecond, the deployment for this sort of air bag should be carefully planned depending on the approaching vehicle speed in relation to the air bag inflation step.

1.3 Objective of the thesis

1.3.1 General objective

The primary goal of this thesis work is modeling and analysis of rear airbag-mounted vehicles to improve crashworthiness for the protection of passengers and automobiles.

1.3.2 Specific Objectives

The specific objective of thesis this work are,

- Size determination of the air bag and estimation of inflation gas amount based on theoretical concepts.
- To decide the size of air filling valves and sensor, based on the hypothetical back ground of Mach number which lead sonic speeds of rear coming vehicle.
- 3-D modeling and analysis of an air bag for its strength matter based on the maximum speed of the rear car using a computational method known as dynamic explicit analysis.
- Analyzing the model of a car without and with airbags to capture their strength, deformation, and energy absorption scenarios as the rear car's speed varies.

1.4 Scope of the thesis work

The study focuses on how air bags are constructed. The airbag's design and inflation in the rear configuration are dependent on the pressure discovered during an initial design calculation.

The purpose of this thesis is to investigate the performance of an airbag-based rear system in a vehicle during a rear collision. The research entails replacing the conventional rear bumper with an airbag-based system and comparing its performance in terms of energy absorption and deformation to that of the conventional system. The study also includes an examination of the stress created in the vehicle's rear collision zone. The study's goal is to see if the airbag-based approach is safer than the conventional system. And the 3d modeling and simulation with Ansys Ls-Dyna for both air bag and vehicle has been done.

1.5 Limitation of the Study

The scope of the study has been constrained to the available materials for the research. Except for the validation of the study, which requires actual vehicles built with airbags that weren't experimentally tested, there are no problems in the design or analyses. The standard ultrasonic sensor and quick filling valve have been chosen to identify the car before the impact, and the Arduino-based code is generated to employ this rear airbag system deployment. However, their use is only confined to demonstration purposes because these materials are not offered on the local market.

1.6 Significance of this thesis work

This study affords a lot of advantages to the scholars, for the designers and to the automobile manufacturer. From numerous the following are;

The relevance of this thesis work is that it suggests a new airbag-based rear system for automobiles that may improve safety in the event of a rear crash. In terms of energy absorption, deformation, and stress caused in the normal rear collision zone, the study compares the performance of the airbag-based system to that of the conventional rear bumper. The study's findings can be used by researchers, vehicle designers, and automakers to improve vehicle safety and lower the chance of injury to passengers in a rear collision. It encourages researchers to conduct additional research on high-speed impact and energy absorption volume.

1.7 Organization of the thesis

This thesis is organized into five chapters. Chapter One describes the introduction, background, statement of problem, objectives, significance and scope of the thesis. Chapter two presents' a literature review of the existing air-bag system and bumper of vehicles. Chapter three describes about Materials and methods used. Chapter four covers results and Discussion, and Chapter five tells about the Recommendation and conclusion.

CHAPTER TWO

LITERATURE REVIEW

2.1 Introduction

Earlier attempts in the air bag and bumper system industry are described in this section. An airbag is a sort of occupant restraint device for automobiles that use a bag that is designed to inflate and deflate quickly. An impact sensor, an inflating module, a flexible fabric bag, and an airbag cushion comprise it. The primary function of an airbag is to softly cushion and confine the occupant of a vehicle during a collision. Injury concerns between the flailing occupant and the interior of the car can be reduced.

The airbag works as an energy-absorbing barrier between the occupants and the steering wheel, instrument panel, body pillar, headliner, and windshield. In current cars, up to ten airbag modules in various configurations may be found, including airbags for the driver, passenger, and side curtains, seats, doors, B and C pillar-mounted side-impact, knee bolster, inflatable seat belt, and pedestrian airbag modules (Barbat et al., 2013). For further information from the previous studies using the analytical system and numerical involving bumper and air bag has been done.

Because, for the general concept present work is to solve airbag replacement with rear bumper space of the vehicle, the following articles and journals are mentioned as related work of this research.

2.2 Review of Related Literature

Rear-end collisions are regular car accidents that involve two vehicles and are frequently triggered by acceleration and deceleration. These incidents occur when a car collides with the rear of the vehicle in front of it, frequently as a result of abrupt acceleration or distracted driving. Previous research has looked into devices to reduce impact load transfer, such as bumper-based rear ends and front bumpers. Therefore passenger safety must be improved to prevent these collisions.

(Tsuchiya & Shiraishi,2015) researched about injure mechanism. Understanding injury trends and demographic changes is essential to developing effective trauma triage standards. This information supports safety guidelines for automakers, new laws, and treatment and preventative methods. The distribution of resources across communities, long-term care facilities, and hospitals will become more difficult as the aging population increases. The healthcare continuum for polytraumatized patients will be impacted by prevention, education, and legislation, necessitating reimbursement and money allocation concerns.

(Tsuchiya & Shiraishi, 1998) investigated the research on collision avoidance that when a driver comes across an obstacle just ahead, there are three different collision avoidance maneuvers that can be used: braking and halting before collision, guiding the car to avoid it, and braking and steering at the same time. Anyhow, each vehicle has a specific crash-unavoidable zone. The design of a crash-unavoidable zone is heavily influenced by a "cross point" established by the behavior of the vehicle, which primarily depends on the speed of the vehicle, friction between the wheels and the road, and steering angle. In this work, this zone is established by taking into account these variables.

(Associate Prof. J is.,2018) studied the amount of energy absorbed by the car's structure and the amount by the restraint system directly correlate with the severity of a collision. The most complicated parts of the restraint system are the airbags, which are a critical part. The design and production of airbag systems are made more difficult by the nonlinear behavior of passengers and vehicles. In addition to investigating a quick design and simulation method for airbag parameters in the concept design phase using an impact issue, this study discusses alternative approaches to developing airbag dynamics equations.

2.3 Review on Modeling Rear Impact and protective device

(Wisch et al., 2014) comprehended and foresee potential issues with electric vehicles, the EVERSAFE project used conventional accident analysis, computer modeling, physical testing, and literature research. Results demonstrated high safety levels, but more research is required to help firefighters identify EVs, turn off electrical systems, and neutralize batteries following a crash. Improvements to post-crash handling and crash protection were the two categories of recommendations.

(Li, 2018) With the aid of the programmers PRO/E and ANSYS/LS-DYNA, a truck rear impact energy-absorbing device has been designed and its simulation analysis is carried out. The device can reduce collision force and absorb energy, breakdown disposable collision energy, and prevent the car from drilling into the truck's bed, according to test results. The results of the simulation are used to propose improvement measures.

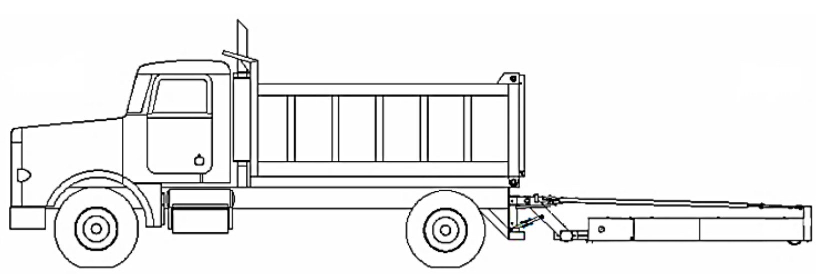

Figure 2.1. Truck Rear Impact Energy -Absorbing Device (Li, 2018)

(Xiaolong Ma et al., 2022) studied on model of Urban Freeway Rear-End Collision Risk (RCP) and Freeway Rear-End Collision Risk (F-RCR) is based on Generalized Pareto Distribution (GPD) and Multi-Layer Perceptron (MLP). Generalized Pareto Distribution (GPD) and Multi-Layer Perceptron (MLP) are the foundations of the suggested model of Urban Motorway Rear-End Collision Risk (RCP) and Motorway Rear-End Collision Risk (F-RCR). The F-RCR model is better suited when the vehicle distribution is unbalanced, the speed difference between neighboring lanes is significant, and the traffic volume is high. The RCP model exhibits continuous change and may quickly identify harmful scenarios. The framework presented in this study is transferable and usable in the motorway proactive traffic safety management system.

(Bennbaia et al., 2023) studied Hybrid Composite Plastic for Automotive Front Bumper Beam in order to reduce risk of injury and absorb impact energy, the bumper beam's protection is critical part for automotive bumper system. The design and testing of a composite-plastic hybrid light construction that was 3D printed with the intention of serving as a foldable energy absorber are presented in this paper. Three different 3D composite construction types were used in the study: printed thermoplastic, both printed thermoplastic and thermoplastic filled with foam are strengthened with Kevlar fiber composite. A strong option for energy absorption applications, the novel design showed great energy absorption capacity as well as a regulated and gradual failure mechanism.

(Dange et al., 2015) studied the characteristics of a front bumper beam on an automobile to enhance its crashworthiness in low-velocity collision. The United Nations Agreement Regulationno.42, 1994 was used to simulate the original bumper under condition impact. A modified SMC bumper beam was found to minimize stress distribution, impact force, and deflection, as well as increase the energy of elastic strain.

(Rambhad et al., 2020) A Reviewed on Design and Analysis of automotive Bumper Beam. The bumper beam is crucial for avoiding serious collisions and minimizing the number of occupant cars. This study examines the design, analysis, and performance of an automotive bumper beam in order to achieve the best design and material sustainability. Additionally, it examines the energy-absorbing mechanism in the front bumper beam and the functionally graded foam-filled bumper beam's crashworthiness design. It also considers the severity of injuries caused by car bumper impacts on pedestrians as well as the weight-saving possibilities of various materials.

(Beyene et al., 2014) The frontal and rear portions of a car serve as the bumper subsystem, which is responsible for absorbing energy during low-velocity impacts. The transverse bumper beam, which is typically formed of steel, is this subsystem's primary component. It appears that the designer is drawn in opposite directions while designing a vehicle subsystem for safety and lightness. Composite materials can be used to create some quite intriguing solutions. For the specific situation involving the front and rear bumpers, this essay analyses some potential other options.

(Maria Segui-Gomez., 2019) conducted a study entitled “Driver Air Bag Effectiveness by Severity of the Crash”. ”The goal of this analysis is to provide net effectiveness estimates of the driver-side air bag in preventing fatal and nonfatal injuries in frontal and near frontal crashes by the severity of the crash, while controlling for characteristics known to influence the frequency and severity of injuries, such as age and sex of the driver, vehicle size and mass, and safety belt use”. For this analysis, the data used was from the CDS years 1993-1996. The Abbreviated Injury Scale (AIS), Injury Severity Score (ISS), and Functional Capacity Index (FCI) were used to calculate the number of injuries and fatalities. A multivariate logistic regression was conducted. Analysis originally pertained to airbag deployment, but was also run about airbag presence and in both cases results were the same.

(Nazari and Nourozi., 2019) studied on Behavioral Analysis of Volvo Cars Instrument Panel during Airbag Deployment. Various component tests are to be performed in the sled environment, as opposed to a real vehicle, to save costs. Various modules are added to the sled once their behavior is verified by testing a simulation. LS-DYNA is used for explicit finite element simulations of the instrument panel (IP) in question with different airbag models. Verification has been achieved by the design of the experiment (DOE); with tests conducted to capture both the movements of the airbag housing and IP movements in response. These movements are broken down in various phases, facilitating implementation in the sled environment.

(Barbat et al., 2013) performed the study on the bumper and grille airbags concept for enhanced vehicle compatibility in side impact. Analytical and computational methods, including Finite Element models, were used to create the notion of deployable external airbags. Phase II ONLY included modifying airbag dimensions, pressure, and deployment procedures, as well as performing additional validation using a via sled test and creating the reaction surface for bumper airbag functionality. Because airbag deployment requires dependable, durable pre-crash sensors for the vehicle environment, the concept focuses on viable packaging, inflators, and reaction surface design.

(Yonghan ju et al., 2023) study about external air bag to support its commercialization, this article suggests a cost-benefit analysis of an external airbag and an autonomous emergency braking system. The National Automotive Sampling System/Crashworthiness Data System (NASS/CDS) data on traffic crashes was utilized to determine the safety performance. According to the findings, the external airbag system saves 46% of passengers with MAIS 3+ injuries and prevents 40% of fatalities. Depending on the situation, the benefit/cost ratios range from 0.496 to 0.509.

(Arbor, 2017) Investigated the Use of Adhesively-Coated External Airbag to Reduce Post-Impact Kinematics. By restricting flight or lowering rebound velocity, adhesive coated airbags can lessen the severity of secondary impacts. It is possible to overcome manufacturing obstacles such laminating onto fabric, release layers, packaging, deployment, and tack time. Adhesively covered airbags can lower exit velocity from main impact, according to modeling and prototyping.

(Alobaidan, 2021) Studied Sensors for airbag systems. This essay addresses a well-known idea that has been shown to be of utmost significance because it continues to save lives on a regular basis. An airbag system is the name for this idea. An automated passenger safety restraint system known as an airbag inflates automatically upon impact to protect the occupants. This issue involves ongoing research and development to improve the design, performance, and efficiency of this life-saving safety device. However, proper use and adherence to safety regulations are essential for any safety restraint system to be successful.

(Edytia and Darmawan ., 2021) investigated airbag is a technology in the automotive sector which was created to save the passenger from fatal risks in vehicle accidents. It is placed on the bumper of the vehicle with a high sensitivity sensor to provide information to the system. The ECU will send a signal to the squib inflator or igniter, which will generate heat to burn propylene airbags and produce nitrogen gas.

(Wook Lee et al.,2008) Investigated an External Explosive Airbag Model for an Innovative Inflatable Bumper (I-bumper) Concept In order to reduce kinetic energy from clashing automobiles before a body-to-body collision, the I-bumper design uses two exploding airbags. To lessen crash energy and peak impact force, a typical airbag type is employed. The I bumper system's ideal design is developed into an analytical model of the explosive airbag, which will be implemented in Matlab and verified with an LS-DYNA simulation. Also being included are design principles and practises.

(Tudruj and Tiechna., 2012) investigated the three-dimensional model of an airbag intended to shield a small city automobile from the impacts of collisions with other vehicles. The airbag is situated outside of the car near the front bumper. Results of airbag operation numerical simulations two different sorts of impediments are provided in the event of collision: a 200 mm-diameter circular pillar and a flat, vertical wall. The physical model that will be the focus of the simulation, together with its mathematical description and the numerical calculation method employed, are all presented in the paper.

(Driver et al., 2004) Airbags were first introduced in the early 1970's and since then, vehicles, as well as their safety features, have developed rapidly. Since model year 1998, all new cars have been required to have air bags on both driver and passenger sides (light trucks came under the rule in 1999). There are many safety features located within the vehicles found on the road today and many more advancements can be expected. However, while these "safety" features are great for protecting the passenger upon impact they can be very hazardous to rescuers, and possibly the passengers, while working to extricate the patients from the vehicle. The dangerous possibilities of airbags were demonstrated by the injuries sustained by two firefighters from Ohio during an extrication. Both rescuers were injured when the multiple airbags deployed during extrication, seriously injuring one of the rescuers.

(*Wonsuk Park*, n.d.2010)The frontal airbag in a vehicle is considered a supplemental restraint to the safety belt restraint system and is important in lowering measured injury assessment values for Anthropomorphic Test Devices (ATD) during vehicle crash testing. Neck injuries for the right front passenger occupant are especially sensitive to the passenger airbag (PAB) shape. Therefore, multiple sled tests and Computer Aided Engineering (CAE) simulations are required for PAB development to arrive at a balanced restraint system and achieve optimal performance for occupant injury metrics. The purpose of this study is to establish a design procedure and optimization process for passenger airbags by using CAE techniques to minimize development time. In this study, a design method to create a new baseline airbag is introduced. Surrogate sled CAE models were generated to make efficient use of computing resource availability. Validation of CAE surrogate models was performed using sled tests. A direct optimization method, not meta-model based, was developed for airbag shape optimization across multiple load cases. Parameterized airbag shape and morphing techniques were used in the optimization. The objective function is US-NCAP performance, however, major injury criteria from FMVSS208 (belted and unbelted) as well as airbag volume were used as constraint conditions. All optimization processes were automated, and airbag shape is optimized per objective functions and constraint conditions. Additionally, different optimization algorithms were compared to find the most efficient method for airbag design.

(Kim et al., 1998) A crash typically occurs within little more than 100 milliseconds (ms). A determination to deploy air bags must be made in the first 20 ms or so in order to get them inflated within about 50 ms, or before an occupant has moved forward more than about 12 cm (5 inches). This timing ensures that the face of the bag has come nearly to rest before the occupant encounters it. A vehicle occupant actually continues at the original vehicle speed until he or she begins to be restrained by the air bag and/or safety belts. The occupant then becomes coupled with the occupant compartment and decelerates at a rate approaching that of the vehicle.

(Factsheet, 2021) They need to inflate at an extremely fast rate in order to be fully inflated by the time a person's body begins to move in reaction to a collision. The bigger the airbag, the faster it has to inflate. In general, European airbags hold 35 liters of gas propellant and fully inflate within 25 milliseconds, which mean that they have to expand at anything up to 160 mph. American air bags, usually holding 60 liters of gas, have to inflate even faster. The area of space within the car taken up by the airbag as it inflates is known as the 'airbag deployment zone'. Sensors within the vehicle monitor the direction and severity of an impact and fire the airbag if the severity and direction warrants it. The impact should be greater than 20mph, and in a frontal direction. Rear end shunts should not fire the airbag. As the airbag module fires, it and the gas it generates are hot, so car occupants may suffer minor burns.

(Yurchenko et al., 2021) done the research on rapid evaluation of autonomous vehicles is necessary in emergency situations, especially for passenger safety. In order to offer 50L airbag inflation in less than 30–40 ms, a novel mechanism for driver airbags is created. A supersonic pulse jet and Prandtl-Meyer problem formulation are used in this procedure. The operability of the aspirated inflator is assessed utilizing pressure fields, high-speed video recordings, and aspiration ratio evaluation after experimental models are put to the test at varied pressures. At 1200 K, the average volume aspiration ratio is anticipated to quadruple.

(Hansae Cho et al., 2018) study about the PAB, a passenger airbag, that it needs to be deployed quickly because of the substantial space between the dashboard and the passenger. The PAB modeling procedure is however difficult and time-consuming. In this study, a feature-based CAD system that builds PAB CAD models and produces PAB FE models for collision analysis is proposed. In order to shorten modeling time and enable effective parametric design studies, the key points and widths of PAB are retrieved from the geometric features of the airbag.

(Bhasin, 2020) study on air bag in the modern era, that airbags are practically universal in automobiles. Numerous airbags are employed to lessen the harm caused by auto accidents. Road car accidents tend to decline when various airbag types are used. To stop the serious injuries that an auto crash might inflict, an airbag is deployed. In the case of an accident, the airbag will instantly begin to inflate. Most airbags are only intended for single usage. Discussing various airbag kinds, along with their uses and applications, is the paper's main goal.

(Bhasin, 2020) overviewed about airbags which have played a critical role in the tremendous rise in automotive safety over the past few years. These safety restraint devices, which include airbags, have prevented fatalities and created new demand for automobile safety. In order to maintain consistent and predictable behavior over time, the textile material used in airbags is crucial. The historical context, various fabric types, characteristics, and airbag finishing techniques are covered in this essay.

(Rohit Kothawale and Amit Chandan., 2020) study on vehicle external airbag system. The initiative is based on auto safety measures. It is motivated by the everyday driving observation of the accidents that happen around us, and occasionally even with us. Increase in traffic is a result of more automobiles on the road. Frequency of traffic accidents, notwithstanding significant progress made in that direction by the auto industry. The airbag system in cars needs some development, as it is seen, by improving the safety systems in the vehicles. Due to the airbag system failing, or the airbags failing to deploy, crashes frequently result in significant casualties. when necessary and the motorist sustains damage.
One of the sensor recommended on his study is ultrasonic sensors, An ultrasonic sensor is a piece of technology that uses ultrasonic sound waves to measure a target object's distance and then turns the sound that is reflected back into an electrical signal. Ultrasonic waves move more quickly than audible sound, or sound that humans can hear. The sensor's job in this system is to transmit the microcontroller the appropriate signal after detecting the presence of any object within a 50-meter range. An ultrasonic sensor's working diagram is displayed below.

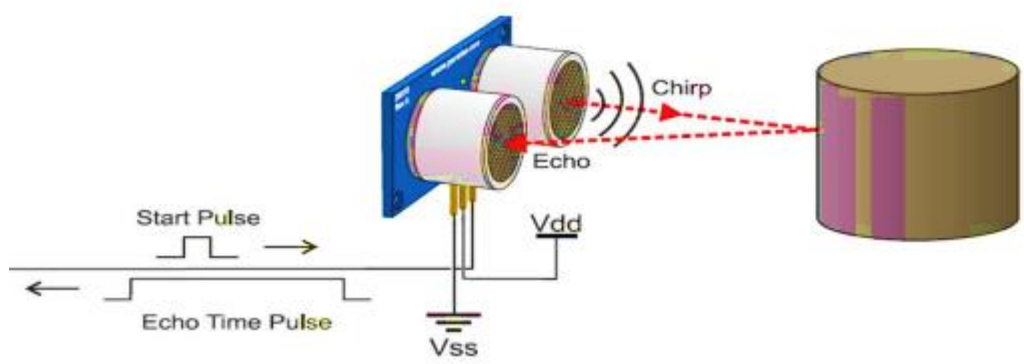

Figure 2.2 working diagram of an ultrasonic sensor (Rohit Kothawale and Amit Chandan., 2020)

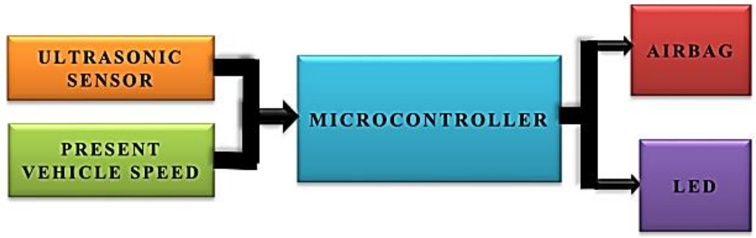

Figure 2.3 the function of the five blocks (Rohit Kothawale and Amit Chandan., 2020)

(Tasnim N. Shaikh et al.,2015) study on Airbags systems. Airbags are a vital safety feature that cushion passengers during collisions and protect them from interior objects like steering wheels and windows. The flexible fabric envelopes that make up these devices quickly expand in the event of a collision. While airbag efficiency is constantly being improved, appropriate use and adherence to safety regulations are essential for their success.

(Arun Kumar.S1 ,Madhu.S2, 2015) The airbag system, a piece of car safety technology, lessens the stress that the steering, windows, and dashboard components impose on the occupants during roll-over incidents. It lessens damage and gives the body protection. While there is still work to be done on developing features, the success of the airbag rests on its effective application and adherence to established guidelines.

2.4 Detail Review of Airbag Materials

(Jab Allah et al., 2019) his study describes a simulation approach for deploying vehicle airbags, with a focus on side-impact airbag deployment in out-of-position scenarios. The FE approach accurately records the airbag deployment process, which reduces passenger injuries and fatalities in car crashes.

The tensile specimens are made in different airbags (P: Peugeot, R: Renault, and VW: Volkswagen) with a length of 200 mm long and a width of 40 mm. Table 2.1 shows the airbag's mechanical characteristics.

Tensile tests were carried out using the Lloyd EZ20 universal testing equipment to ascertain the mechanical characteristics of the airbag material used in the test pieces. These tests are conducted using rectangular samples. The axial force and axial displacement acquired during a test are converted into stress and the strain to be used for the fabric material model. The continuous recording of the stress-strain data is performed during both the load and unload phases. A minimum of five samples are made to check the repeatability of the measurements. All the data is collected by using a PC-based data acquisition system and analyzed by commercial software.

Table 2.1. Mechanical properties of the airbag (D. Bend jab Allah et al., 2019)

Parameters	Values
Density (kg/mm3)	9.100E−07
Young's modulus (GPa)	2.500
Poisson's ratio	0.345
Thickness (mm)	0.150

Finite element model of airbag simulation: Numerical simulations of airbags use very complex techniques such as an orthotropic model to identify the mechanical behaviors during the airbag inflation and the fluid mechanics (gas flow) to describe the inflator gas flow (pressure gradient) and improve the representation of the pressures within the airbag. To model the airbag as an orthotropic model, three material constants have to be provided. Assuming a plane stress condition, the material constitutive equations are given by

$$\begin{Bmatrix} \sigma_1 \\ \sigma_2 \\ \tau_{12} \end{Bmatrix} = \begin{bmatrix} Q_{11} & Q_{21} & 0 \\ Q_{12} & Q_{22} & 0 \\ 0 & 0 & Q_{66} \end{bmatrix} \begin{vmatrix} \varepsilon_1 \\ \varepsilon_2 \\ \gamma_{12} \end{vmatrix} \tag{1}$$

Where σ is the normal stress and τ is the shear stress, the subscript refers to the principal material directions, i.e., the fill and warp directions. Also, ε and γ are the strain components. The material elastic constants Qij are given by the following equations:

$$Q_{11} = \frac{E_1}{1 - v_{12}.v_{21}} \ , Q_{12} = \frac{v_{12}E_2}{1 - v_{12}.v_{21}} = \ Q_{21} = \frac{v_{21}E_2}{1 - v_{12}.v_{21}}, Q_{22} = \frac{E_2}{1 - v_{12}.v_{21}}, Q_{66} = G_{12} \tag{2}$$

Where E_1 and E_2 are Young's modulus in the fill and wrap directions and G_{12} is the shear modulus of the fabric material. ν_{ij} is the Poisson ratio of the material. The gas exerts a pressure load on the airbag causing it to expand. This expansion puts the airbag under tensile stress lowering the expansion rate. In this study, heat conduction and heat transfer are not taken into account

Table 2.2. Physical and mechanical properties of the airbag D. Bend jab Allah et al. (2019)

Properties	Airbag					
	Peugeot		Renault		Volkswagen	
	P0	P90	R0	R90	VW0	VW90
Initial yield strength (MPa)	285	292	155	154	210	213
Young's modulus (GPa)	2.43	2.46	2.51	2.53	2.48	2.52
Poisson's ratio	0.341	0.346	0.349	0.342	0.345	0.346

2.4.1 Necessary components for installation

Finally, the researcher incorporated the visual alert system for the Arduino ultrasonic sensor. This allows visualizing whether we are near or far from an obstacle. With 3 LEDs (green, yellow and red) we can determine if we are far, near or in a danger zone. The following list shows all the necessary material.

Arduino UNO

Breadboard

Cables to make connections

3220 Ω resistors

1 green LED

1 yellow LED

1 red LED

4 Arduino Ultrasonic Sensor (HC-SR04)

1 buzzer

Ultrasonic sensor, mounting circuit

It is a very simple circuit. On the one hand, there is alerts, acoustic and visual, and on the other hand the ultrasound sensor. In the following diagram the connection can be observed.

Things to keep in mind: The resistors are 220 Ω and are placed in series with the LEDs. The Arduino ultrasonic sensor connects to two digital pins, one for the trigger and one for the echo or receiver. The Arduino buzzer connects to a PWM output.

[icon name = »exclamation-triangle» class = »» unprefixed_class = »»]

Try to put the Arduino ultrasonic sensor as close to the edge of the breadboard as possible.

2.4.2 Mounting Air Bag with Volkswagen Vehicle

The total distance of pre-crash consideration for car at rear end is 450mm. This is standard for any hatch back and sedan batch cars according to Society of automotive engineering SAE. There for the air bag mounting place should not exit out of this distance limited. Figure 3.11 shows free crash lengths for the rear impact.

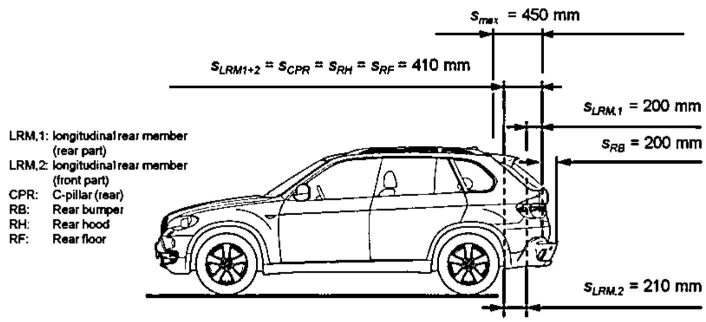

Figure 2.4 Free crash lengths for the rear impact (Andreas Meier et al, 2014)

2.5 Numerical Simulation Using Ansys LS DYNA

The most popular explicit simulation program in the world, Ansys LS-DYNA, can simulate how materials react to brief bursts of intense loading. With its numerous components, contact formulas, material models, and other controls, complex models can be simulated while maintaining complete control over the problem's specifics.

Incremental Time Step

Nodal Mass spring system

Rewrite the forces in terms of the nodal displacements:

$$T = -f_{1x} = k(u_2 - u_1) \quad \Rightarrow \quad f_{1x} = k(u_1 - u_2)$$

$$T = f_{2x} = k(u_2 - u_1) \quad \Rightarrow \quad f_{2x} = k(-u_1 + u_2)$$

$$\begin{bmatrix} k & -k \\ -k & k \end{bmatrix}\begin{bmatrix} u_1 \\ u_2 \end{bmatrix} - \omega^2 \begin{bmatrix} m_1 & 0 \\ 0 & m_2 \end{bmatrix}\begin{bmatrix} u_1 \\ u_2 \end{bmatrix} = \begin{bmatrix} 0 \\ 0 \end{bmatrix} \tag{3}$$

$$\mathrm{Det}\begin{bmatrix} \mathrm{k} - \mathrm{m}_1\omega^2 & -\mathrm{k} \\ -\mathrm{k} & \mathrm{km}_2\omega^2 \end{bmatrix} = 0 \tag{4}$$

$$\omega = \sqrt{\frac{\mathrm{k}(\mathrm{m}_1 + \mathrm{m}_2)}{\mathrm{m}_1 \mathrm{x} \mathrm{m}_2}} \tag{5}$$

2.6 Summary of review

The examined studies' overall concept investigates design elements for bumper structure, such as shape, material, and impact situations. They compare traditional metals and recommend a high-strength SMC bumper. The research also looks into counts and thickness for car front bumper beam design, with the goal of enhancing crashworthiness in low-velocity impacts. The energy-absorbing property of the airbag is investigated, and the deployment process is carefully captured.

Furthermore, driver Air Bag Effectiveness by Crash Severity." The analysis of driver-side air bags provides net effective estimates for preventing fatal and nonfatal injuries in frontal and near frontal crashes based on the severity of the crash. Controlling for parameters known to influence the frequency and severity of injuries, performed on Bumper and Grille Airbags Concept for Enhanced Vehicle Compatibility in Side Impact. Analytical and numerical methodologies, as well as hardware testing, were employed to support and develop the deployable external airbags concept.

2.7 Research gap

- The research gap in earlier studies on rear vehicle crash analysis is focused on bumper material optimization and design changes for low-speed crashes. However, research on moderate and high speed effect analyses is lacking.
- The air bag system proposed in the preceding study demonstrates that most researchers were primarily concerned with testing and effective implementation of the existing air-bag system, which is only employed in the vehicles inside, front, and sides. However, the original idea in this research work is to integrate the notion of an airbag system to the back area of the vehicle as safeguard against crashes. Because rear impact is common in metropolitan areas, particularly during traffic jams. In this thesis, the predictable output from the concept of an airbag system combined at the rear bumper portion is to boost energy absorption capacity, reduce vehicle body deformation during smash, and reduce vehicle body stress concentration level at high-speed impact.
- For this type of external rear air bag system, the deployment should be carefully designed based on coming vehicle speed relative to the inflation speed of the air-bag, with a fast filling valve strategy within a millisecond. After assessed of all this work, a conclusion has been made that, the protection of the passenger car is increased.

CHAPTER THREE
MATERIAL AND METHOD

3.1 Introduction

Materials and methods are the most crucial heading to evaluate the overall quality of any study distribution product-, because they explain to readers what processes, approaches, designs, and treatments were used in the research, allowing us to duplicate the studies. A thorough review of the literature aided in the selection of working materials, research methods, and simulation software. The designs in this study were created using a suitable working material selection.

3.2 Materials used

This may include testing instruments, technical equipment, or other materials used during research. The following table 3.1 shows the materials used on proposed thesis.

Table 3.1. Materials used

Characteristics of material	Materials Name
Simulation Software Tool	Ansys LS DYNA Software
Computer	Minimum Processor Unit, 32 RAM
Flash Card	64GB
Flexible Meter Tape	Meter Tape

3.3 Methodology

This section describes the methodology used to completed objectives of the research. It means the section involves studying the methods used in the theories or principles behind them, to develop an approach that matches the objectives. The work flow or methodology summary is described as, Literature Review, Concept on Rear air bag system, Air bag shape Design with 3D Model, Numerical Simulation Using Ansys LS DYNA, Designed shape of Air bag, 3D Model of Car, Car with Final shape of air bag assembly, Numerical Simulation of assembled system, Summary and conclusion. Figure 3.1 below shows the detail of work flow on this thesis.

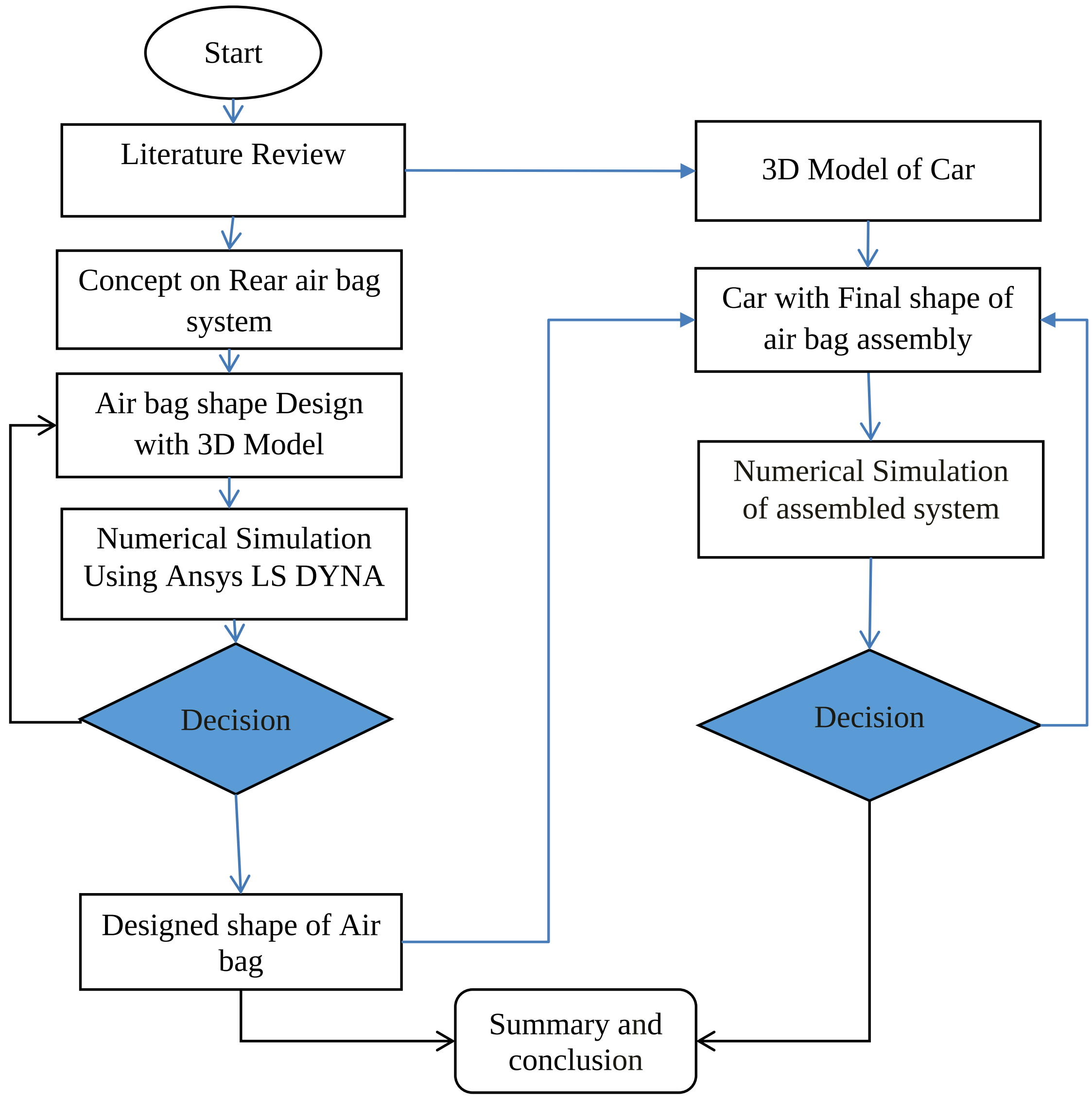

Figure 3.1. Methodology of the study

3.3.1 Data Collection (Primary)

For this kind of analysis, extensive vehicle data is obviously necessary. So, utilizing model numbers obtained from motor insurance companies, the researcher made an effort to gather primary data. The two randomly selected vehicle data are presented in tables 3.2 and 3.3 due to the fact that many cars are sedans, hatchbacks, and pickups that are prominent and well-known throughout the nation.

Vehicle Specification

The specification of the model of vehicle used for the model and design analysis is labeled in table 3.2,

Table 3.2. Pick-up Car Specifications

Parameters	Data Value
Gross Weight (kg)	4500
Maximum vehicle Speed (m/s)	50
Maximum brake Torque (SAE certified)	515Nm @ 4200rpm
Six-speed automatic (6.6L gas)	4.03, 2.36, 1.53, 1.15, 0.85 and 0.67
Displacement	8,127 cc

Table 3.3. Volkswagen Specifications

Parameters	Data Value
Gross Weight (kg)	1650
Maximum vehicle Speed (m/s)	50
Maximum brake Torque (SAE certified)	450Nm @ 4500rpm
Six-speed automatic (4L gas)	3.25, 2.36, 1.53, 1, 0.8 and 0.65
Compression Ratio	16.0:1

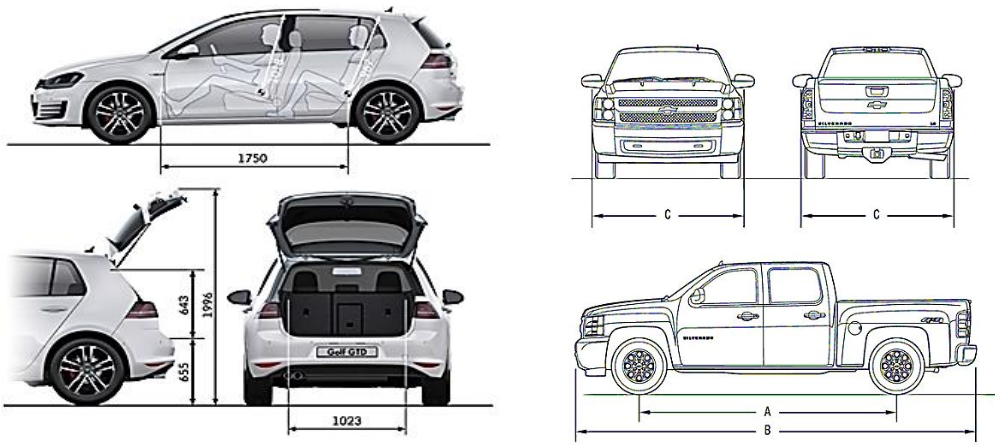

(a) (b)

Figure 3.2 (a) & (**b**) Volkswagen car and Cholveret Silverado 2500 pick up

The automobiles selected for this study purpose is pick up Cholveret Silverado 2500, 2018 and the hatchback Volkswagen. The bumper of the existing model had steel bumper.

Material for bumper

Many existing automobile bumpers are made of AISI 1006 steel, which contains primarily carbon as an alloying ingredient and is known as carbon steels. They have 0.4% silicon and 1.2% manganese. Carbon steels also contain trace amounts of chromium, nickel, aluminum, copper, and molybdenum. AISI 1006 carbon steel structures are mostly soft and ductile and selected one. More information about AISI 1006 carbon steel may be found in the table below (Dange et al., 2015). Table 3.4 shows properties of steel.

Table 3.4. Properties of Steel 1006

Property	Value
Density	7896 Kg/m3
Yield Strength	350 MPa
Hardening Constant	275 MPa
Hardening Exponent	0.36
Strain rate constant	0.022
Melting Temperature	1538 0C
Shear Modulus	81.8 GPa
Specific Heat	452 J/Kg

3.3.2 Material properties of the body of vehicles

The development of several car body variants challenges established development processes and requires the introduction of enhanced knowledge-based 3D-CAD methods. In addition, the need for fuel consumption reduction leads to the amplified application of lightweight technologies in automotive body design. This comprises both, lightweight materials and new design solutions including joining technology. Exemplary, the potential for weight reduction with high-strength steel is about 10 % about conventional steel. A whole carbon fiber body weighs roughly 50% less than a comparable standard steel body in the same vehicle class, and aluminum indicates possibilities between 30% and 40% according to (Hirz & Rossbacher, 2017)

In this thesis, the materials used to test the vehicle are conventional steel (mild steel) for both automobiles, with the strength-to-weight ratio and energy absorption capabilities for the selected car's own material. Table 3.5 shows mechanical properties of conventional steel.

Table 3.5. Mechanical Properties of Conventional Steel

Properties	Values
Young’s Modulus	200Gpa
Poisson’s ratio	0.31
Density	7750kg/m3
Tensile Yield Strength	320Mpa
Tensile Ultimate Strength	400Mpa

3.3.3 3D model pick-up of front bumper beam

This section presents the geometrical development of the front Bumper of Pick up Car model released 2018 vehicle system with steel-made bumper. Here the conventional front bumper model has been referred from the Chevrolet Silverado pick up car model released in 2018 vehicle and actual dimensions are measured and compared with the literature before proceeding to the geometrical development in the space claim 3d design of ANSYS Work bench. The standard dimension of pick-up model released in 2018 is depicted in the figure below and these values are utilized to perform the 3D model on ANSYS space claim 3d design.

Geometrical overall dimensions of the Conventional Front Bumper Model is,

1. Length of the bumper =1200 mm
2 .Width of the bumper = 300mm
3. Thickness of the conventional steel bumper beam = 5mm
4. Height of the bumper = 500mm

From the dimensional value the 3D modeling and geometrical configuration are presented in the figure 3.2.

Figure 3.3. Bull bar Bumper

3.3.4 Data Collection (Secondary Data)

Theory of Airbag

In 1998, the NHTSA mandated two frontal airbags to provide maximum protection in head-on accidents. The crash sensor, a steel ball, detects rear-end crashes and activates the airbag. The sensor activates an electrical circuit, resulting in the production of nitrogen gas (N_2), which fills a nylon or polyamide bag and propels the front face at speeds ranging from 150 to 250 miles per hour. The airbag must deflate by the time the tow vehicle collides with it, lowering its internal pressure. The NHTSA's crash sensor inflates the airbag when an impact force of 10-15 mph is detected, using data from an accelerometer integrated into a microchip. This guarantees that the airbag is effective in averting head-on crashes and protecting passengers and drivers (Alobaidan, 2021). Figure 3.3 shows Sensor and airbag operating systems in the car.

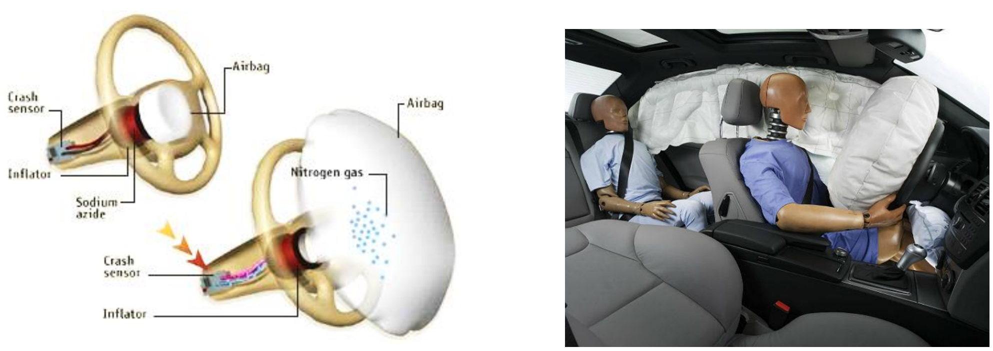

Figure 3.4. Sensor and airbag operating systems in the car

Think of the airbag inflation system as a solid rocket booster. The airbag ignites a solid propellant which burns very rapidly and creates a large volume of gas to inflate the bag. The airbag actually bursts from its storage at up to 200 mph. A second later the nitrogen gas dissipates through small holes in the bag which completely deflates it. Figure 3.4 shows Detail of the air-bag inflation device.

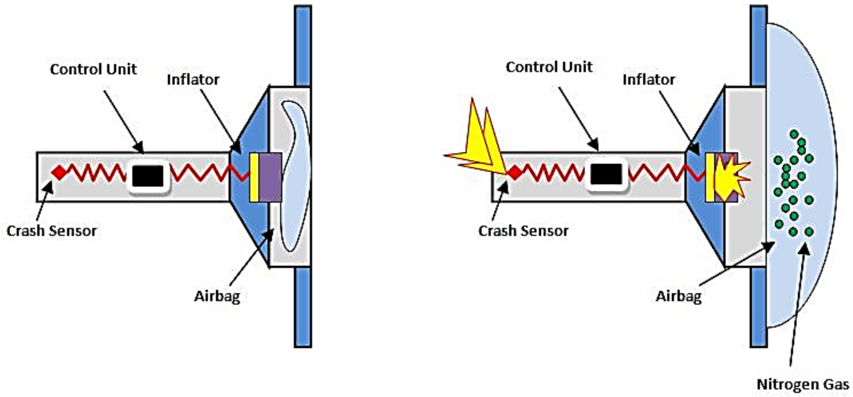

Figure 3.5. Detail of the air-bag inflation device

From impact to full deployment, a driver's airbag takes approximately 30 - 40 milliseconds (0.030 - 0.040 seconds) - an eye blink takes 0.2 seconds - while the larger passenger airbag takes 40- 80 milliseconds to inflate. Side impact airbags must inflate and deploy much quicker because there is no crumple zone and very little space between the passenger and the door. Side-collision detection must take place within 3 milliseconds (0.003 seconds) and complete deployment of the side or curtain airbags must happen within 10 - 15 milliseconds (0.010 - 0.015 seconds).

Chemical Reactions Used to Generate the Gas

During head-on crashes, the airbag's gas generator, which is composed of NaN_3, KNO_3, and SiO_2, conducts three chemical processes. These processes generate nitrogen gas (N_2), which fills the airbag and converts sodium metal (Na) to the innocuous sodium and potassium silicate. At 300oC, sodium azide (NaN3) decomposes, releasing sodium metal and nitrogen gas (N_2). The reaction between KNO_3 and SiO_2 removes sodium metal, turning it to a harmless substance. This procedure is carried out in commercial airbags using sodium azide, a hazardous chemical.

$$2\mathrm{NaN}_{3(\mathrm{s})} = \mathrm{Na}_{\mathrm{s}} + 3\mathrm{N}_{2(\mathrm{g})}$$

It is the nitrogen gas that inflates the airbag to provide a safety cushion for the passengers in the car. Some airbags, like the one shown below can deploy in 0.015-sec for high-speed crashes and 0.025-sec for low-speed crashes. All and all, the deployment and inflation processes are quicker than a blink of an eye. We guess you can say this is a pretty quick reaction.

For isotropic materials within the elastic region, it is possible to relate Poisson's ratio (ν), Young's modulus of elasticity (E), and the shear modulus of elasticity (G).According to (Volz K et al 2011) and (Romeo M. Flores.2014). Table 3.6 shows properties of Nitrogen gas

Table 3.6. Properties of Nitrogen gas.

Density (Kg/m3)	1.1606
Shear Modulus (Gpa)	1.37
Bulk Modulus (Gpa)	2.44
Poison Ratio for gas(v)	0.5
Molecular Weight (g/mol)	28.02
Specific heat volume C_v	701
Specific heat volume C_p	1001
Specific heat constant (k)	1.4
Gas Constant –R (J/kg K)	296.80

Types of Air Bags

Air bags are designed to protect occupants during crashes, with three types: driver-side air-bag, passenger side air-bag, and side impact air-bag. Frontal air-bags absorb kinetic energy, allowing occupants to rest without injury. Side impact air-bags exert force and move occupants away from the crash area, providing head protection during side collisions.

Dynamics theory of Air bag System Design

An estimate for the pressure required to fill the airbag in milliseconds can be obtained by a simple mechanical analysis shown in the calculation below. When the airbag inflates during a collision, the front face of the airbag begins at rest (v_i = 0.00 m/s) and travels a distance (x) equals to the thickness of the fully inflated airbag. If the front face travels at 89.4 m/s by the end of the inflation (v_f), and the thickness of a fully-inflated airbag is 40.0 cm, what is the acceleration of the front face. The airbag's acceleration (a) can be computed from one of the Equations of Linear Motion encountered in a basic physics text: When Chemical Reactions to Generate the Gas to Fill an Airbag start Decomposition of Sodium Azide (NaN_3) Reactions to Remove Harmful Products.

Ideal-Gas Law

$$PV = nRT \tag{6}$$

To Estimate this Pressure for Fill an Airbag the terms must considered are Acceleration, Force, and Pressure. Airbags Decrease the Force Acting on the Body by Spreading the Force over a Larger Area. The airbag's acceleration (a) can be computed from one of the Equations of Linear Motion encountered in a basic physics. What is the force exerted on the front face of the airbag that can cause this acceleration. The force can be calculated using Newton’s Second Law of Motion, Pressure is defined as the force exerted by a gas per unit area (A) on the walls of the container, so the pressure (in Pascals) in the airbag immediately after inflation can be determined using the force and the area of the front face of the airbag (the part of the airbag that is pushed forward by this force).

The amount of gas needed to fill the airbag at this pressure is then computed by the ideal-gas law. Note that the pressure used in the ideal gas equation is absolute pressure. Therefore, the absolute pressure inside the bag is greater than the gauge pressure.

Absolute pressure = Gauge pressure + atmospheric pressure

The airbag's absolute pressure P, its internal area A_o, the loads F on it, and the atmospheric pressure P_o are all related to one another.

$$F = A_O(P - P_O) \tag{7}$$

The variation law solves the gas state equation when the load changes the airbag's thickness, causing corresponding changes in its volume and internal pressure:

$$P = P_O\left(\frac{V_O}{V}\right)^n \tag{8}$$

Where V stands for the volume of the airbag at any location, Po for the absolute pressure of the volume of the airbag at static equilibrium, V_o for the volume of the airbag at static equilibrium, and n for the polytrophic index. The gas state changes near the adiabatic process when there is an impact; therefore, n = 1.4; otherwise, accept n = 1.33 for the sake of this research study. When there is no impact, n = 1. The simulated vehicle is moving at 50 m/s. The air bag springing is stiff, as follows:

$$k = \frac{dF}{dx} = \frac{A_O d(P - P_a)}{dx} + \frac{dA_O(P - P_a)}{dx} \tag{9}$$

$$k = (P - P_a)\frac{dA_O}{dx} - A_O n P_o \frac{{V_O}^n}{V^{n+1}}\frac{dV}{dx} \tag{10}$$

Where,

$$\frac{dA_O}{dx} = 0, \qquad\qquad \frac{dV}{dx} = -A_O$$

$$k = -A_O n P_o \frac{{V_O}^n}{V^{n+1}}\frac{dV}{dx}$$

Take into account the airbag's static equilibrium position. It is possible to measure spring stiffness in a static equilibrium position:

$$k_o = {A_O}^2 n P_o \frac{{V_O}^n}{{V_O}^{n+1}} = \frac{{A_O}^2 P_o n}{V_O} \tag{11}$$

The dynamic force applied by internal gas flow of air bag is,

$$F = \sum F = ma = m\frac{dv}{dt} = m\frac{dv}{dt} = m\frac{d^2x}{dt^2} \tag{12}$$

$$v = \frac{dx}{dt} => \quad a = \frac{dv}{dt} = \frac{vdv}{dx}$$

$$a = \frac{vdv}{dx}$$

$$F = m\frac{vdv}{dx} => Fdx = mvdv \tag{13}$$

The work done by flowing gas through air bag is given by

$$dU = \int Fdx = \int -kxdx = -\frac{1}{2}kx^2 \tag{14}$$

The above equation (12&13) become equalized, at energy level which is internal energy of air bag become equal with the kinetic energy of moving front face of air bag.

$$\int Fdx = m\int vdv = \int kxdx = \frac{1}{2}kx^2 \tag{15}$$

$$KE = U_e = \frac{1}{2}mv^2 = \frac{1}{2}kx^2$$

Calculating the air mass flow rate for the airbag inflator

The net external force on a constant mass object obeys Newton's second law, F_{net} external = ma. The most straightforward way to approach the concept of average force is to multiply the constant mass times the average acceleration, and in that approach the average force is an average over time. Another approach that is valuable for assessing the impact force in high speed collisions is to use the impulse of force. When you strike a golf ball with a club, if you can measure the momentum of the golf ball and also measure the time of impact, you can divide the momentum change by the time to get the average force of impact. This average force is also an average over time.

$$kdx = -A_O nP_o \frac{{V_O}^n}{V^{n+1}} dV = \frac{1}{2}v\sqrt{mk} \tag{16}$$

$$\frac{V^{n+1}}{dV} = -2A_O nP_o \frac{{V_O}^n}{v\sqrt{mk}}$$

$$\int \frac{dV}{V^{n+1}} = \frac{v\sqrt{mk}}{-2A_O nP_o {V_O}^n}$$

When the kinetic energy of moving particle is converted into potential or internal energy of restrain part (air bag). The equation of stiffness can be determined as,

$$KE = \frac{1}{2}mv^2 = \frac{1}{2}kx^2$$

$$F = \left(\frac{mv^2}{x}\right)$$

In order to evaluate air bag gas mass flow overtime, it is possible to use substituted equation with stiffness.

$$\int \frac{dV}{V^{n+1}} = \frac{\frac{mv^2}{x}}{-2A_O n P_o {V_O}^n} = \frac{\frac{mv^2}{vt}}{-2A_O n P_o {V_O}^n} = \frac{mv}{-2A_O nt P_o {V_O}^n}$$

$$V = V_O \left[\frac{2tA_O P_o}{mv}\right]^{\frac{1}{n}}$$

$$\frac{V}{t} = \frac{V_O}{t}\left[\frac{2tA_O P_o}{mv}\right]^{\frac{1}{n}} = \frac{V_O}{t^{1-\frac{1}{n}}}\left[\frac{2A_O P_o}{mv}\right]^{\frac{1}{n}} \tag{17}$$

The relationship between mass flow rate and volume flow rate is given by the following equation.

$$A_c u = \frac{\dot{m}}{\rho} = \frac{V}{t} \tag{18}$$

Volume term is given by,

$$\frac{\dot{m}}{\rho} = \frac{V}{t} = \frac{V_O}{t^{1-\frac{1}{n}}}\left(\frac{2A_O P_o}{mv}\right)^{1/n}$$

$$\dot{m} = \frac{\rho V_O}{t^{1-\frac{1}{n}}}\left(\frac{2A_O P_o}{mv}\right)^{1/n} \tag{19}$$

$$\dot{m} = \left(\frac{V_O \rho}{t^{1-\frac{1}{n}}}\right)\left(\frac{2A_O P_o}{mv}\right)^{\frac{1}{n}} \tag{20}$$

The parametric Value for Air Bag Inflation mass flow determination is described in the table 3.3.

Air bag Inflation time

When polytrophic number is equal to 1 the initial starting time of inflator can be determined as,

$$\dot{m} = \left(\frac{V_O \rho}{t^{1-\frac{1}{n}}}\right)\left(\frac{2A_O P_o}{mv}\right)^{\frac{1}{n}}$$

$$m_a = \left(\frac{V_O \rho}{t^{-\frac{1}{n}}}\right)\left(\frac{2A_O P_o}{mv}\right)^{\frac{1}{n}} = \rho V = \left(\frac{V_O \rho}{t^{-\frac{1}{n}}}\right)\left(\frac{2A_O P_o}{mv}\right)^{\frac{1}{n}}$$

$$V = V_O \left(\frac{2A_O P_o t}{mv}\right)^{\frac{1}{n}}$$

Total distance that can rear vehicle moved with addition to crash zone displacement is,

$$S = vt_i + vt_d + vt_a = vt \tag{21}$$

$$t_f = (t_d + t_a) = t - t_i \tag{22}$$

Number of time step

$$N = \frac{t^{1-\frac{1}{n}}}{\Delta t} = \frac{(t - t_i)^{1-\frac{1}{n}}}{\Delta t} \tag{23}$$

From the above equation of initial inflator starting time, as speed of impactor increase the starting time become decrease to make compensating of instant impacting period. The conservation of mass is a fundamental concept of physics. Within some problem domain, the amount of mass remains constant; mass is neither created nor destroyed. The mass of any object is simply the volume that the object occupies times the density of the object. For a fluid (a liquid or a gas) the density, volume, and shape of the object can all change within the domain with time and mass can move through the domain. The conservation of mass (continuity) tells us that the mass flow rate m_{dot} through a tube is a constant and equal to the product of the density r, velocity V, and flow area A. Figure 3.5 shows Conservation of mass in diverging tube cal., 2019).

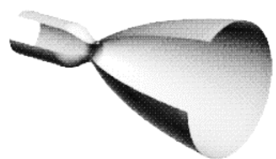

Figure 3.6 Conservation of mass in diverging tube (cal., 2019)

$$\dot{m}_a = \rho\left(\frac{2A_O {V_O}^n P_o}{kvt}\right)^{\frac{1}{n}} = \left(\frac{V_O \rho}{t^{1-\frac{1}{n}}}\right)\left(\frac{2A_O P_o}{mv}\right)^{\frac{1}{n}} \tag{24}$$

$$\dot{m}_t = C_d A_{or} P_{atm} \sqrt{kRT}\left[\left(\frac{2}{k+1}\right)^{\frac{k+1}{2(k-1)}}\right] \tag{25}$$

$$\dot{m}_a = \dot{m}_t$$

From the conservation equation orifes cross sectional area can be obtained as the following equation. The orifes area must be determined at maximum flow rate over the entire time step. From the time step graph the maximum mass flow time is first time step.

$$A_{or} = \frac{\left(\frac{V_O \rho}{t^{1-\frac{1}{n}}}\right)\left(\frac{2A_O P_o}{mv}\right)^{\frac{1}{n}}}{C_d P_{atm} \sqrt{\frac{k}{RT}}\left[M\left(1 + \frac{k-1}{2} M^2\right)^{-\frac{k+1}{2(k-1)}}\right]} \tag{26}$$

3.3.5 Sizing and Selection of Air Bag filling Valve

a) Determination of Mach number (M)

Mach number is a dimensionless quantity in fluid dynamics representing the ratio of flow velocity past a border to the local speed of sound. It can represented by

$$M = \frac{v}{c} = \frac{90}{686.4} = 0.2623$$

$$\text{Where,}\quad c = \sqrt{kRT}$$

Where, c is the speed of sound represent the distance travelled per unit of time by a sound wave as it propagates through an elastic medium. And for the typical airbag deployment speed is between 100 and 200 mph.

Automotive airbags are subjected to extreme temperatures (up to 900°C) during deployment which is achieved by using pyrotechnic inflators. Although the airbag fully inflates within a few milliseconds, the heat often causes physical damage to the airbags fabric and seams in this short period of time.

$$A = \frac{\left(\frac{0.0011577*1.16}{0.00000025^{0.285}}\right)\left(\frac{2*1.16*101000}{2*90}\right)^{\frac{1}{1.4}}}{0.9*101000\sqrt{\frac{1.4}{296.8*1173}}\left[0.2623\left(1+\frac{1.4-1}{2}0.2623^{2}\right)^{-\frac{1.4+1}{2(1.4-1)}}\right]} = 0.01m^{2}$$

Then the selected air bag based on valve opening cross sectional area is become $0.01m^2$. Figure 3.6 shows fast airbag filling valve.

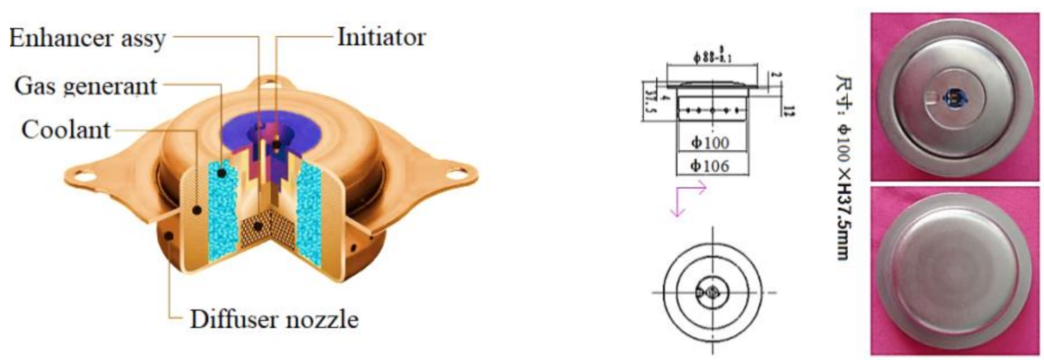

Figure 3.7. Fast Air bag filling Valve

3.3.6 Sensor Selection for Air Bag inflation

The main purpose of the Sensor is high precision measurement of speed and traveling distance of the vehicle relative to ground (automotive and railroad application) and speed and length of objects moved relative to the sensor (industrial application). Using Ultrasonic Sensors for Distance Measurement, also known as Sonar sensors, are among the most common distance measuring sensors, as they measure distance to objects by transmitting high-frequency ultrasonic waves. Ultrasonic Sensor Module Distance Measuring Meter Ranging Sensor can be from 1cm-600cm Adjustable Relay Output with Probe and Display 12V/24V DC. The basic principle behind the working of ultrasonic sensor is to note down the time taken by sensor to transmit ultrasonic beams and receiving the ultrasonic beams after hitting the surface. Figure 3.7 shows Ultrasonic beams

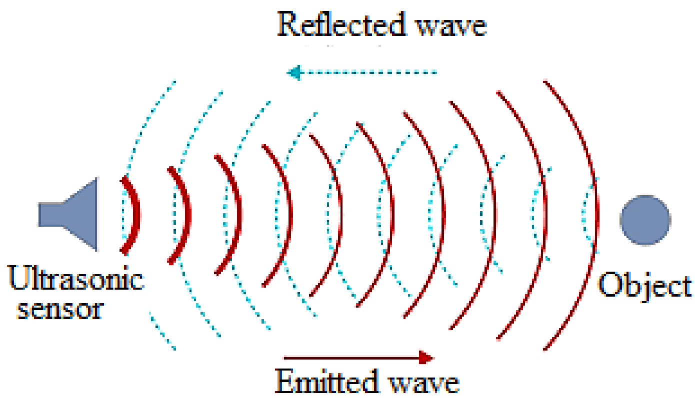

Figure 3.8. Ultrasonic beams

The distance can be calculated with the following formula:

$$L = 1/2 \times T \times C$$

Where L is the distance, T is the time between the emission and reception, and C is the sonic speed. (The value is multiplied by 1/2 because T is the time for go-and-return distance)

Selection criteria for Ultrasonic sensor

Choosing the ideal sensor depends on numerous variables, including:

- The measurement application
- The distance of the object being measured
- The output requirements
- The environmental conditions

In this project, the widely available HC-SR04 Ultrasonic Sensor is used. The HC-SR04 Ultrasonic Range Sensor Features has described below.

If a sensor is too close to an object, it may not be able to measure the distance accurately. If a sensor is too far from an object, it may not detect the object at all. The sensor chosen for a distance measurement application must be properly rated for the expected minimum and maximum measurement distances. Factors to consider when determining the useful operating range required (i.e., the material window) include: Table 3.7 shows HC-SR04 Ultrasonic Sensor.

The HC-SR04 Ultrasonic Range Sensor Features

Table 3.7. HC-SR04 Ultrasonic Sensor

Parameters	Characteristics value
Input voltage	5V
Current draw	20mA (Max)
Digital output	5V
Digital output	0V (Low)
Working temperature	-15°C to 70°C
Sensing angle	30° Cone
Angle of effect	15° Cone
Ultrasonic frequency	40kHz
Range	2cm - 400cm=0.2m - 4m

Table 3.8. HC-SR04 Ultrasonic Sensor Size

Dimensions of selected Ultrasonicsensor device	**Size**
Length	43mm
Height	15mm
Centre screw hole distance	40mmx15mm
Screw hole diameter	1mm (M1)
Transmitter diameter	8mm

3.3.7 Installation position adjusted for sensor

The following figure shows the sensor installation position for air bage inflation.

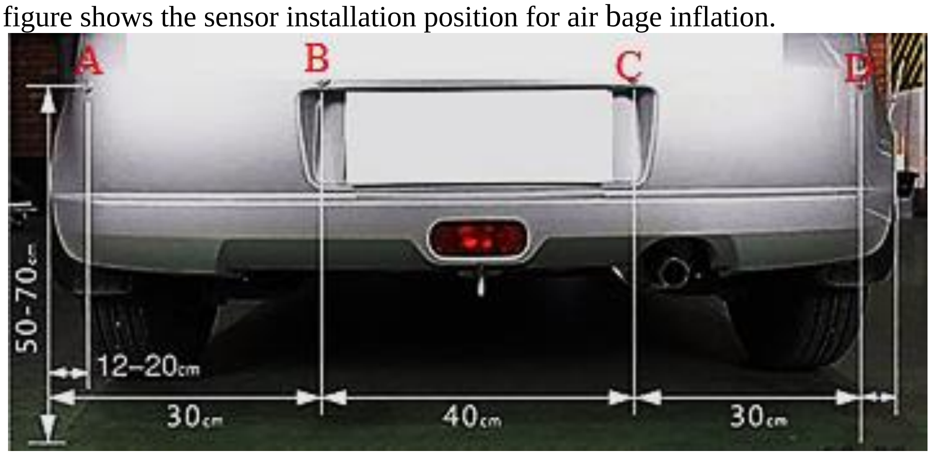

Figure 3.9 Sensor Installation position

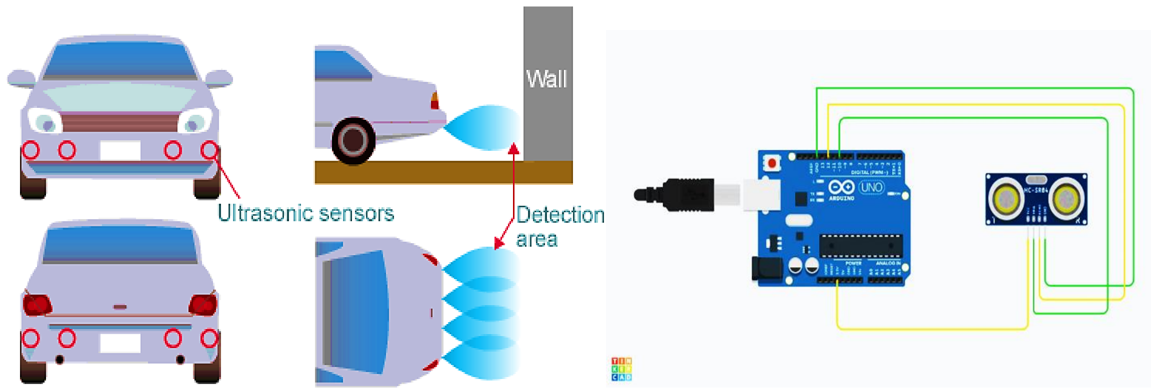

Figure 3.10 working of ultrasonic sensor on vehicle

3.3.8 Programming the Arduino ultrasonic sensor to measure distance

It began with the programming portion. The first is a succinct explanation of our goals. This will make it easier to state the overall issue and then divide it into more manageable chunks. Computational thinking, which incorporates logic, analysis, patterns, automation, and generalization, is what this is. The idea comes from parking systems, which detect objects using ultrasonic sensors and issue warnings via light and sound signals. As a result, the first division has already been completed: obstacle detection and sound and light alarms.

Threshold 1: it is in the green zone from 30 cm to 20 cm.

Threshold 2: it is in the yellow zone, from 20 cm to 10 cm.

Threshold 3: it is in the red zone, less than 10 cm.

[icon name = »exclamation-triangle» class = »» unprefixed_class = »»]

It is important to know the operating range of the ultrasound sensor. It normally ranges from

3.4 Concept on Rear air bag system

On this research the concept of air bag on rear bumper system is started from material properties of bag. Airbag textiles must be flexible and strong enough to bear explosive charge and impact loads during high-speed deployment. Because of its energy absorption capacity and ageing characteristics, Nylon 6, a material with high specific strength, abrasion resistance, and toughness, is the ideal material. This study emphasizes the significance of selecting the appropriate material for airbags during the selection stage. The two basic alternative material has been described in the following table 3.8 (D. Bend jab Allah et al., 2019). Table 3.9 shows Properties of Nylon 66 and Polyester.

Table 3.9. Properties of Nylon 66 and Polyester.

	Nylon 66	Polyester
Density (Kg/m^3)	1140	1390
Specific heat capacity (kJ/kg/K)	1.67	1.3
yield strength (MPa)	213	27.0
Young's modulus (GPa)	2.52	0.92
Poisson's ratio	0.35	-0.65
Melting point (° C)	260	258
Point of softening (° C)	220	220
Melting energy (kJ/kg)	589	427

Air bag for Rear bumper portion system

During a collision, air bag systems absorb kinetic energy from the vehicle, minimizing body deformation. The rear bumper beam functions as an outside air bag system, boosting energy absorption capacity and decreasing mortality rates. To create a successful bumper and improve collision performance, technological advancement is required. Extending the rear end during or before a collision would have a substantial impact on the crash energy absorption system.

3.5 Conceptual Design of Air bag shape with 3D Model

Conceptual design is a framework for establishing the underlying idea behind a design and a plan for how it will be expressed visually. It includes the design of interactions, experiences, processes, and strategies. It is the first or a very early phase of the design process. In this thesis conceptual design phase explore ideas for the research using a variety of tools including drawings, physical models and 3d modeling, preliminary ideas and parameters used. Therefor the following figure shows bumper with air bag considered at the rear of the vehicle. Figure 3.10 shows 3d model of bumper and Concept of airbag Shape.

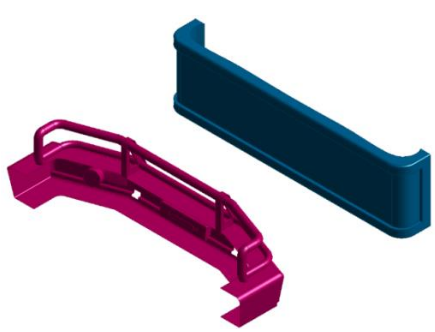

(a)

Figure 3.11.3d model of bumper and Concept of airbag Shape

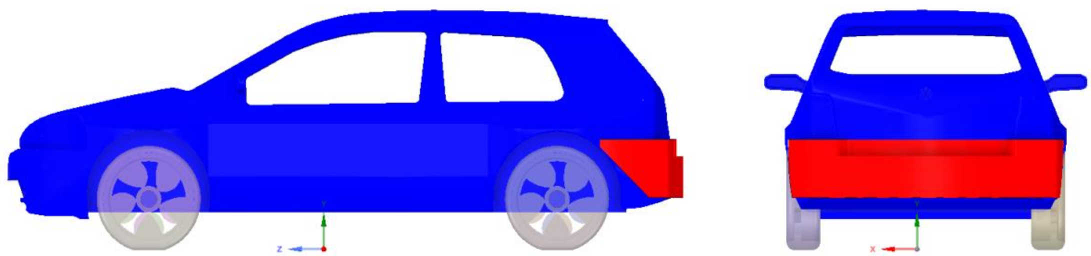

Figure 3.12 Vehicle with designed air bag mounted at rear

3.5.1 Parametric of air bag Design

Parameter design is a process that seeks to set main factors so as to achieve a response objective (Maximum, Minimum, Target) while at the same time allowing subsidiary factors to vary in a "customary" way.

Input Parameters Design (1)

Table 3.10 Air bag Shape Size based on rear crash zone of car

Air bag Sized Concept	Sized Shape thickness (mm)
Shape Size based on rear crash zone of car with dimensions 1000x500x10	5 10 15 20

Table 3.11. Air bag Shape based on fixing location

Air bag Fixing Concept location	**Sized Shape Fixing location images**
Air bag Shape Size based on	fixing at rear crash zone of car
Airbag Shape Size based on	fixing cornering

Output Parameters

Table 3.12. Output Parameters on analysis

Names	**Results-oriented**
Speed of both Car at the end of Simulation	Reference to pre-crash speed
Failure or Fracture Test of Air bag	Based on deformation and internal Energy
Stress Concentration	Based on average maximum
Total Deformation	Based on average maximum

3.5.2 3D Modeling

On this study the 3Dmodel of two cars has been obtained from professional engineers and imported to ANSYS space claim in order clean unnecessary feature from geometry that reduce the quality of discretization.

Continuum theory of sound propagation through elemental rod

Sound waves can propagate through solids in the form of longitudinal, transverse, dilatational or flexural waves. An elastic longitudinal wave propagates along a rod by means of a periodic sequence of expansion and contraction along the length of the rod. The propagation period is given by the following equation.

$$\Delta t = \frac{l}{c} = \frac{l}{\sqrt{\frac{E}{\rho}}} = l\sqrt{\frac{\rho}{E}} \tag{27}$$

$$E \ = 2G(1 + v) \tag{28}$$

$$\Delta t = \frac{\sqrt{2}}{\sqrt{\frac{k(m_1+m_2)}{m_1 x m_2}}} = \sqrt{\frac{2(m_1 x m_2)}{(m_1 + m_2)}\frac{1}{k}} = x\sqrt{\frac{2m_2}{(m_1 + m_2)}\frac{1}{v^2}} \tag{29}$$

Computational model with domain of analysis is used to guide if the geometry or vehicle is moved away from the center of road. The figure 3.13 below shows the control rigid wall with two vehicles prepared for upcoming simulation.

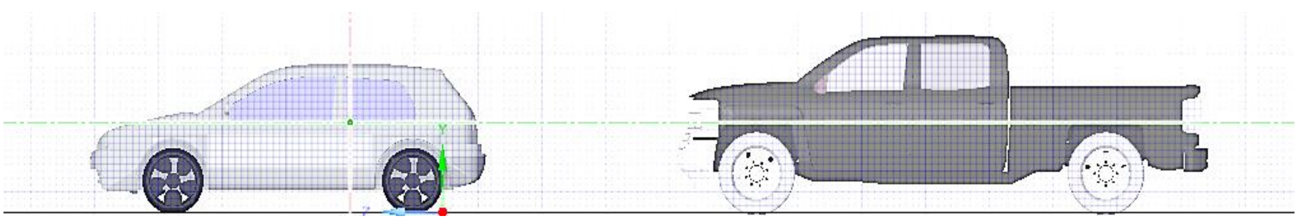

Figure 3.13. Vehicle without air bag mounted at rear

3.5.3 Ansys LS Dyna Boundary/Initial Condition's

For a boundary value problem to be solved, boundary conditions (B.C.) are restrictions. A boundary value problem is a differential equation (or system of differential equations) that needs to be solved within a domain whose boundary has a given set of conditions. And the starting circumstances are essential for setup. They are crucial to the simulation because they specify the condition of the system at zero time. This is defined as initial conditions. Table 3.13 shows the detail of boundary condition used on simulation.

3.5.4 Assumption

Many researchers have done crash analysis at speeds up to 6 m/s, which is called a low speed level. The speed of the rear car vehicle is stepped by the averaged speed variations between successive speeds, starting from the maximum vehicle speed to the minimum vehicle speed, which is described as 50 m/s, 25 m/s, 12.5 m/s, and 12.5 m/s. This means considering the maximum, moderate, and minimum speed of the vehicle during a crash depending on the driving condition. The collision is not considered the brake on this thesis. Because the analysis is to investigate the performance and strength of airbag equipped vehicles under worst case condition.

Table 3.13. Boundary/Initial Condition's

Terms	**Frame of Reference**	**Descriptions**
Rear Car Speed	Started + 2m from global axis	50m/s, 25m/s, 12.5m/s, 6.25m/s
Frontal Car Speed	Free stand to the origin of global axis	Stationer
Simulation end Time	Start with 0sec	0.017sec
Simulation Time Step	_	2.55×10^{-7}sec
Standard Earth Gravity	_	9.81m/s^2
Specific heat volume C_v	_	701
Specific heat pressure C_p	_	1001
Air bag Inflation Time	_	0.01sec
Air bag mass flow rate	_	Tabular Data
Pre-crash distance	_	0.23m
The face of airbag	Fixed with the car body at the rear bumper position	

Table 3.14. Parametric Value for Air Bag Inflation mass flow

Name	Value
Air Density	1.16kg/m3
Initial volume of air bag	0.0011577m^3
Air bag inflation speed	90m/s
Polytrophic number	1.4
Airbag mass	8kg
Initial impact face area of air bag	1.16m^2
Initial inflator pressure of air bag	101kpa

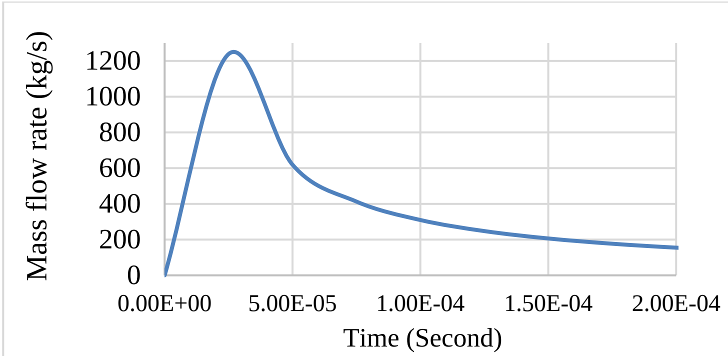

Figure 3.14 plot of Air Bag Inflation mass flow Rate

3.5.5 Ansys LS Dyna Meshing

The geometrical model developed in previously is imported to the ANSYS LS dyna tool. The first case of analysis has been started with traditional steel made bumper as per the model developed in the ANSYS space claim and the airbag based rear bumper meshing is done using tetrahedron elements with fine mesh and the quality check has been done to see the mesh quality.

3.5.6 Grid independent Test based on grid convergence index (GCI)

It has a restriction that necessitates the researcher's subjective judgement in choosing the reference grid, despite the fact that there is a guideline for the ratio between the grid conditions for GCI calculation. The convergence error of the grid is calculated using Richardson's extrapolation as a basis for the GCI indicator, which is used to identify the best grid. It is used to assess the appropriateness of the grid as an indication that quantifies the mistake of the numerical analysis by grid. The grid refinement ratio (r) calculation is used to determine the GCI.

$$r = \left(\frac{\Delta_{\mathrm{fine}}}{\Delta_{\mathrm{coarse}}}\right)^{1/3} \tag{30}$$

Where Δr_{fine} denotes the quantity of grids in the fine grid condition and Δr_{coarse} denotes the quantity of grids in the coarse grid condition. To distinguish the discrete error from other mistakes, the grid refinement ratio should be greater than 1.3. The medium grid was used in this study as the grid resolution that was determined to be ideal by the grid independence test. With this grid serving as a guide, it was determined which grid resolutions' coarse and fine grids satisfied the grid refinement ratio. According to Richardson's extrapolation, the GCI is calculated with

$$\mathrm{GCI} = \frac{F_s \varepsilon}{r^p - 1} \tag{31}$$

Where p is the order of convergence, Fs is the safety factor, and denotes the relative inaccuracy of two grid conditions in the simulation. When comparing three or more grids, Fs are calculated using a value of 1.25. This is how p is determined:

$$p = \frac{\ln/(f_{coarse} - f_{medium})/(f_{medium} - f_{fine})/}{\ln r} \quad (32)$$

$$\varepsilon = \frac{f_{coarse} - f_{fine}}{f_{fine}} \quad (33)$$

By using the mean equivalent stress of the model, the numerical solution error of the GCI is computed. On the basis of this, the GCI between the medium and coarse grids, as well as between the fine and medium grids, is determined. According to the grid, a bigger GCI number indicates a larger inaccuracy, necessitating a finer grid construction. The GCI between the medium and fine grids as well as between the medium and coarse grids were compared in order to assess the medium grid's suitability.

Table 3.15. Grid Refinement ratio of different Model

e/t size of air bag(mm)	20	15	10	5	Grid Ratio	
e/t size of car(mm)	47.5	37.5	27.5	10		
Model. sno	e/t_1	e/t_2	e/t_3	e/t_4	r_{21}	r_{32}
Air Bag Model	10343	15087	23655	46054	1.318	1.451
Two Car Model	40465	65198	83808	10027	1.315	1.447

Table 3.16. Grid Refined Stress value of different Model

Model. Sno	Stress1	Stress 2	Stress 3	Stress 4	P_{21}	P_{32}
Air bag model	8.97E+07	1.02E+08	9.80E+07	1.00E+08	4.322	0.677
Two car model	9.26E+08	1.33E+09	9.93E+08	1.055E+09	3.640	2.362

Table 3.17 GCI of different Model

P_{21}	P_{32}	$Error_{21}$	$Error_{23}$	$Error_{43}$	Safety	GCI_{21}	GCI_{32}
4.322	0.677	0.0842	0.00796	0.00796	1.25	5%	3%
3.640	2.362	0.0669	0.0224	0.0224	1.25	5%	2%

3.5.7 The selected models mesh Generated

From table 3.17, the minimum convergence index shows that the airbag model has 3% and the two car models have 2%–5%. This shows that the result from finite element analysis based on stress concentration decided to select a 5mm element size for all air bag analyses, and 27.5mm was selected for two cars. It's known that 10mm element size is better than 27.5mm, but on a computational system, 27.5mm element size can be solved quickly. And their error is also not out of the confidence interval, which is up to 5%.

The geometric Meshing is the process of turning irregular shapes into more recognizable volumes called “elements.” Before starting meshing, it must first upload a geometry or CAD model into, Ansys Mechanical to begin the simulation process. The following figures show the final mesh generated for numerical analysis.

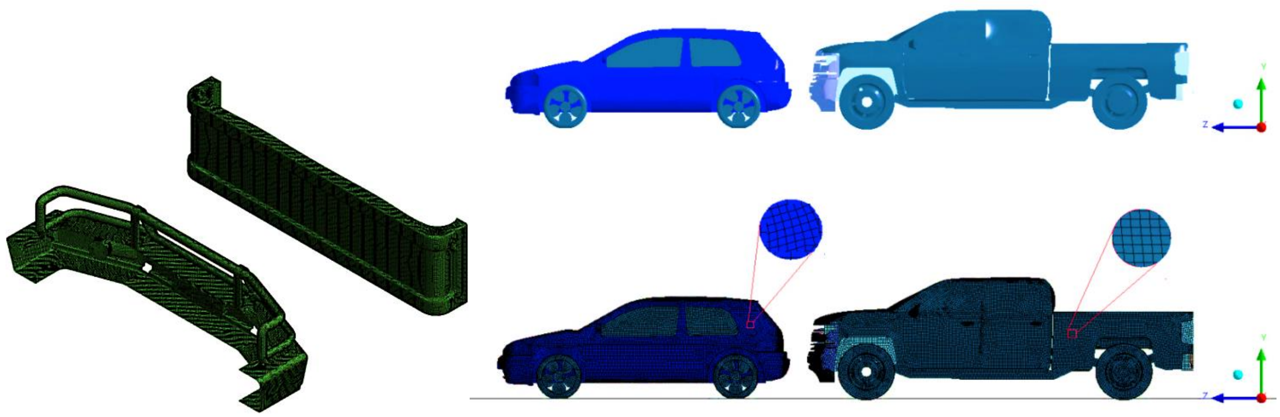

(a) (b)

Figure 3.15 (a) Airbag- Mesh and (b) Two Cars, Mesh Generated

CHAPTER FOUR

RESULT AND DISCUSSION

This chapter contains the results section which is unit containing a description about the main findings of this research, whereas the discussion section interprets the results for readers and delivers the significance of the findings.

4.1 Numerical Result of Airbag Design

The numerical simulation has been applied for airbag design to choose better thickness which can overcome failure state under maximums dynamic load which obtained from maximum speed of rear car or bulbar bumper, around 50m/s. There for the designated thickness of airbag is based on 50m/s. The stimulated result has been shown with figure 4.1 a, b, c and d.

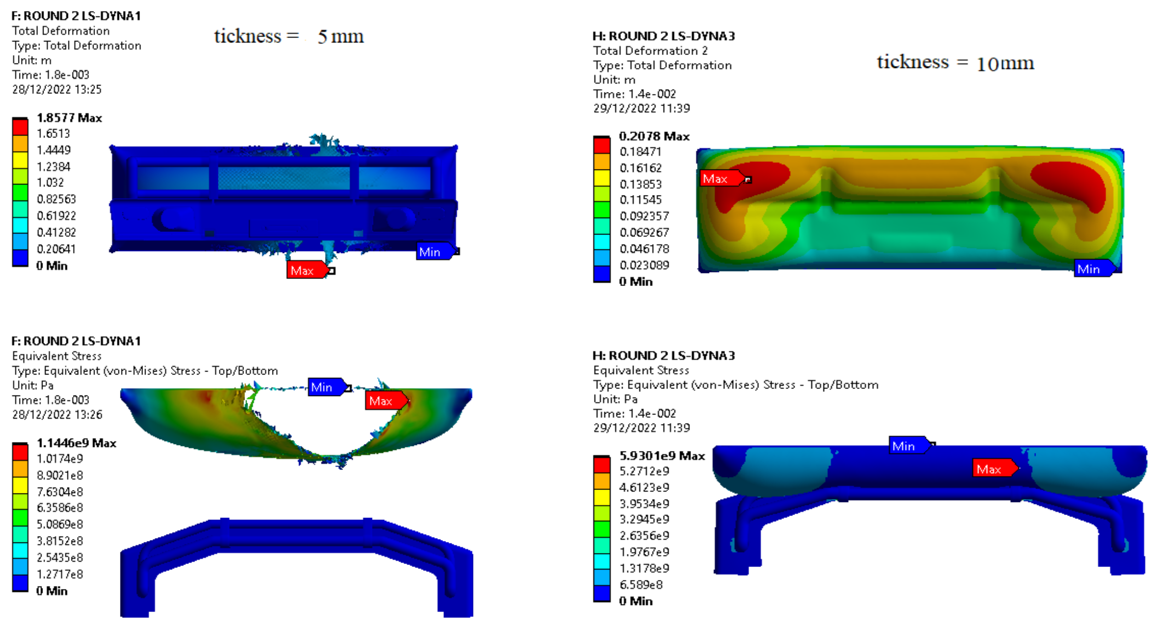

(a) Tickness air bag = 5mm (b) Tickness of air bag =10mm

Figure 4.4.1. a & b, Stress distribution and total deformation of air bag at maximum speed of rear vehicle 50m/s

According to the illustration figure 4.1 a, b, an airbag that is 5 mm thick is ruptured before the impactor even touches it. This demonstrates that the airbag collapsed before much energy was absorbed, reaching fracture level right away. Additional it shows that it releases the stress level or it failed under lower stress values 1144Mpa when it is compared with this of 10mm which still subjected to 5930Mpa but didn't failed. The following figure 4.1 c, d thickness of 15mm and 20mm are also the other option to use the same thing as a result of this failure.

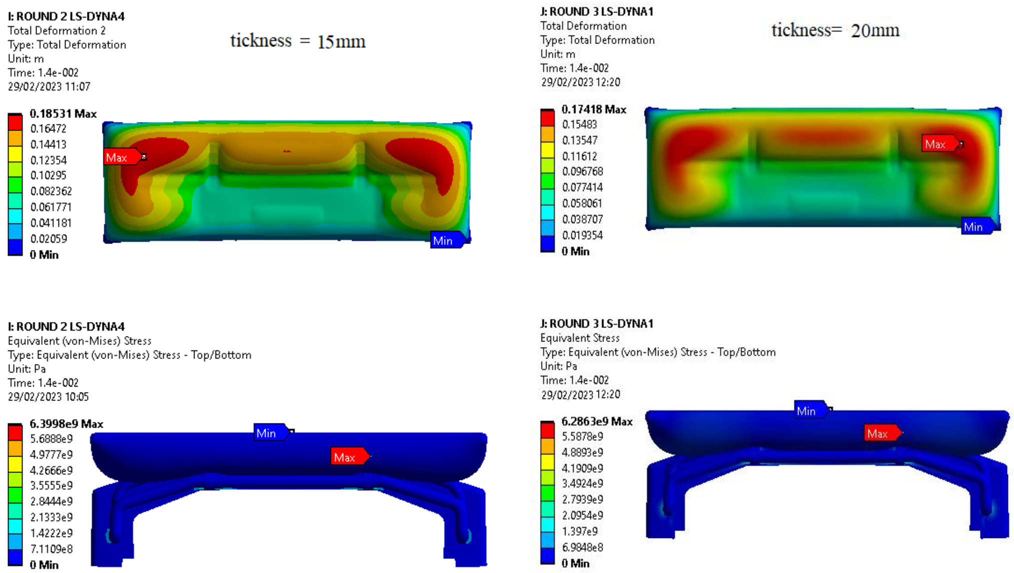

(c)Tickness air bag = 15mm (d) Tickness of air bag =20mm

Figure 4.4.2. c & d, Stress distribution and total deformation of air bag at maximum speed of rear vehicle 50m/s

The air bag simulation result shown in Figures 4.2 a, b, c, and d demonstrates that as airbag thickness varies or raises the concentration of stress decreases, as does deformation. However, based on their energy absorption, they can be secured. For instance, the failure status of 10mm, 15mm, and 20mm is avoided. The chosen thickness is that, found between 10mm and 20mm, which is 15 mm, this is required for the coming simulation of a car with a rear airbag mounted.

4.2 Vehicle crash analysis

Vehicle crashes involve non-linear transient dynamics, necessitating a crashworthiness investigation to assure safety, strength, and the integrity of the vehicle's structural components depends heavily on internal energy, including microscopic forms.

ANSYS LS Dyna analyzed vehicle models with and without airbags, evaluating the crash worthiness of the rear system as a unique component. This analysis provides a justification for the rear end impact safety and protection.

There is four simulation tests run for the rear impact. In Simulation 1, the rear speed of the vehicle is 6.25 m/s; in Simulation 2, the rear speed is 12.5 m/s; in Simulation 3, the rear speed is 25 m/s; and in Simulation 4, the rear speed is 50 m/s for both case studies.

4.2.1 Car without Air Bag Tested Result

Here the rear portion airbag mounted car is collide with the coming pickup car from rear end which has speed varied from 6.25 m/s, 12.5 m/s, 25m/s and 50m/s. the equivalent stress and total deformation as well as front car speed after specified time of collision. The detail has been explained and all figures are labeled according to the contour plot and graphical plots.

Result on automobile without air airbag at pick up car speed of 25m/s and 50m/s

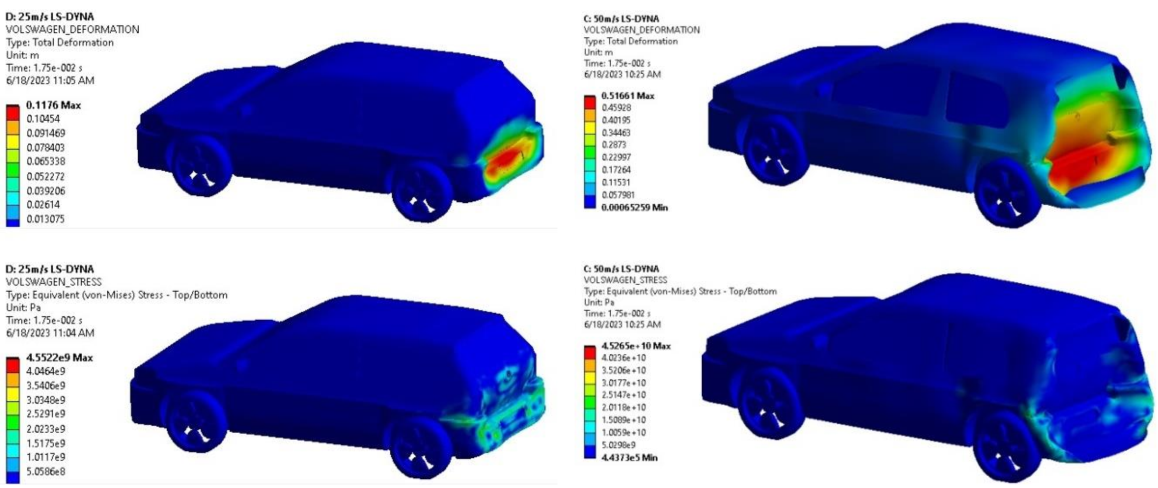

(a) (b)

Figure 4.4.3 a & b, Stress distribution and total deformation of Frontal car at rear car speed of (25m/s & 50m/s)

The simulation duration for an automobile without an airbag is 0.017 seconds, as shown in Figures 4.3 a and b. At this time, the maximum stress and deformation on the rear zone of the pickup car were 4526.5 MPa and 516.6mm, respectively. 117.6mm at 25 m/s of pick-up car, and 4552 Mpa. However, it is hard to say whether the maximum value has ever been used at this time. Because the structure's analysis results vary depending on the dynamic circumstances during a certain simulation period at distinct nodes, three states of dynamic conditions, minimum, maximum, and average dynamic value—are used to express the results of transient dynamic analysis. The minimum and maximum values are challenging to interpret because they change with each simulation time step. As a result, the dynamic average state is chosen to represent the analysis's findings. From the average dynamic state result, all stress, deformation, and internal energy are measured and shown.

i) Average Dynamic stress during impact 25m/s & 50m/s

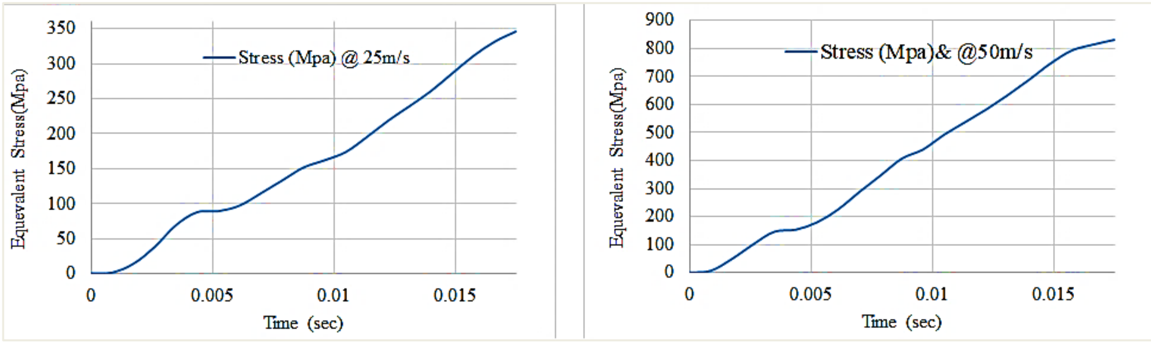

Figure 4.4.4 Average Dynamic stress on front vehicle during 25m/s & 50m/s speed of rear car

ii) Average Dynamic Deformation during impact

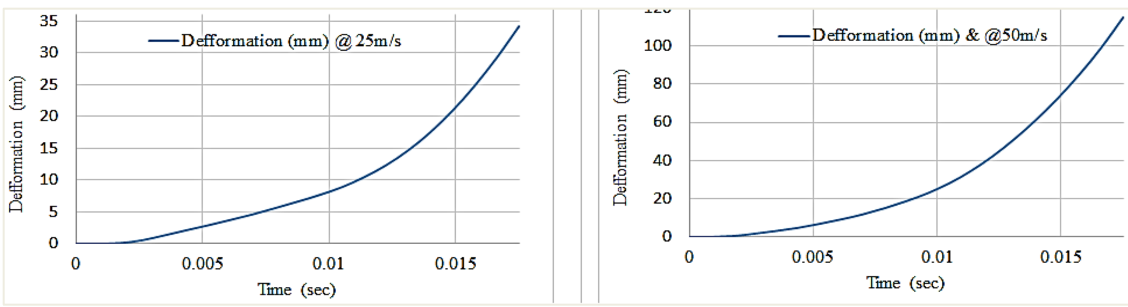

Figure 4.4.5 Average dynamic deformation on front vehicle during 25m/s & 50m/s speed of rear car

iii) Average Dynamic internal Energy absorbed during impact

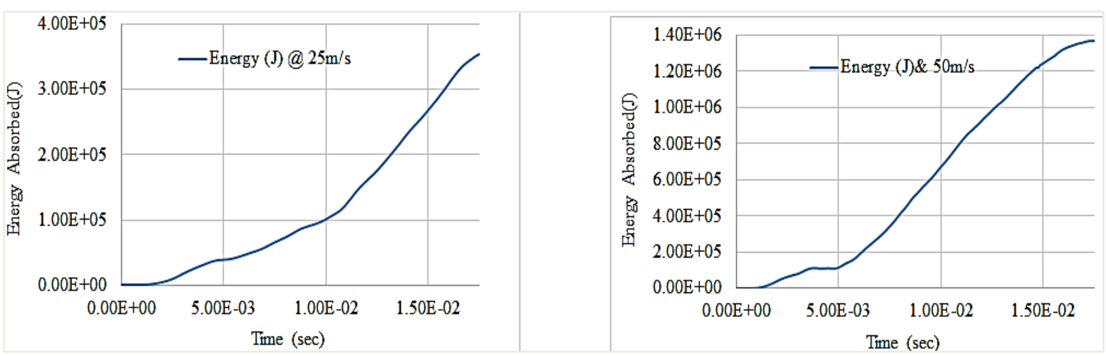

Figure 4.4.6 Average dynamic internal energy absorbed on front vehicle during 25m/s & 50m/s speed of rear car

At rear car speeds of 25 m/s and 50 m/s prospectively, Figure 4.4–4.6 displays the average dynamic state results of stress, deformation, and internal energy. All output parameters are raised with increasing collision times as a result of these dynamic state results. The average dynamic result for each graphical scenario is at its highest value at the time. The maximum average dynamic stress, deformation, and internal energy are, respectively, 346 MPa and 829 MPa, 34.2mm and 115mm, and 0.35 MJ and 1.37 MJ.

Result of automobile without airbag at pick up car speed of 6.25m/s and 12.5m/s

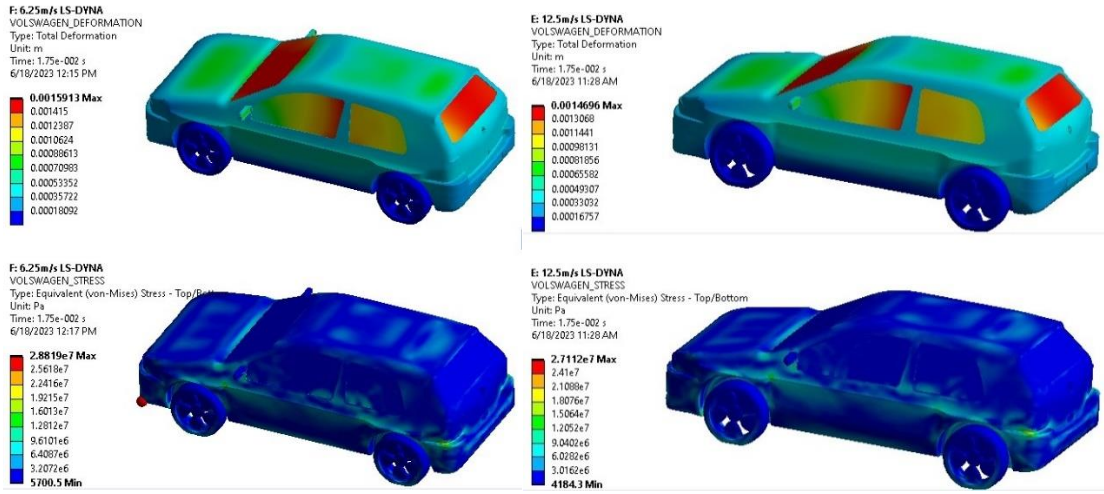

(a) (b)

Figure 4.4.7 a & b, Stress distribution and total deformation of Frontal car at rear car speed of (6.25m/s & 12.5m/s)

The simulation period for an automobile without an airbag is 0.0175 seconds, as shown in figures 4.7a and b. At this time, the maximum stress and deformation on the vehicle's rear zone at 12.5 m/s for a pick-up car are 27.11 MPa and 1.47mm, respectively. And for a pick-up car travelling at 6.25 m/s, 28.8 MPa, and 1.59 mm. To record the outcome of this analysis's dynamic situations, the dynamic average state is allocated. The average dynamic state result is used to calculate all stress, deformation, and internal energy.

i) Average Dynamic stress during impact

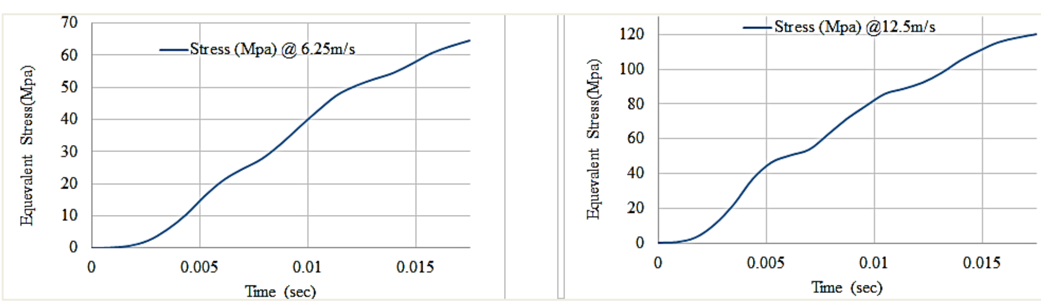

Figure 4.4.8 Average dynamic stress on front vehicle during 6.25m/s & 12.5m/s speed of rear car

ii) Average Dynamic Deformation during impact

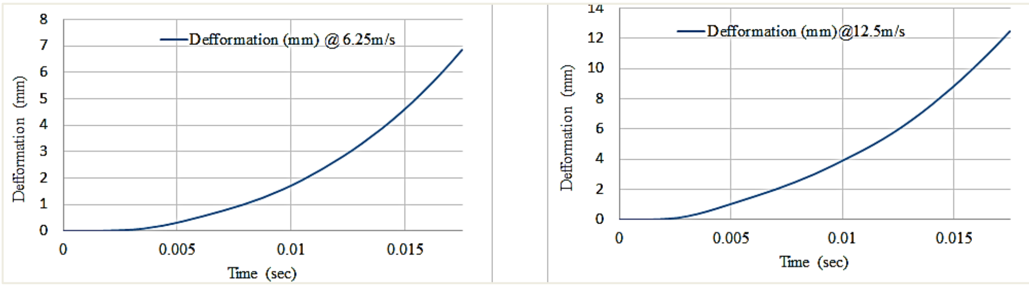

Figure 4.4.9 Average dynamic deformation on front vehicle during 6.25m/s & 12.5m/s speed of rear car

iii) Average Dynamic internal Energy absorbed during impact

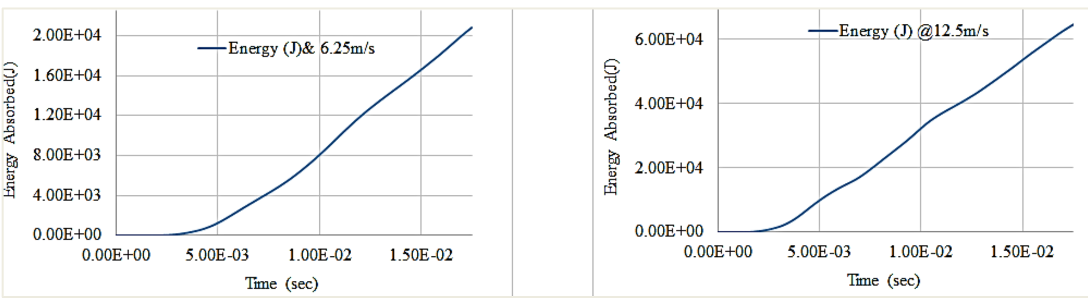

Figure 4.4.10 dynamic internal energy absorbed during 6.25m/s & 12.5m/s speed

The average dynamic state values for stress, deformation, and internal energy are shown in Figures 4.8–4.10 for rear vehicle speeds of 6.25 m/s and 12.5 m/s, respectively. All output parameters increase with increasing collision times as a result of these dynamic state results. The maximum value of the average dynamic outcome for each graphical example is currently available. The highest levels of average dynamic stress, deformation, and internal energy were attained, and they are 64.75 MPa, 120.7 MPa, 6.8 mm, and 12 mm, respectively.

Table 4.1 Summary of Crash analysis without air bag

Speed of the car (m/s)	Energy absorbed (E_{ab}) average maximum over time (MJ)	Stress (σ) average maximum over time (Mpa)	Deformation (δ) average maximum over time (mm)
6.25	0.02	64.75	6.80
12.5	0.064	120.7	12.0
25.0	0.350	346.0	34.2
50.0	1.370	829.8	115
Weighted average	0.834	555.24	72.5

From the table 4.1 above, the internal energy within the system increases with the speed of the rear car. The simulation is recorded for up to 0.0175second. Here the internal energy change from 6.25m/s to 12.5m/s is around 0.044MJ and also the others 12.5m/s -25 m/s is 0.286MJ and 25m/s -50 m/s is 1.02MJ increased. Therefor the internal energy of the frontal vehicle increases until both vehicles speed is the same and moving together. The deformation is, 6.8mm, 12mm, 34.2mm and 115mm at vehicle speed of 6.25m/s,12.5m/s,25m/s and 50m/s respectively. The highest average stress created on the front vehicle, is 64.75MPa, 120.7MPa, 346MPa, and 829.8 MPa with the speed of the rear car, respectively.

4.2.2 With Air Bag mounted at the rear end

Here the rear portion airbag mounted car is collide with the coming pickup car from rear end which has speed varied from 6.25 m/s, 12.5 m/s, 25m/s and 50m/s. the equivalent stress and total deformation as well as front car speed after specified time of collision. The detail has been explained and all figures are labeled according to the contour plot and graphical plots.

Result of automobile with airbag at pick up car speed of 25m/s and 50m/s

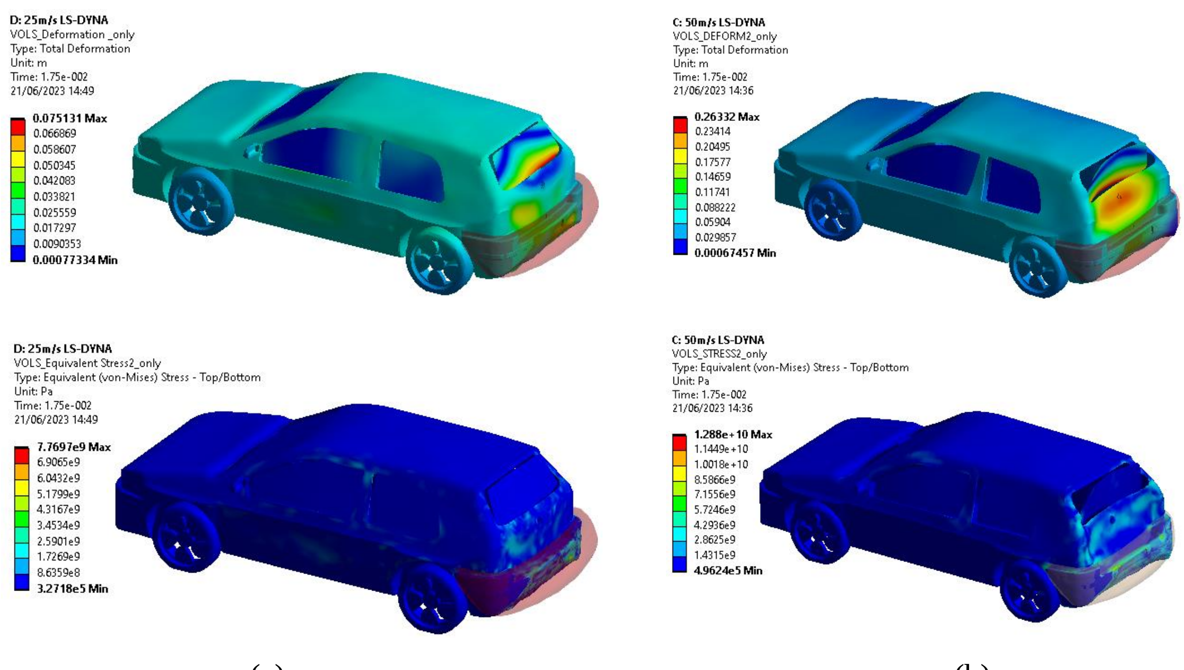

(a) (b)

Figure 4. 4.11 a & b, Stress distribution and total deformation of Frontal car at rear car speed of (25m/s & 50m/s)

Figure 4.11 a and b depict an airbag-equipped car with a simulation time of 0.0175 seconds. At this time, the pickup car's rear zone experienced a maximum stress development of 12880 MPa and a deformation of 263.3 mm, respectively. As well as 75.1mm at 25 m/s in a pick-up car and 7769.9 MPa. But to claim that this simulation period's highest value is available is intolerable. Therefore, it is best to speak from figure 4.12-4.14's average dynamic state graphical plot.

i) Average Dynamic stress during impact 25m/s & 50m/s

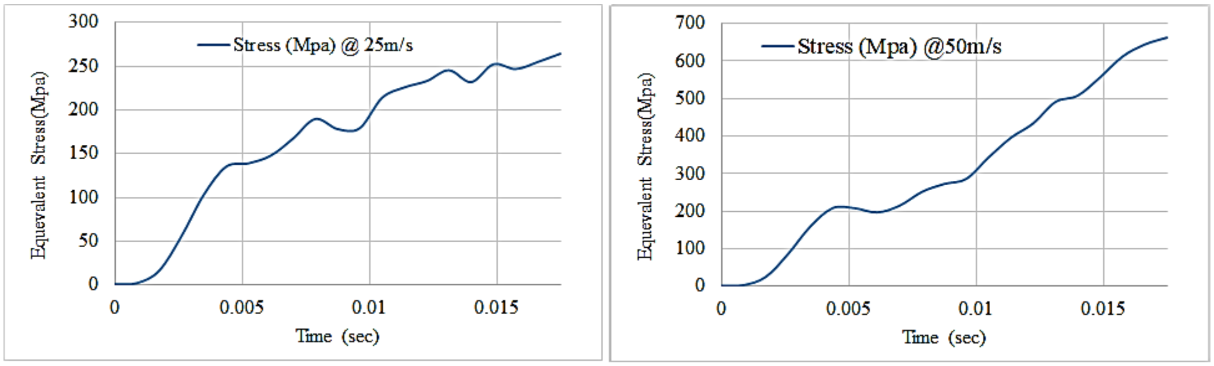

Figure 4.4.12 Average dynamic stress on conventional automobile body during 25m/s & 50m/s speed of rear car

ii) Average Dynamic Deformation during impact

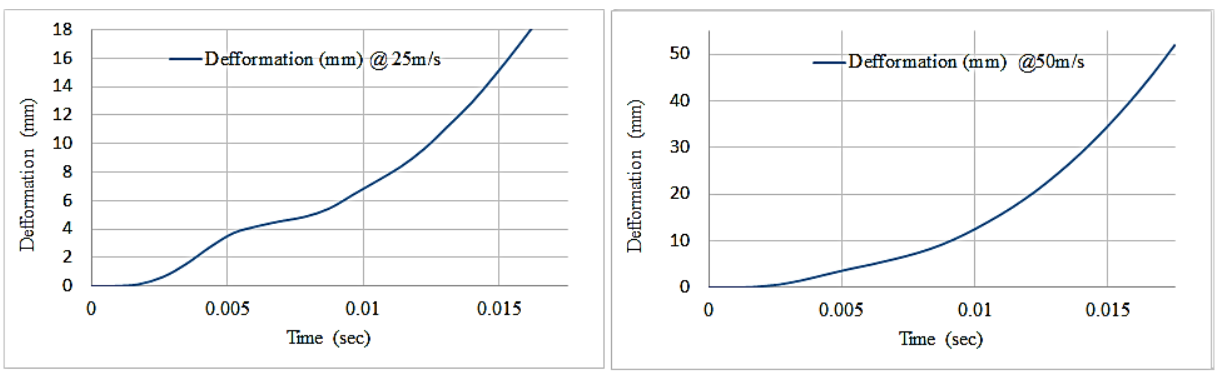

Figure 4.4.13 Average deformation of conventional automobile body during 25m/s & 50m/s speed of rear car

iii) Average Dynamic internal Energy absorbed during impact

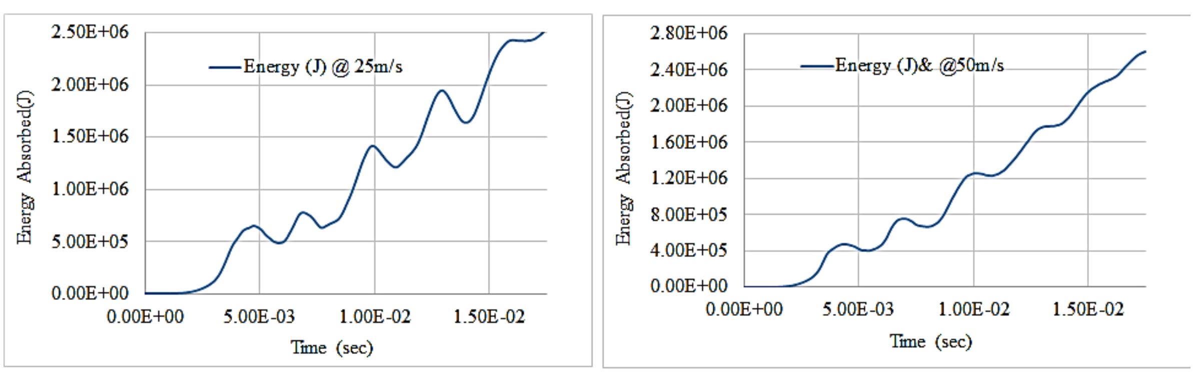

Figure 4.4.14 Average dynamic internal energy absorbed of conventional automobile body during 25m/s & 50m/s speed of rear car

At rear car speeds of 25 m/s and 50 m/s, Figures 4.12-4.14 show average dynamic state outcomes of stress, deformation, and internal energy. The yield parameters are advanced with collision periods derived from these dynamic state outcomes. At the designated time, the average dynamic outcome for each graphical scenario is at its highest value. The highest possible average dynamic stress, deformation, and internal energy were attained at 269 MPa, 664 MPa, 21 mm, and 51 mm, respectively.

Result of automobile with airbag at pick up car speed of 6.25m/s and 12.5m/s

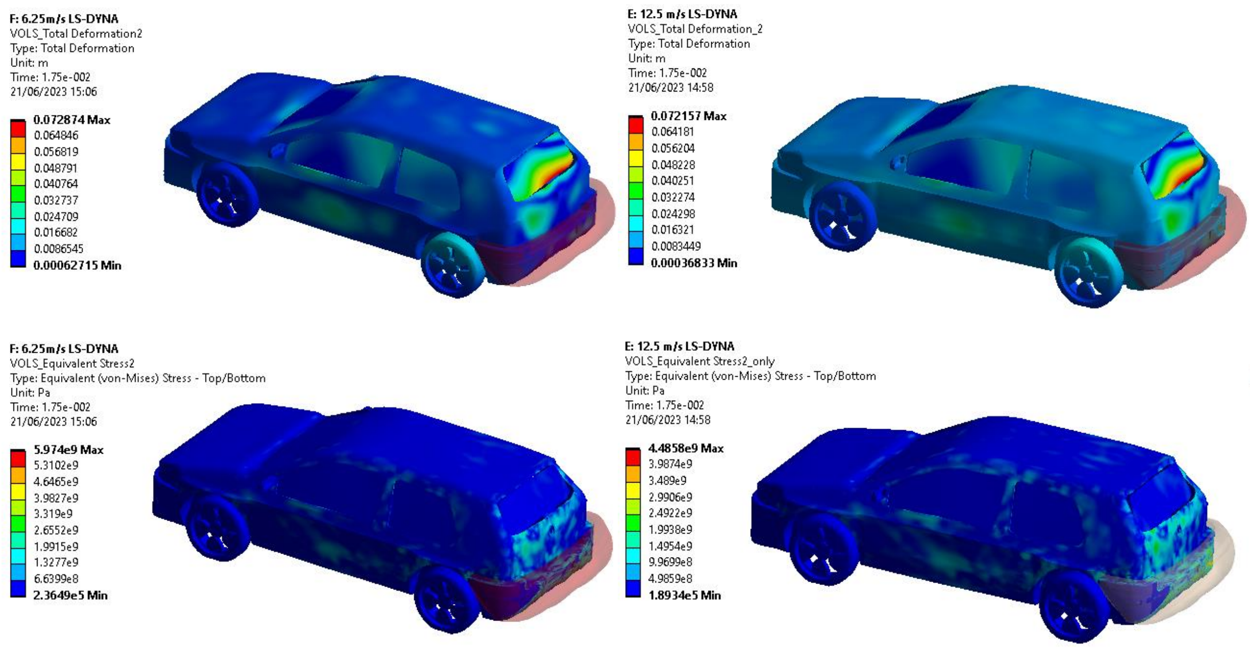

(a) (b)

Figure 4. 4.15 a & b, Stress distribution and total deformation of Frontal car at rear car speed of (6.25m/s & 12.5m/s)

Figure 4.15 a and b depict an airbag-equipped car with a simulation time of 0.0175 seconds. At this time, the pickup car's rear zone had the maximum amount of stress development and deformation, measuring 4485 MPa and 72.15 mm, respectively. And a pick-up car at 6.25 m/s with 5974 MPa and 72.8 mm. However, it is unacceptable to claim that the simulation period's maximum or minimum value is always available. Because of this, it is preferable to read from the average dynamic state graphical plot in figures 4.16-4.18.

i) Average Dynamic stress during impact

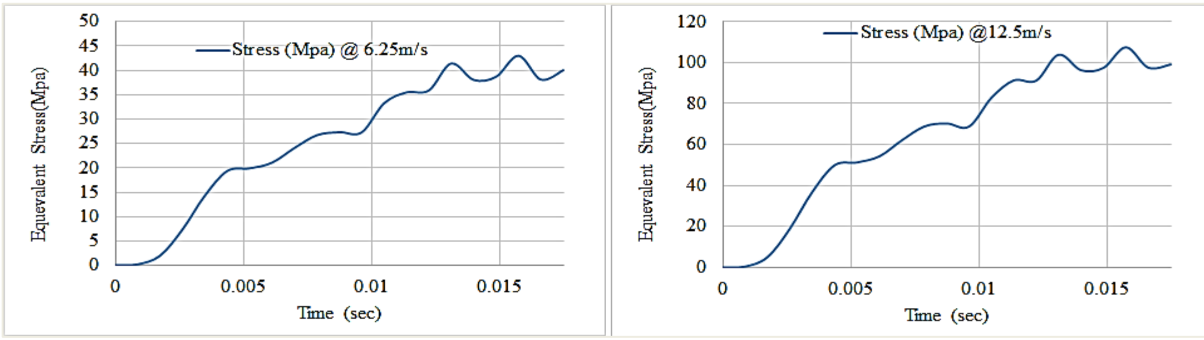

Figure 4.4.16 Average dynamic stress on airbag based automobile during 6.25m/s & 12.5m/s speed of rear car

ii) Average Dynamic Deformation during impact

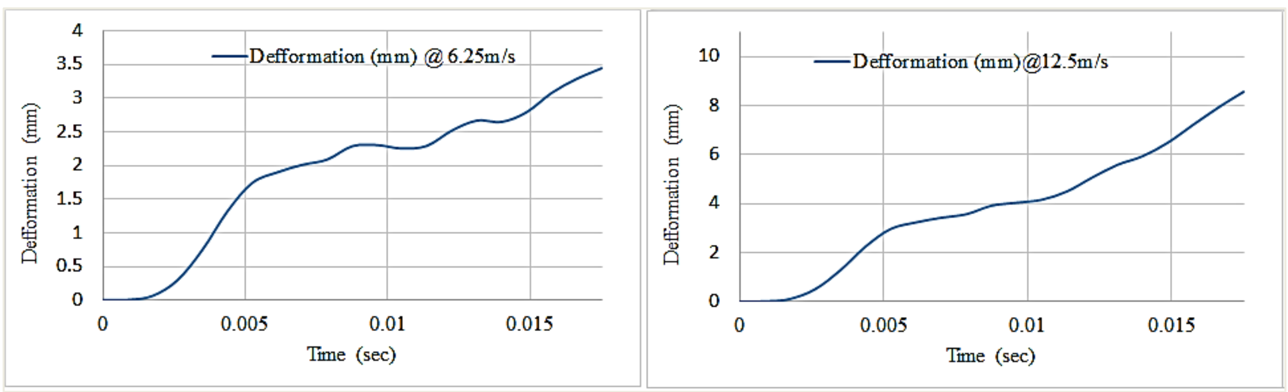

Figure 4.4.17 Average dynamic deformation on airbag based automobile during 6.25m/s & 12.5m/s speed of rear car

iii) Average Dynamic internal Energy absorbed during impact

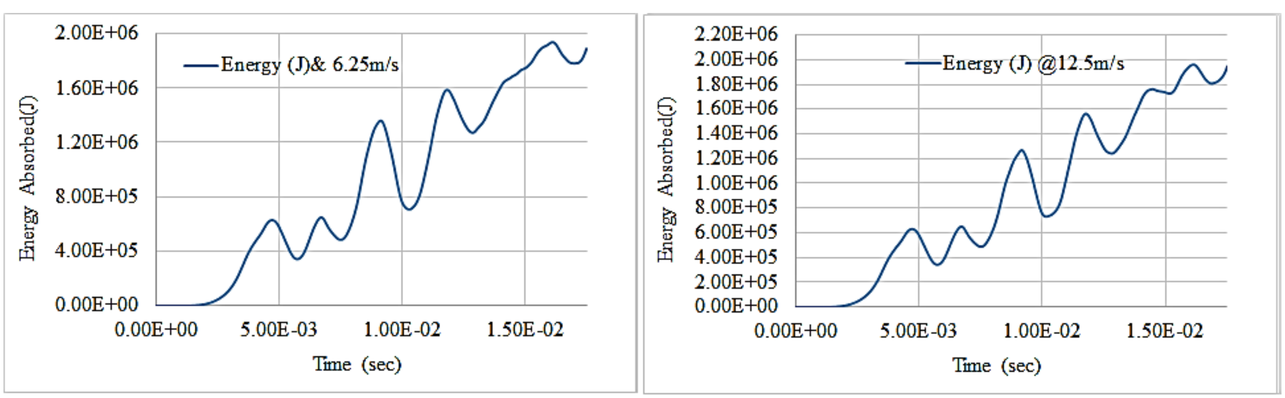

Figure 4.4.18 Average dynamic internal energy absorbed of airbag based automobile during 6.25m/s & 12.5m/s speed of rear car

At rear car speeds of 6.25 m/s and 12.5 m/s, Figure 4.16-4.18 illustrates the average dynamic state outcomes of stress, deformation, and internal energy. The yield factors progress over the impact periods as a result of these dynamic state impacts. At the specified time, the average dynamic result for each graphical case is at its highest value. The highest independent average dynamic stress, deformation, and internal energy values were 43 MPa and 107.6 MPa, 3.41 mm and 8.51 mm, and 1.93 MJ and 1.95 MJ.

Table 4.2 Summary of crash analysis for airbag based automobile

Speed of the car (m/s)	Energy absorbed (E_{ab}) average maximum over time (MJ)	Stress (σ) average maximum over time (Mpa)	Deformation (δ) average maximum over time (mm)
6.25	1.93	43.00	3.41
12.5	1.95	107.6	8.51
25.0	2.50	269.0	21.0
50.0	2.63	664.0	51.8
Weighted average	2.458	443.08	34.59

The simulation of rear air bag mounted frontal car collides with impacted car speed at 6.25m/s, 12.5m/s, 25m/s and 50m/s has been analyzed. The results summary of rear portion air bag mounted frontal car is shown in above table 4.2. The simulation period is recorded for up to 0.0175second. Here the internal energy change from 6.25m/s to 12.5m/s is 0.02MJ , 12.5m/s to 25 m/s is 0.55MJ and 25m/s to 50 m/s is 0.13MJ increased. Therefore the internal energy of the frontal vehicle increases until both vehicles speed is the same and moving together. The deformation is, 3.41mm, 8.51mm, 21mm and 51.8mm with the same speed. The highest average stress induced on the front vehicle, is 43.75MPa, 107.6MPa, 269MPa, and 664MPa with the variation speed of rear car, respectively. And the other collision state at graphical plots is drawn at 6.25m/s, 12.5m/s, 25m/s and 50m/s is obtained and shown by figures ,

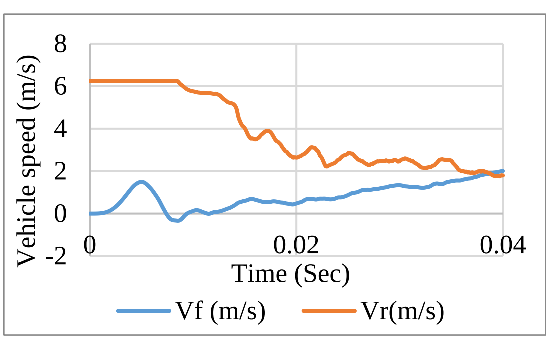

(a)

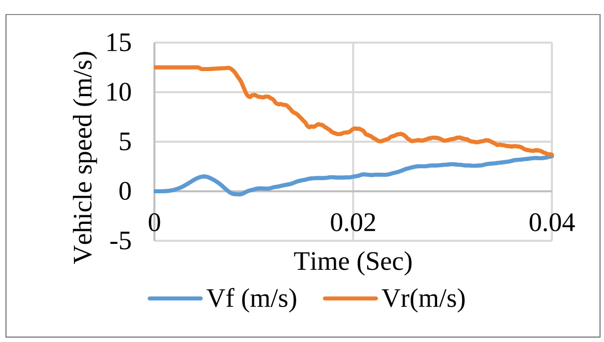

(b)

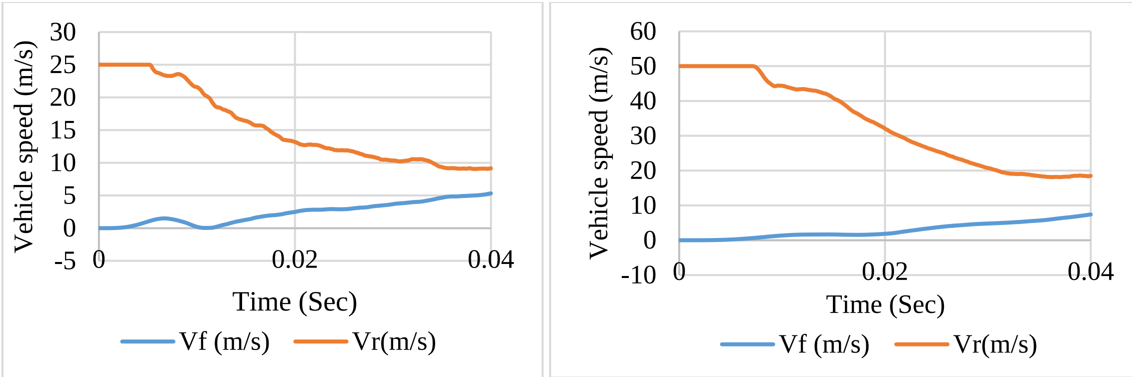

(c) (d)

Figure 4. 4.19 a, b, c & d, both rear car speed and Frontal car respectively during collision

Feasibility of outside airbag

- According to the findings from (Yonghan ju et al., 2023), the external airbag on front and side bumper system saves 46% of passengers injuries and prevents 40% of fatalities.
- Depending on the circumstances, the benefit/cost ratios range from 49.6% to 50.9% in percentage.
- On other hand, ZF Company of Commercial vehicles and industrial technology, recently gave a live demonstration of the prototype of its new pre-crash occupant safety system with an external side airbag in Memmingen, Germany.
- ZF said that the pre-crash safety system could reduce the penetration of the intruding vehicle by up to 30 percent, helping to significantly reduce the occupants' risk of injury.
- ZF said that biggest challenge in the development of this system was reliably recognizing an unavoidable collision and deploying the external side airbag before the collision takes place.
- The system has approximately 150 milliseconds to make the decision to deploy the airbag and fill it – roughly the amount of time it takes a person to blink.
- The vehicle's sensors first have to identify a potential impact quickly and accurately. This is possible with connected cameras, radar and lidar.

Figure 4. 5 Feasibility of outside airbag

CHAPTER FIVE

SUMMARY AND CONCLUSION

5.1 Summary

The rear pre-crash zone is an important in automobile member from the safety point of view. These study studied by adding a new feature airbag on the rear pre-crash system ,as it explained the analysis in the chapter four it gives better result compare with the conventional normal pre-crash zone one.

- The rear pre-crash zone or vehicle without airbag has a deformation of, 6.8mm, 12mm, and 34.2mm and 115mm at vehicle speed of 6.25m/s,12.5m/s,25m/s and 50m/s respectively where the new airbag based rear beam has a deformation of 3.41mm, 8.51mm, 21mm and 51.8mm with the same speed. Therefore the new airbag based rear system highly performed than the conventional one.
- The internal energy which is absorbed by the conventional is 0.02MJ, 0.064MJ, 0.35MJ and 1.37MJ at vehicle speed of 6.25m/s, 12.5m/s, 25m/s and 50m/s where the new airbag based rear system has 1.93MJ, 1.95MJ, 2.5MJ and 2.63MJ with the same speed. Therefore the new airbag based system has better than the conventional.
- The existing and the new airbag based is analyzed in ANSYS 2020R1 and the stress induced in the normal rear crash zone is 64.75Mpa, 120Mpa, 346Mpa and 829.8Mpa within a given speed of 6.25m/s, 12.5m/s, 25m/s and 50m/s. Where the new airbag based rear system has 43.75Mpa, 107.6Mpa, 269Mpa, and 664Mpa with the same speed. Therefore, the new airbag based rear system is better than the conventional one. From the study, it is concluded that airbag based rear system has better energy absorption and deformation than rear crash zone.

5.2 Conclusion

- The rear pre-crash zone without airbag has a deformation of, 6.8mm, 12mm, and 34.2mm and 115mm at vehicle speed of 6.25m/s, 12.5m/s, 25m/s and 50m/s respectively where the new airbag based rear beam has a deformation of 3.41mm, 8.51mm, and 21mm and 51.8mm with the same speed. Therefore the new airbag based rear system has better than the conventional one.
- The internal energy within the system increases with the speed of the rear car. Here the weighted average internal energy of car without air bag is 0.834MJ respectively where the new airbag based car has weighed average internal energy 2.458MJ. The percentage of energy absorption with air bag is 194% more than vehicle without airbag. Therefor air bag based rear

beam is better than conventional.

- The highest stress created on the front vehicle without airbag is, 64.75Mpa, 120Mpa, 346Mpa and 829.8Mpa with the speed of the rear car, respectively. The highest stress created on the front vehicle with air bag is 43.75Mpa, 107.6Mpa, 269Mpa, and 664Mpa with the speed of the rear car, respectively.

5.3 Recommendation

The following recommendations for future work can be noted as:

- It recommend to applying a complete controller design to control the dynamic operating system of airbag deployment during smashing or collision.
- It is recommended that using designed airbag is limited to the medium and light duty vehicle but not to heavy duty.

5.4 Future scope

- Testing the experimental of rear airbag mounted vehicle and validating the result with numerical study.
- It is recommended including side impacts along with rear impacts for accurate safety concern results.
- Better for researchers to design a control system and integrate it with the rear air bag mounted sensors.

REFERENCES

Supriya, M. S., N. D. Gangadhar, & A. G. Manjunath (2017). Reliable automotive crash detection using multi sensor decision fusion. SAS Tech-Technical Journal of RUAS 16.2 (2017): 46-49.

Raj Kumar, G., Balasubramaniyam, S., Senthil Kumar, M., Vijayanandh, R., Raj Kumar, R., & Varun, S. (2019). Crash Analysis on the Automotive Vehicle Bumper. International Journal of Engineering and Advanced Technology (2019), 8, 1602-160710.

Sonawane, C. R.,& Shelar, A. L. (2018). Strength enhancement of car front bumper for slow speed impact by FEA method as per IIHS regulation. Journal of the Institution of Engineers (India) (2018): Series C, 99(5), 599-606.

Tasnim N. Shaikh, SatyajeetChaudhari and Hiren Rasania (2013). Airbags for safety system in automobile engineering.Int. Journal of Engineering Research and Applications Vol. 3, Issue 5, Sep-Oct 2013, pp.615-621

MOTGI, N. S., KULKARNI, P., & BANSODE, S. S. (2017). Design improvement in front bumper of a passenger car using impact analysis-a review (2017).

Srikantha, B. M. and Kumar, M.(2017). Impact Analysis of Toyota Land Cruiser Car Bumper Using AnsysAutodyn D, 3, 28-37.

Wagh, M. P., and More, O. A (2020). “Vibration and Impact Analysis of Optimized Automotive Front Bumper. International Journal of Engineering Research & Technology (IJERT) (2020).

Nazari, A., and Nourozi, B. (2016). Behavioral Analysis of Volvo Cars Instrument Panel during Airbag Deployment. (2016)

The Global Automotive Airbag Market Outlook ". Valiet (2015). Automotive Market Research. Archived from the original on 23 June 2015. Retrieved 22 June 2015.

Standard, I. S. O., & ISO, B. (2019). Plastics—Determination of flexural properties. ISO Geneva, Switzerland.

Aikyo, Y., Kobayashi, Y., Akashi, T., & Ishiwatari, M. (2015). Feasibility study of airbag concept applicable to motorcycles without sufficient reaction structure. Traffic injury prevention, 16(sup1), S148-S152.

D. Bendjaballah, A. Bouchoucha1 , M. L. Sahli1, and J-C. Gelin (2017). Numerical analysis of side airbags deployment in out-of-position situations. International Journal of Mechanical and Materials

Engineering (2017) 12:12 DOI 10.1186/s40712-016-0070-2

Uber Cloud Inc. (2017). Airbag Simulation with ANSYS LS-DYNA on Uber Cloud and Azure: An Uber Cloud Technical Case Sudy (2017).

I. H. Hassanien, S. Shabaan & E. E. Khalil. (2017). Numerical simulation and investigation of an atrium fire experiment: International Journal of Advances in Mechanical & Automobile Engineering, vol. 4, pp. 35–39, 2017

Romeo M. Flores. (2014).Coalbed gas production. Copyright 2014 Elsevier Inc. All rights reserved

Mario Hirz & Patrick Rossbacher. (2016). Enhanced knowledge-based 3d-cad methods supporting automotive body-in-white production engineering'motsp2016 - International Conference Management of Technology – Step to Sustainable Production June 2016, Croatia

Lerdmanus Bumrungsup & Kunnawee Kanitpong. (2022). Analysis of rear-end crash potential and driver contributing factors based on car-following driving simulation, Traffic Injury Prevention, 23:5, 296-301, DOI: 10.1080/15389588.2022.2062334

Hsinjurylaw.(2017). Steps to take after a Rear-End Collision in North Carolina. https://www.hsinjurylaw.com/blog/steps-to-take-after-a-rear-end-collision.cfm October 16, 2017.

Avery, Maria Krafft, Anders Kullgren. (2012). Acceleration pulses and crash severity in low velocity rear impacts – real world data and barrier tests, Chalmers University of Technology Sweden

Alobaidan, H. (2021). Sensors for airbag systems. 11(8), 1–5. https://doi.org/10.9790/9622-1108020105

Arbor, A. (2017). IRC-17-63 IRCOBI Conference 2017. 494–507.

Arun Kumar, S., & Madhu, S. (2015). A research review on airbag in automobile safety system. International Journal of Applied Engineering Research, 10(33), 26815–26819.

Barbat, S., Li, X., & Prasad, P. (2013). Bumper and Grille Airbags Concept for Enhanced Vehicle Compatibility in Side Impact: Phase II. Traffic Injury Prevention, 14(SUPPL1). https://doi.org/10.1080/15389588.2013.811720

Bennbaia, S., Mahdi, E., Abdella, G., & Dean, A. (2023). Composite Plastic Hybrid for Automotive Front Bumper Beam. Journal of Composites Science, 7(4). https://doi.org/10.3390/jcs7040162

Beyene, A. T., Koricho, E. G., Belingardi, G., & Martorana, B. (2014). Design and manufacturing issues in the development of lightweight solution for a vehicle frontal bumper. Procedia Engineering, 88, 77–84.

https://doi.org/10.1016/j.proeng.2014.11.129

Bhasin, K. (2020). Airbags for Safety System in Automobile Engineering. International Journal of Automobile Engineering Research and Development, 10(1). www.tjprc.org

Dange, M. V, Buktar, R. B., & Raykar, N. R. (2015). Design and Analysis of an Automotive Front Bumper Beam for Low-Speed Impact. IOSR Journal of Mechanical and Civil Engineering Ver, 12(2), 2320–2334. https://doi.org/10.9790/1684-12241727

Das, S., Minjares-Kyle, L., Wu, L., & Henk, R. H. (2019). Understanding crash potential associated with teen driving: Survey analysis using multivariate graphical method. Journal of Safety Research, 70, 213–222. https://doi.org/10.1016/j.jsr.2019.07.009

Driver, M., Program, C., & Squad, R. (2004). MCFRS Driver Certification Program Page 1 Rescue Squad - Module 12. 1–26.

Factsheet, A. (2021). Road Safety Factsheet. March.

Hirz, M., & Rossbacher, P. (2017). Enhanced Knowledge-Based 3D-Cad Methods Supporting Automotive Body-in-White Production Engineering. Acta Technica Corviniensis - Bulletin of Engineering, 10(2), 123–128. https://search.proquest.com/docview/1916673708?accountid=26636%0Ahttp://link.periodicos.capes.gov.br/sfxlcl41?url_ver=Z39.88-2004&rft_val_fmt=info:ofi/fmt:kev:mtx:journal&genre=article&sid=ProQ:ProQ%3Aengineeringjournals&atitle=ENHANCED+KNOWLEDGE-BASED+3D

Kahane J, C. (2013). Injury Vulnerability and Effectiveness of Occupant Protection Technologies for Older Occupants and Women. National Highway Traffic Safety Administration, May, 349.

Kim, E., Moore, N. R., & Vanzandt, T. R. (1998). Advanced Air Bag Technology Assessment.

Kleisner, V., & Zemčík, R. (2009). Analysis of composite car bumper reinforcement. Applied and Computational Mechanics, 3, 287–296.

Kurebwa, J., & Mushiri, T. (2019). A Study of Damage Patterns on Passenger Cars Involved in Road Traffic Accidents. Journal of Robotics, 2019, 22–24. https://doi.org/10.1155/2019/3927935

Lee, S. E., Llaneras, E., Klauer, S. G., & Sudweeks, J. (2007). Analyses of Rear-End Crashes and Near-Crashes in the 100-Car Naturalistic Driving Study to Support Rear-Signaling Countermeasure Development. Distribution, October, 1–125.

Li, M. (2018). Design and Simulation Analysis of the Truck Rear Impact Energy -Absorbing Device. 166(Amcce), 819–824. https://doi.org/10.2991/amcce-18.2018.143

Luo, Q., Chen, X., Yuan, J., Zang, X., Yang, J., & Chen, J. (2020). Study and Simulation Analysis of Vehicle Rear-End Collision Model considering Driver Types. Journal of Advanced Transportation, 2020. https://doi.org/10.1155/2020/7878656

Ma, X., Yu, Q., & Liu, J. (2022). Modeling Urban Freeway Rear-End Collision Risk Using Machine Learning Algorithms. Sustainability (Switzerland), 14(19). https://doi.org/10.3390/su141912047

Mohamed, S. A., Mohamed, K., & Al-Harthi, H. A. (2017). Investigating Factors Affecting the Occurrence and Severity of Rear-End Crashes. Transportation Research Procedia, 25(June), 2098–2107. https://doi.org/10.1016/j.trpro.2017.05.403

Muhammad, N. S., Hambali, A., Rosidah, J., Widodo, W. S., & Ahmad, M. N. (2017). A review of energy absorption of automotive bumper beam. International Journal of Applied Engineering Research, 12(2), 238–245.

Raj Kumar, G., Balasubramaniyam, S., Senthil Kumar, M., Vijayanandh, R., Raj Kumar, R., & Varun, S. (2019). Crash analysis on the automotive vehicle bumper. International Journal of Engineering and Advanced Technology, 8(6 Special Issue 3), 1602–1607. https://doi.org/10.35940/ijeat.F1296.0986S319

Rambhad, K., Sutar, V., Sonwane, P., & Suryawanshi, S. (2020). A Review on Automotive Bumper Beam Design and Analysis. Journal of Automotive Engineering &Technology, 5(1), 21–35. https://doi.org/10.13140/RG.2.2.23423.23205

Report, N. T. (1981). Evaluation of the Bumper Standard. 4(April).

Sonawane, C. R., & Shelar, A. L. (2018). Strength Enhancement of Car Front Bumper for Slow Speed Impact by FEA Method as per IIHS Regulation. Journal of The Institution of Engineers (India): Series C, 99(5), 599–606. https://doi.org/10.1007/s40032-017-0365-y

Sudin, M. N., Din, A. T., Abdullah, M. F., & Shamsudin, S. A. (2018). Conceptual design of automotive bumper beam. 9.

Supriya, M. S., Gangadhar, N. D., & Manjunath, A. G. (2017). Reliable Automotive Crash Detection using Multi Sensor Decision Fusion. RUAS-SASTech Journal, 16(2), 46–49.

Tsuchiya, Y., & Shiraishi, M. (1998). A study on a critical car-crash region for an external airbag system. Seimitsu Kogaku Kaishi/Journal of the Japan Society for Precision Engineering, 64(3), 394–398. https://doi.org/10.2493/jjspe.64.394

Wang, W., Li, Y., Lu, J., Li, Y., & Wan, Q. (2019). Estimating Rear-End Accident Probabilities with Different Driving Tendencies at Signalized Intersections in China. Journal of Advanced Transportation, 2019. https://doi.org/10.1155/2019/4836908

Wisch, M., Ott, J., Thomson, R., Léost, Y., Abert, M., & Yao, J. (2014). Recommendations and Guidelines for Battery Crash Safety and Post-Crash Safe Handling. EverSafe, D3.1(3). http://www.eversafe-project.eu/files/pages/554/deliverables/d3-1-eversafe-guidelinesforbatterysafetyandsafehandling-recommendationscrashcompatibility.pdf

Xi, J., Guo, H., Tian, J., Liu, L., & Sun, W. (2019). Analysis of influencing factors for rear-end collision on the freeway. Advances in Mechanical Engineering, 11(7), 1–10. https://doi.org/10.1177/1687814019865079

Yurchenko, N. F., Breed, D. S., & Zhang, S. (2021). Design of the Airbag Inflation System Applicable to Conventional and Autonomous Vehicles. Automotive Innovation, 4(4), 390–399. https://doi.org/10.1007/s42154-021-00156-y

APPENDIX I
VEHICLE BODY MATERIAL TICKNESS

Table Carbon Steel Gauge Chart

Gauge Number	Inches	mm
7	0.1793	4.554
8	0.1644	4.175
9	0.1495	3.797
10	0.1345	3.416
11	0.1196	3.038
12	0.1046	2.656
14	0.0747	1.897
16	0.0598	1.518
18	0.0478	1.214
20	0.0359	0.911
22	0.0299	0.759
24	0.0239	0.607
26	0.0179	0.454
28	0.0149	0.378

APPENDIX II
SPEED OF CAR IN SPECIFIED AREA

Table Typical speed of Car in specified area

Speed	Typically found
50 km/h	Typical car speed on residential roads or busy city roads
80–90 km/h	Vehicle on main road, travelling reasonably fast
100–120 km/h	Fast car on motorway, typical speed of a cheetah running, freight trains

APPENDIX III
RESULT SUMMARY OF CRASH ANALYSIS

Vehicle Speed = 6.25m/s

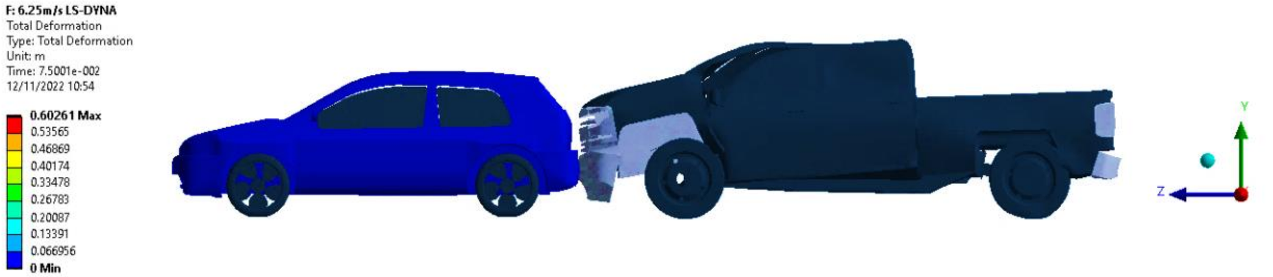

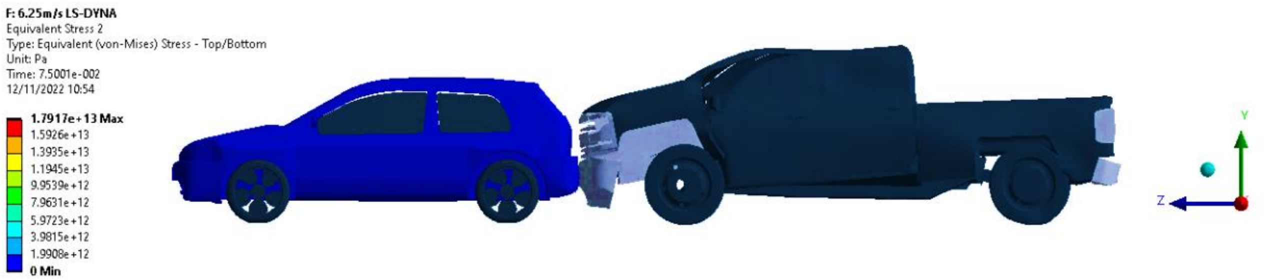

Vehicle Speed =12.5m/s

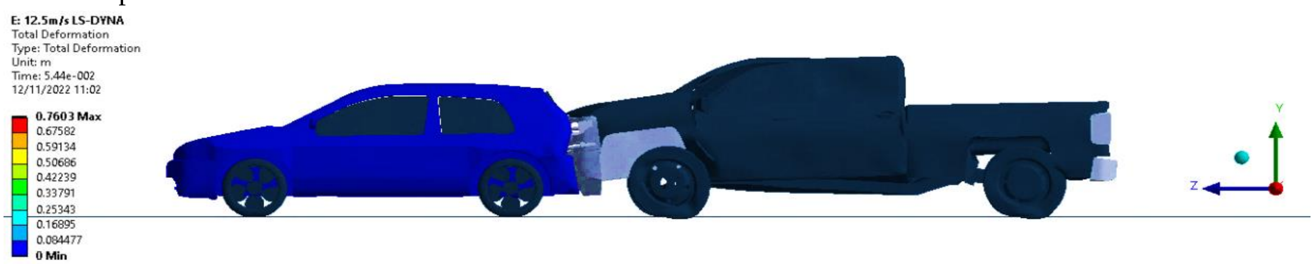

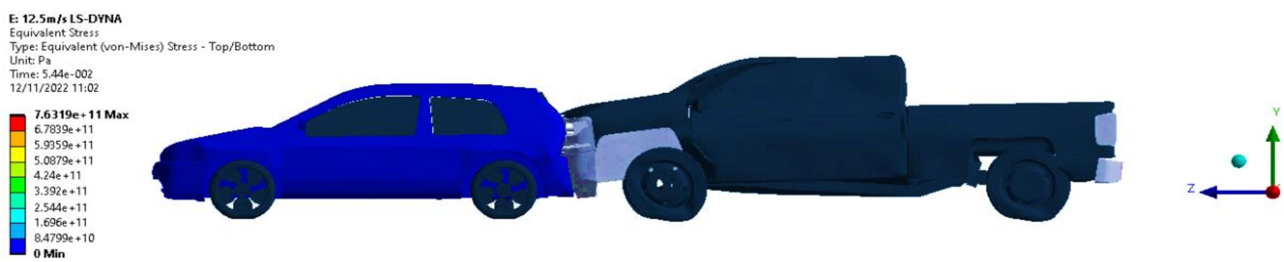

Vehicle Speed = 25m/s

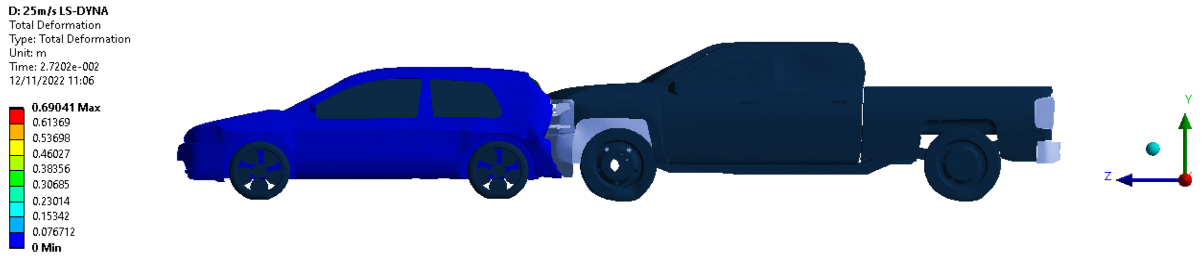

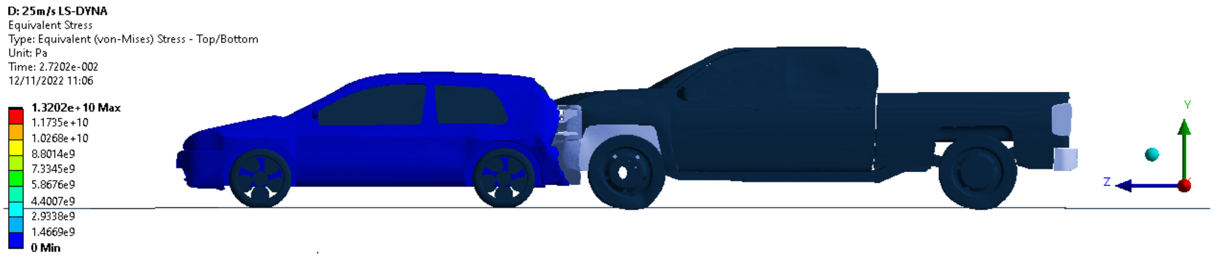

Vehicle Speed = 50m/s

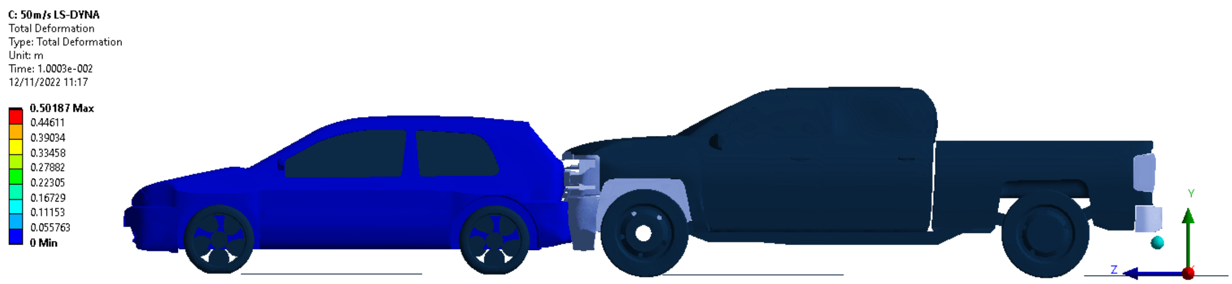

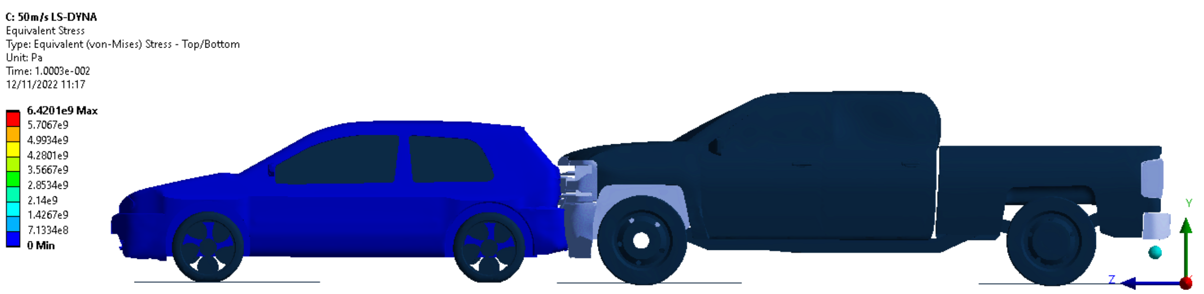

APPENDIX IV

RESULT UNDER MORE SEVERE DAMAGE CONDITION

When a vehicle sustains severe damage, it must either be completely replaced or undergo significant reconstruction of the component and catalog before it can be utilized once more for its proper purpose. The following images illustrate the more severe damage to the car and its strong behaviors at these various speeds. On this location, the damaging size is also quite large when the vehicle moves for a longer period of time.

Rear zone pre-crash analysis (0.06 second)

Vehicle speed = 50m/s

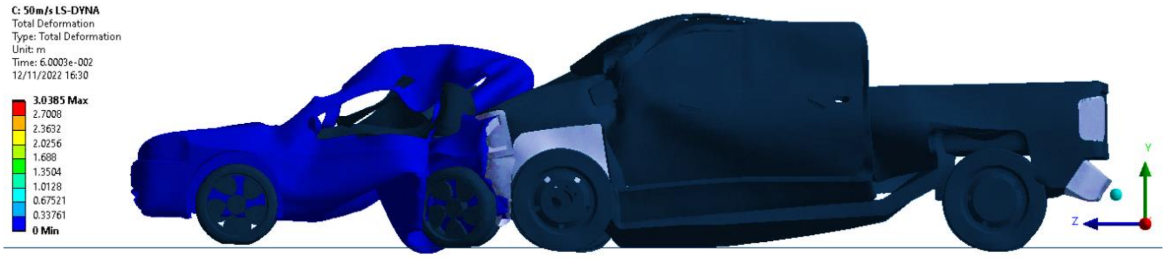

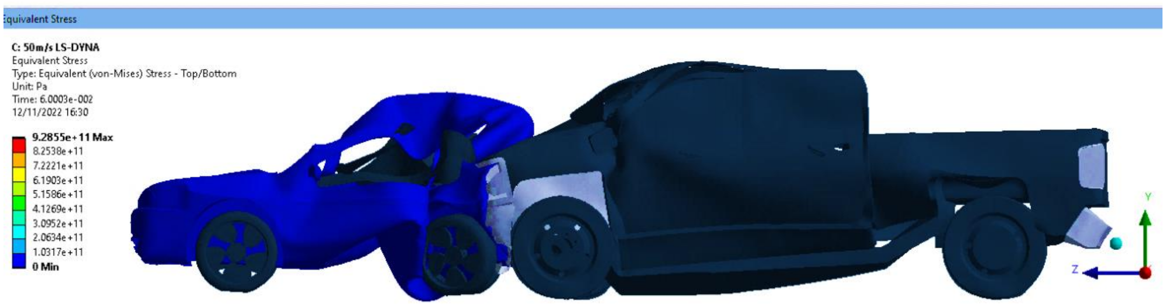

Rear zone pre-crash analysis (for 0.06 second)

Vehicle speed = 25m/s

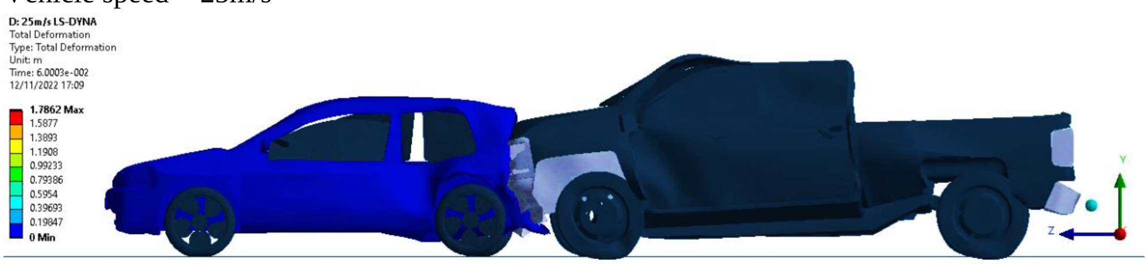

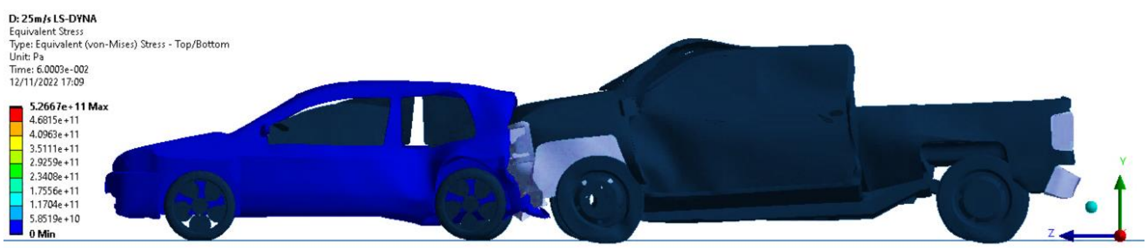

Rear zone pre-crash analysis (for 0.06 second)

Vehicle speed = 12.5m/s

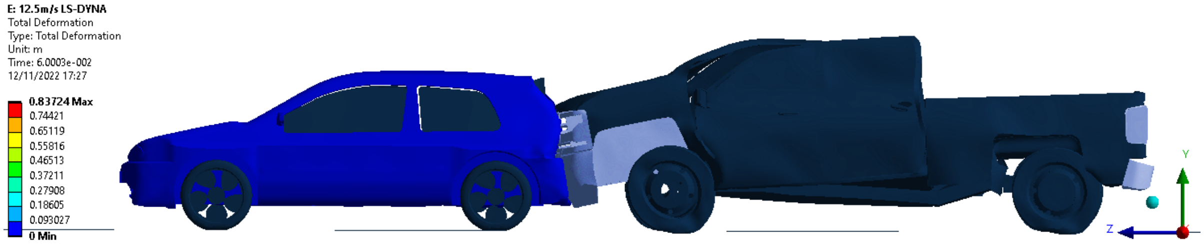

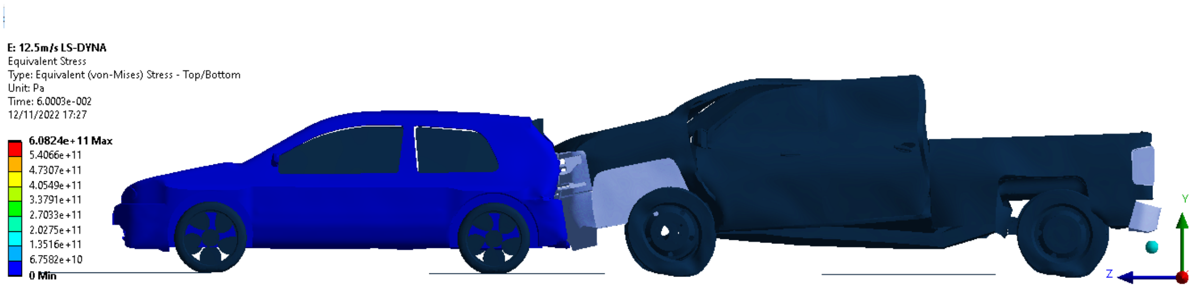

Rear zone pre-crash analysis (for 0.06 second)

Vehicle speed = 6.25m/s

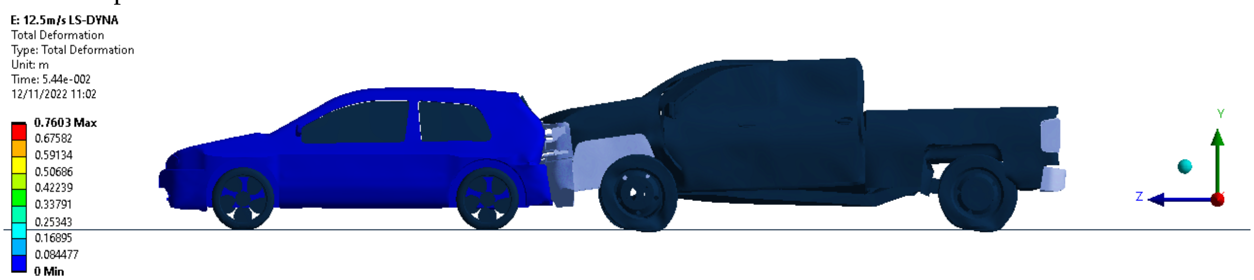

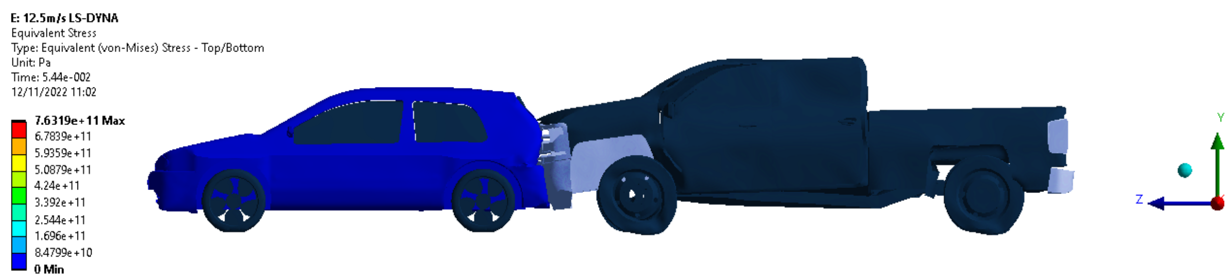

APPENDIX V
FRONT CAR WITH AIR BAG

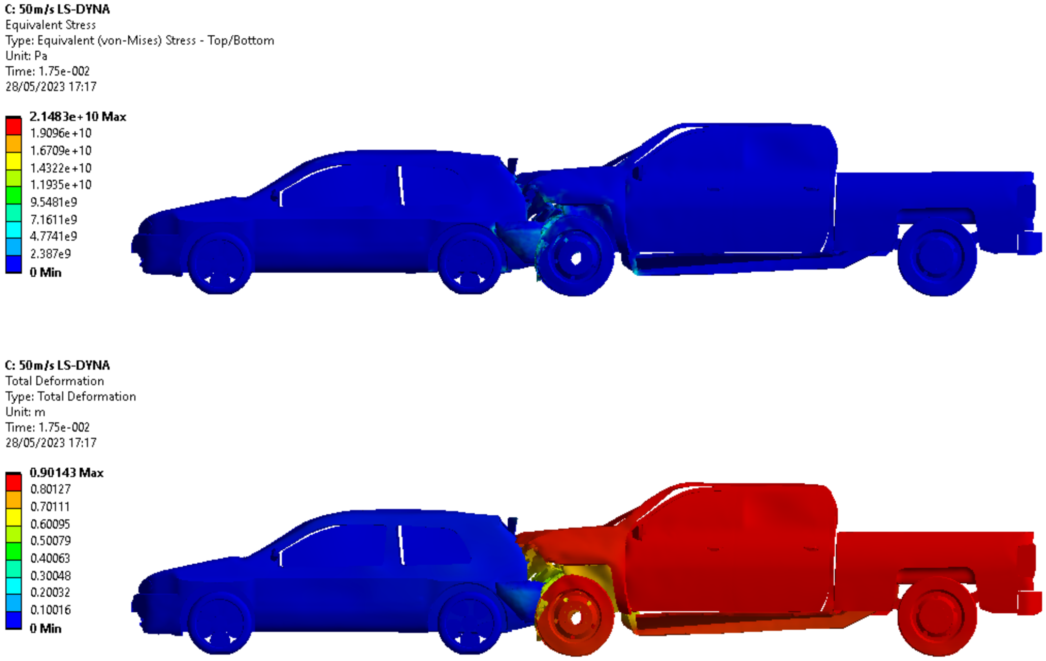

(a)

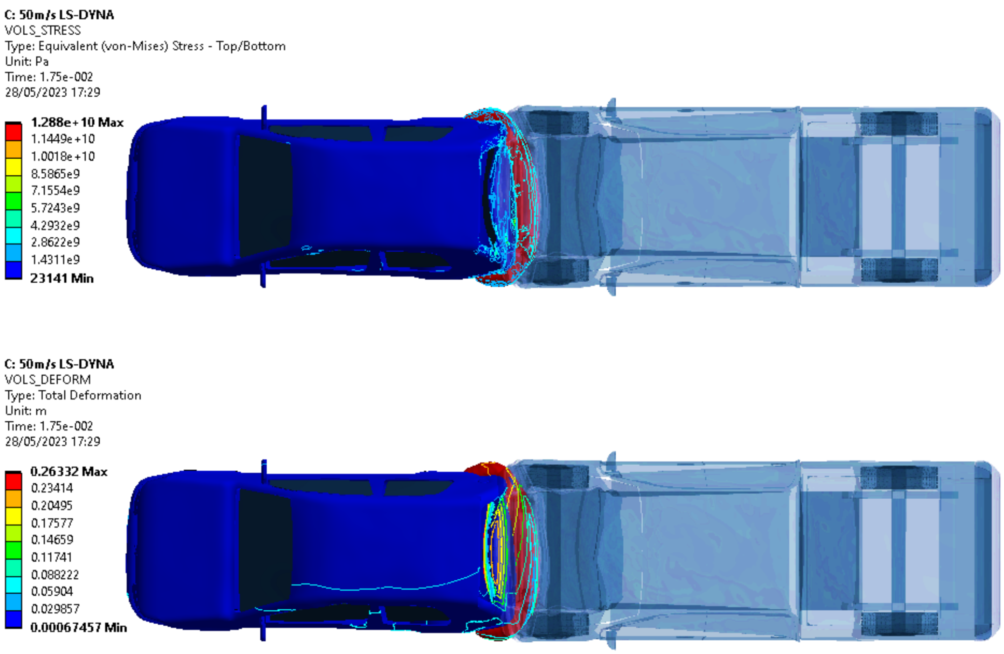

(b)

Figure. a & b, Stress distribution and total deformation of both cars and Frontal car respectively at rear car speed of (50m/s)

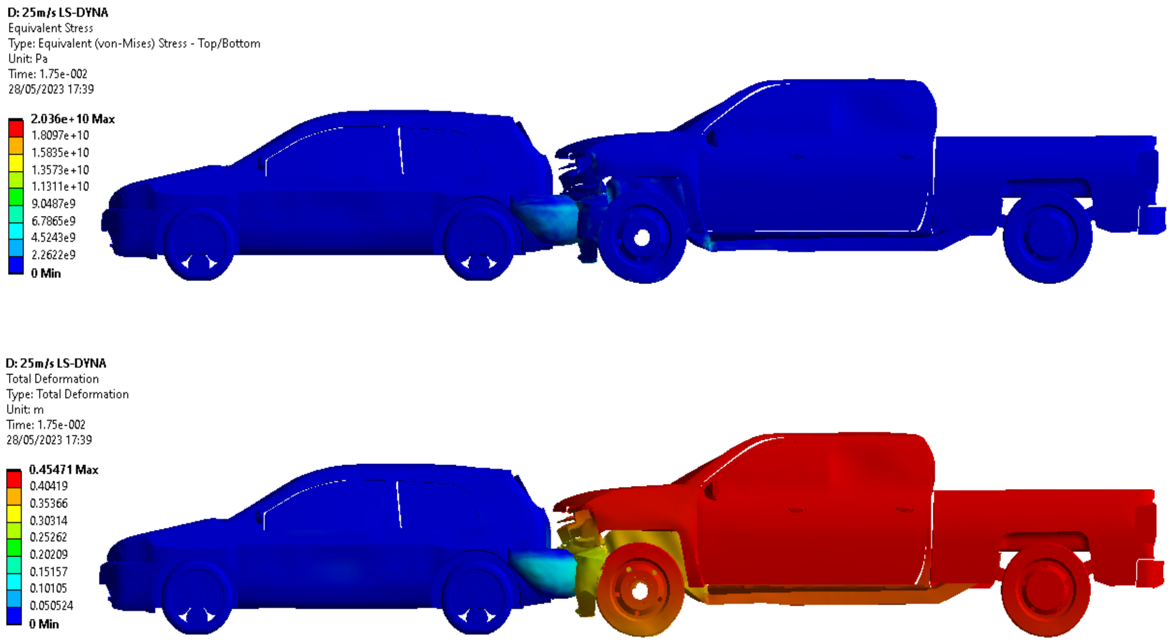

(a)

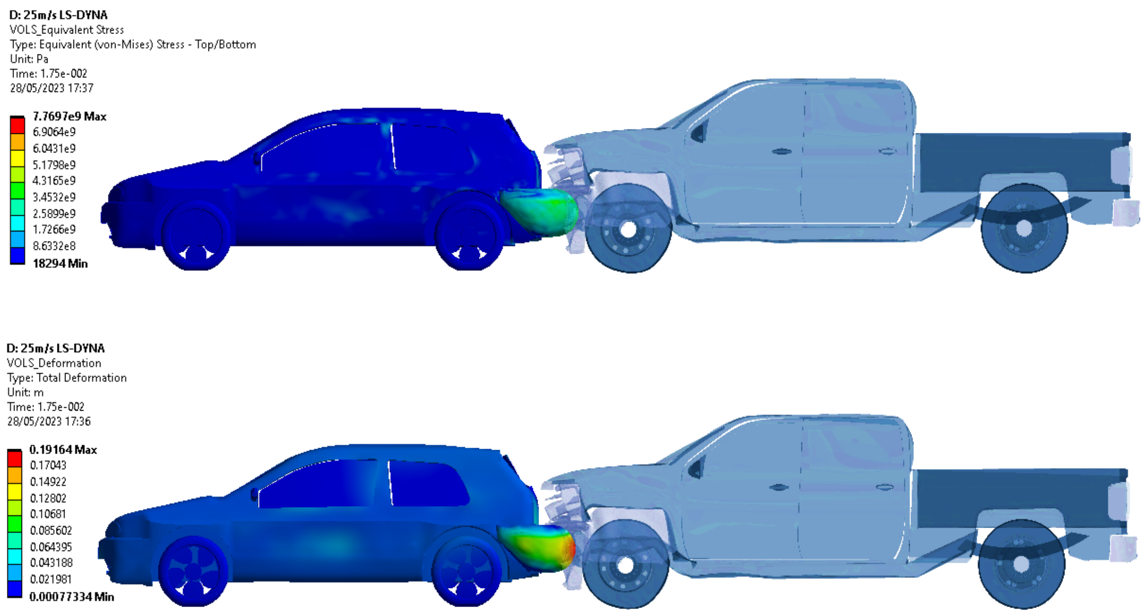

(b)

Figure. a & b, Stress distribution and total deformation of both cars and Frontal car respectively at rear car speed of (25m/s)

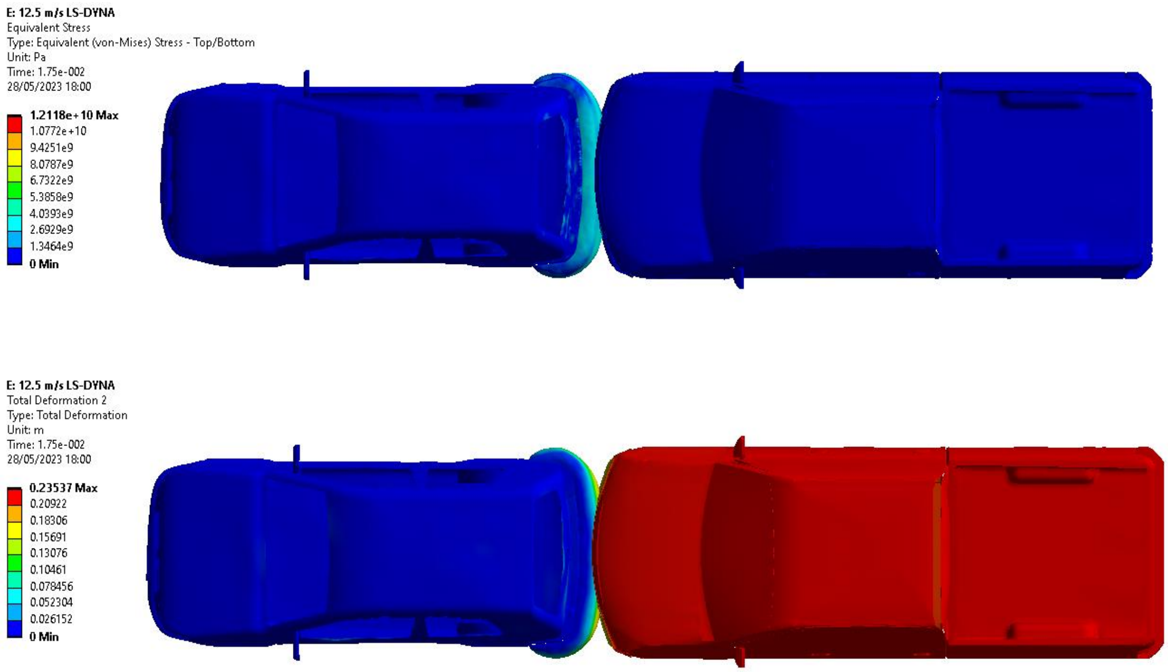

(a)

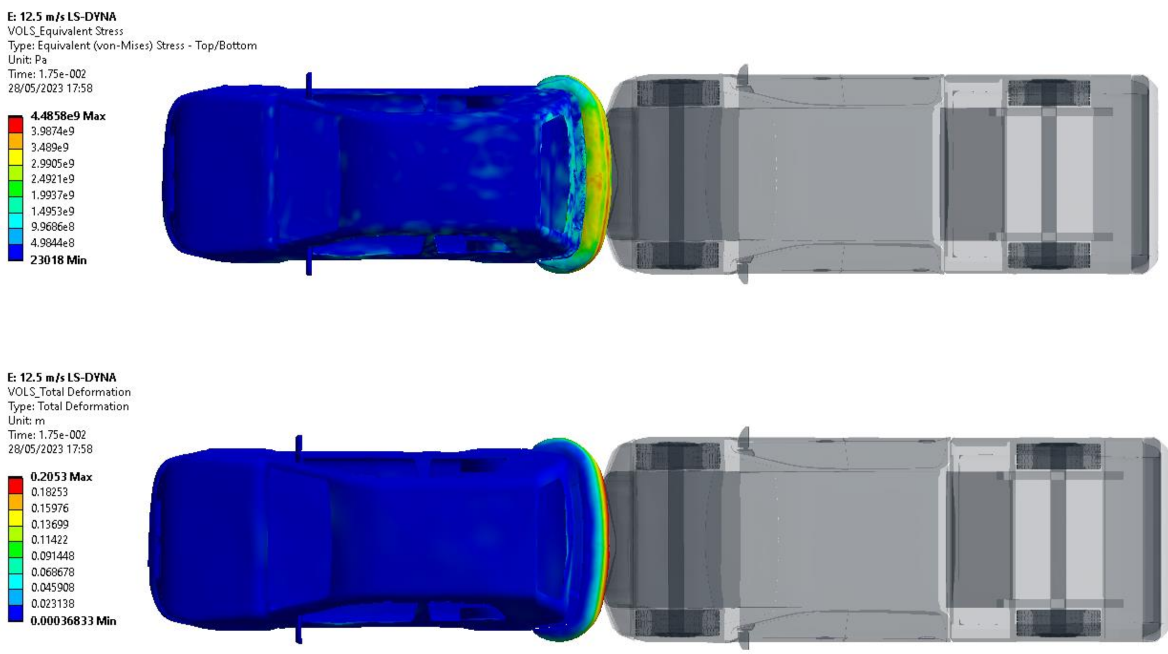

(b)

Figure 0.1 a & b, Stress distribution and total deformation of both cars and Frontal car respectively at rear car speed of (12.5m/s)

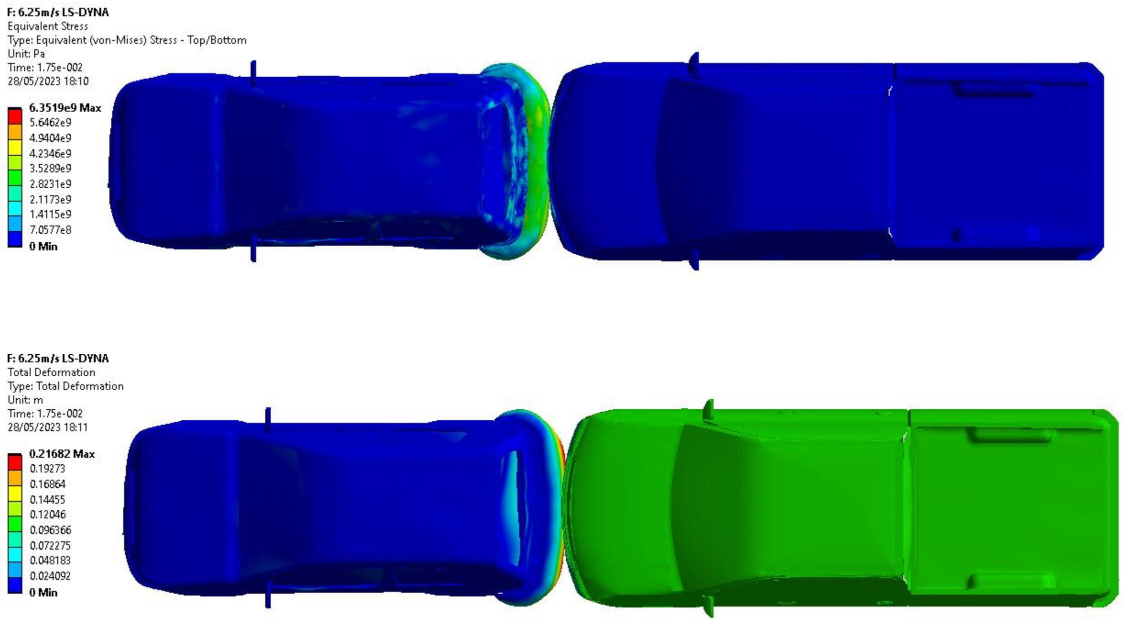

(a)

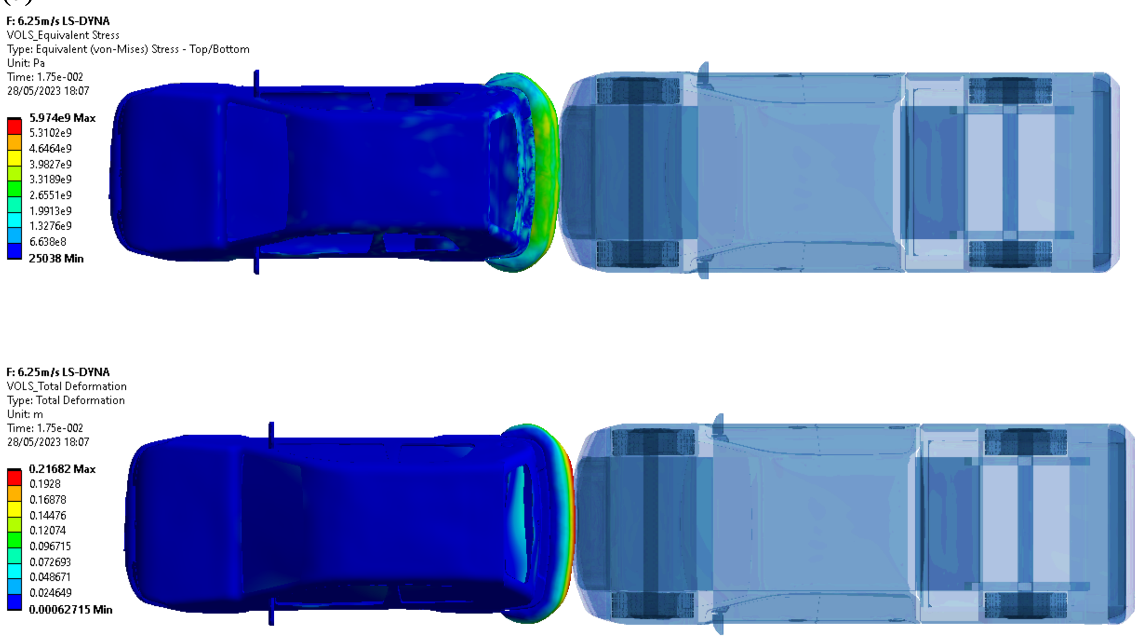

(b)

Figure. a & b, Stress distribution and total deformation of both cars and Frontal car respectively at rear car speed of (6.25m/s)

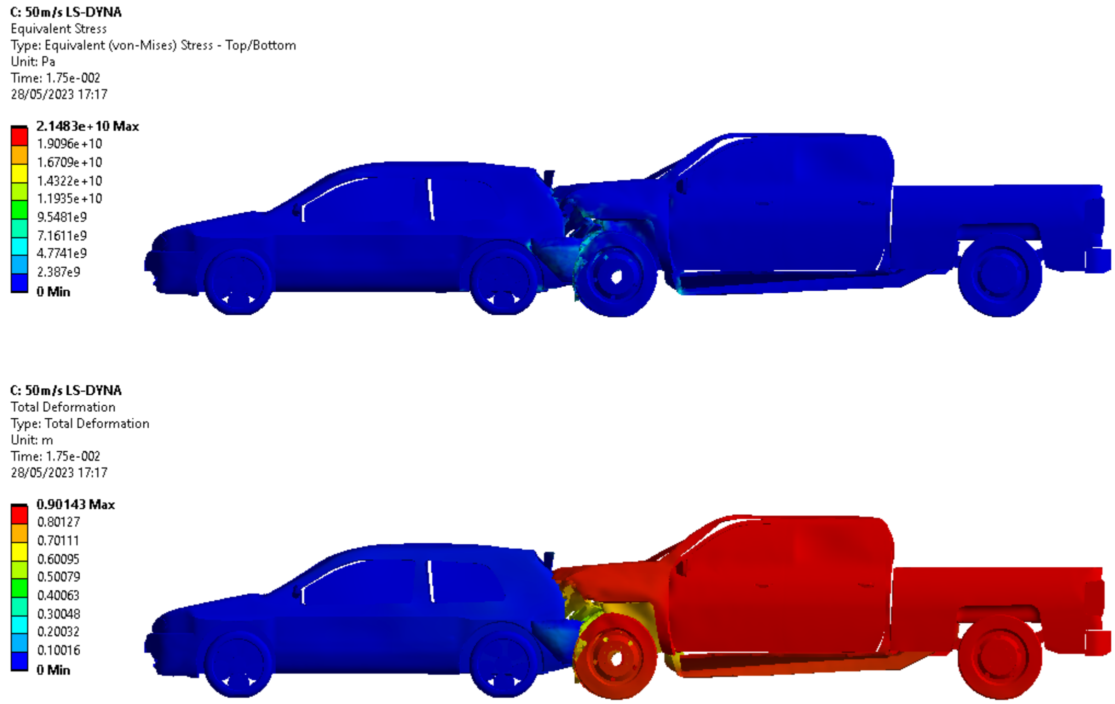
C: 50m/s LS-DYNA
Equivalent Stress
Type: Equivalent (von-Mises) Stress - Top/Bottom
Unit: Pa
Time: 1.75e-002
28/05/2023 17:17
2.1483e+10 Max
1.9096e+10
1.6709e+10
1.4322e+10
1.1935e+10
9.5481e9
7.1611e9
4.7741e9
2.387e9
0 Min
C: 50m/s LS-DYNA
Total Deformation
Type: Total Deformation
Unit: m
Time: 1.75e-002
28/05/2023 17:17
0.90143 Max
0.80127
0.70111
0.60095
0.50079
0.40063
0.30048
0.20032
0.10016
0 Min

(a)

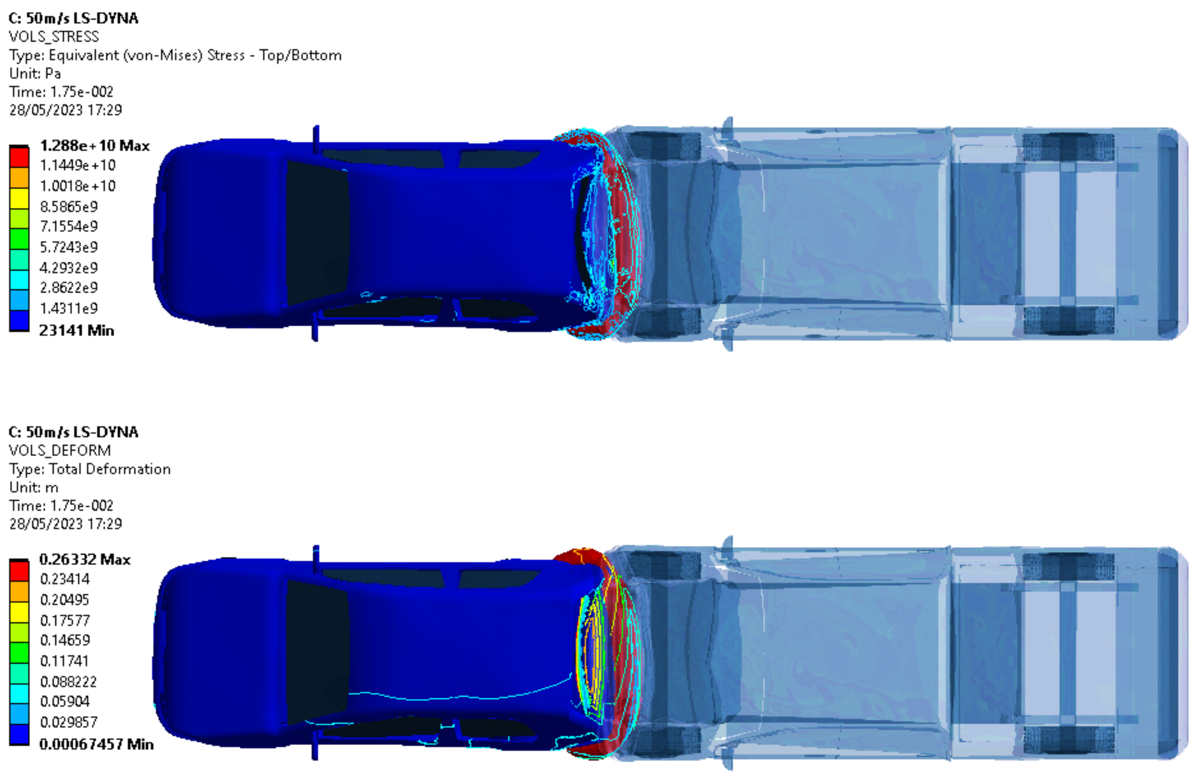
C: 50m/s LS-DYNA
VOLS_STRESS
Type: Equivalent (von-Mises) Stress - Top/Bottom
Unit: Pa
Time: 1.75e-002
28/05/2023 17:29
1.288e+10 Max
1.1449e+10
1.0018e+10
8.5865e9
7.1554e9
5.7243e9
4.2932e9
2.8622e9
1.4311e9
23141 Min
C: 50m/s LS-DYNA
VOLS_DEFORM
Type: Total Deformation
Unit: m
Time: 1.75e-002
28/05/2023 17:29
0.26332 Max
0.23414
0.20495
0.17577
0.14659
0.11741
0.088222
0.05904
0.029857
0.00067457 Min

(b)

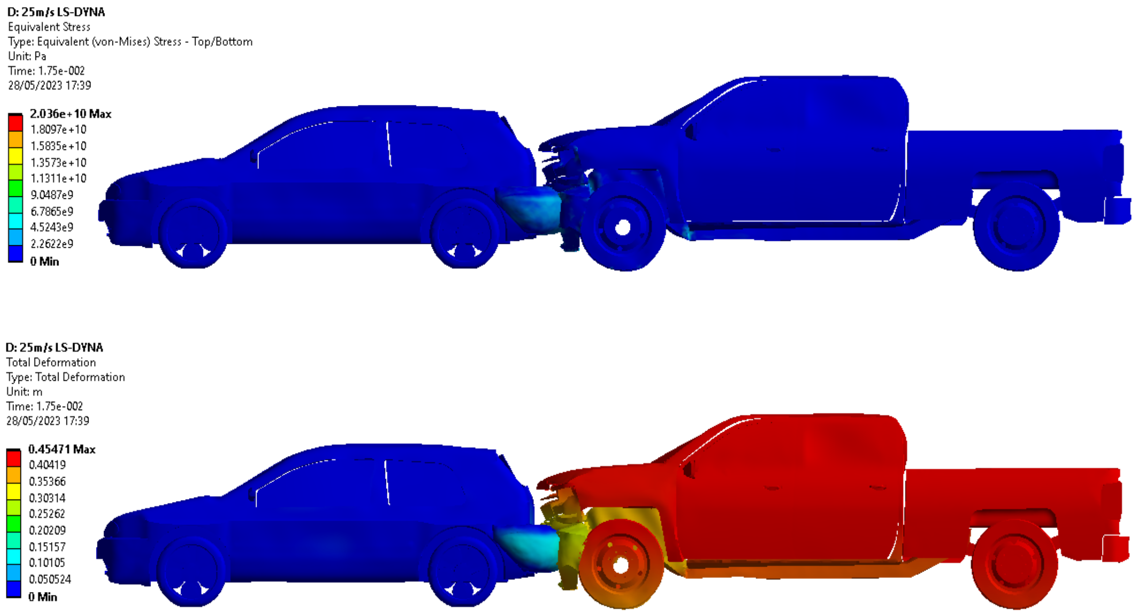
D: 25m/s LS-DYNA
Equivalent Stress
Type: Equivalent (von-Mises) Stress - Top/Bottom
Unit: Pa
Time: 1.75e-002
28/05/2023 17:39
2.036e+10 Max
1.8097e+10
1.5835e+10
1.3573e+10
1.1311e+10
9.0487e9
6.7865e9
4.5243e9
2.2622e9
0 Min
D: 25m/s LS-DYNA
Total Deformation
Type: Total Deformation
Unit: m
Time: 1.75e-002
28/05/2023 17:39
0.45471 Max
0.40419
0.35366
0.30314
0.25262
0.20209
0.15157
0.10105
0.050524
0 Min

(a)

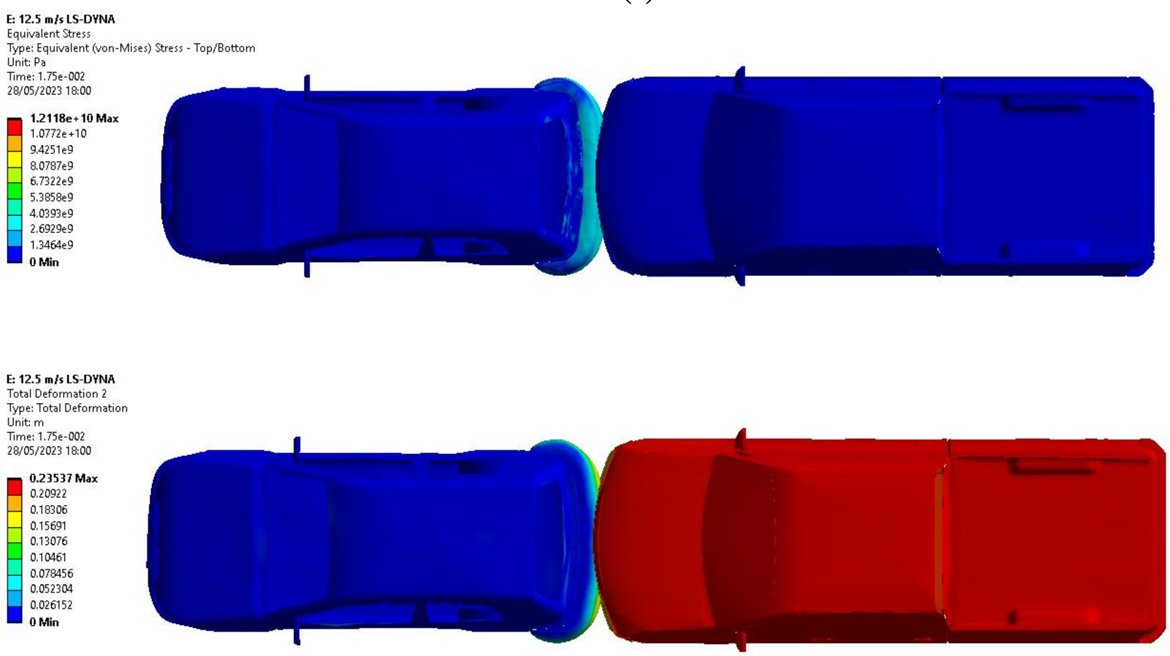
E: 12.5 m/s LS-DYNA
Equivalent Stress
Type: Equivalent (von-Mises) Stress - Top/Bottom
Unit: Pa
Time: 1.75e-002
28/05/2023 18:00
1.2118e+10 Max
1.0772e+10
9.4251e9
8.0787e9
6.7322e9
5.3858e9
4.0393e9
2.6929e9
1.3464e9
0 Min
E: 12.5 m/s LS-DYNA
Total Deformation 2
Type: Total Deformation
Unit: m
Time: 1.75e-002
28/05/2023 18:00
0.23537 Max
0.20922
0.18306
0.15691
0.13076
0.10461
0.078456
0.052304
0.026152
0 Min

(a)

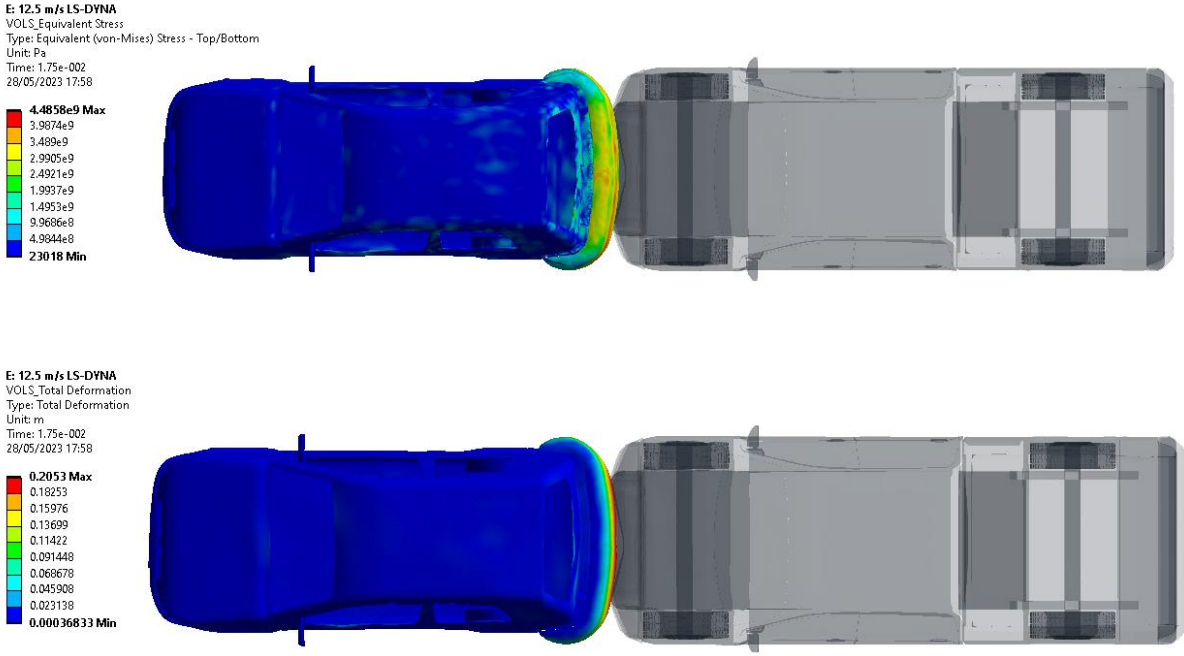

(b)

Figure. a & b, Stress distribution and total deformation of both cars and Frontal car respectively at rear car speed of (12.5m/s)

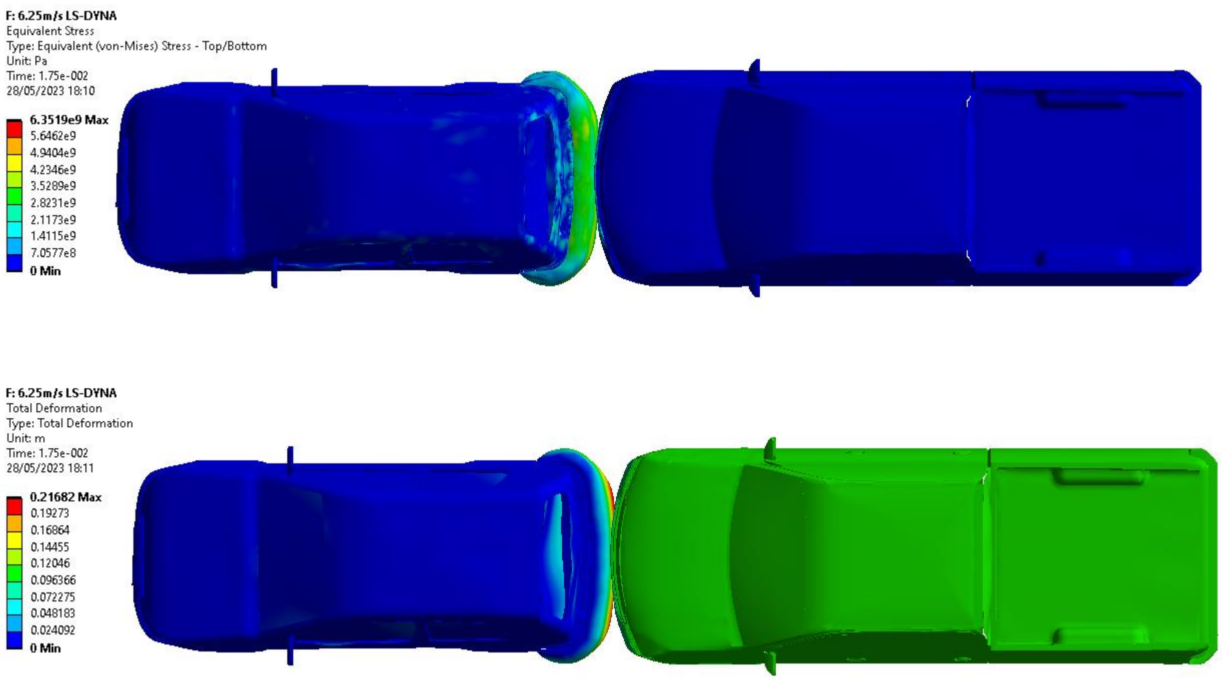

(a)

APPENDIX VI
CAR SPECIFICATION

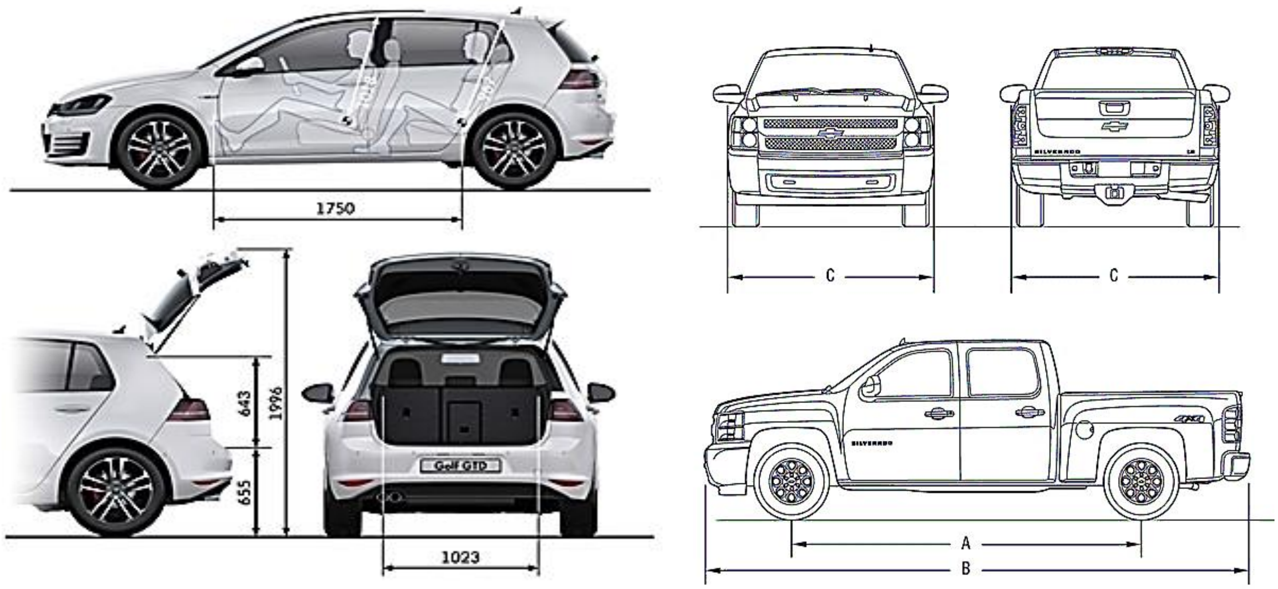

(a) (b)

Figure. Volkswagen car and Cholveret Silverado 2500 pick up

APPENDIX VII

AIR BAG ARDINO BASED SENSOR CODE

Code:

```
// Pins used
#define LEDGREEN 2
#define LEDYELLOW 3
#define LEDRED 4
#define TRIGGER 5
#define ECHO 6
#define BUZZER 9
// Constants
const float sound = 34300.0; // Sound speed in cm/s
const float threshold 1 = 200.0;
const float threshold 2 = 100.0;
const float threshold 3 = 50.0;
void setup() {
  // Initiate mounting circuit
  Serial.begin(9600);
  // Modo entrada/salida de los pines
  pinMode(LEDGREEN, OUTPUT);
  pinMode(LEDYELLOW, OUTPUT);
  pinMode(LEDRED, OUTPUT);
  pinMode(ECHO, INPUT);
  pinMode(TRIGGER, OUTPUT);
  pinMode(BUZZER, OUTPUT);
  // Turn off the LEDs
  turnoffLEDs();
}

void loop() {
  // Prepare Ultrasonic sensor
  initiateTrigger();
  // Obtain distance
```

```
  float distance = calculatedistance ();
  // Turn off LEDs
  turnoffLEDs();
  // Alert if within danger zone
  if (distance < threshold 1)
  {
    // Launch alerts
    alerts(distance);
  }
}
// Turn off LEDs
void turnoffLEDs()
{
  // Turn off LEDs
  digitalWrite(LEDGREEN, LOW);
  digitalWrite(LEDYELLO, LOW);
  digitalWrite(LEDRED, LOW);
}
// Check if any visual or sound alert is required
void alerts (float distance)
{
  if (distance < threshold 1 && distance >= threshold 2)
  {
    // Turn on LED Green
    digitalWrite(LEDGREEN, HIGH);
    tone(BUZZER, 2000, 200);
  }
  else if (distance < threshold2 && threshold > threshold3)

  {
    // Turn on LED yellow
    digitalWrite(LEDYELLOW, HIGH);
    tone(BUZZER, 2500, 200);
```

```
  }
  else if (distance <= threshold3)

  {

    // Turn on LED red

    digitalWrite(LEDRED, HIGH);
    tone(BUZZER, 3000, 200);
  }
}
// Calculate distance between sound and the object
float calculatedistance()
{
  unsigned long time = pulseIn(ECHO, HIGH);
  float distance = time* 0.000001 * sound / 2.0;
  Serial.print(distance);
  Serial.print("cm");
  Serial.println();
  delay(500);
  return distance;
}
 void initiateTrigger()
{
 digitalWrite(TRIGGER, LOW);
  delayMicroseconds(2);
  digitalWrite(TRIGGER, HIGH);
  delayMicroseconds(10);
  digitalWrite(TRIGGER, LOW);
}
```